UNIVERSITY OF CALIFORNIA SAN DIEGO

Biomaterial-based devices for liver cell transplantation

A dissertation submitted in partial satisfaction of the

requirements for the degree Doctor of Philosophy

in

Bioengineering

by

Nailah Seale

Committee in Charge:

Professor Shyni Varghese, Chair
Professor Pedro Cabrales
Professor Shankar Subramaniam
Professor Prashant Mali
Professor Pradipta Ghosh
Professor Tatiana Kisseleva

2018

The dissertation of Nailah Seale is approved, and it is acceptable in quality and form for publication on microfilm and electronically:

_____

_____

_____

_____

_____

_____

Chair

University of California San Diego

2018

Epigraph

“Not everything that is faced can be changed, but nothing can be changed until it is faced.”

-James Baldwin

Table of Contents

List of Figures

List of Tables

List of Abbreviations

3D, Three-dimensional

ANOVA, Analysis of variance

CD31, platelet endothelial cell adhesion molecule (PECAM-1)

CK18, Cytokeratin-18

DA, daltons

DAPI, 4',6-diamidino-2-phenylindole

DNA, deoxyribonucleic acid

ECM, extracellular matrix

ELISA, enzyme linked immunosorbent assay

FBS, fetal bovine serum

GM, growth medium

HA, hyaluronic acid

HAMA, hyaluronic acid Methacrylate

HM, human umbilical vein endothelial cells medium

HUVECS, human umbilical vein endothelial cells

hA1AT, human alpha-1-antitrypsin

hMSCs, human bone marrow stromal cells

MA, methacrylate

MEFs, mouse embryonic fibroblasts

NaBH3, sodium borohydride

NIH, national institute of health

OCT, optimum cutting temperature

PBS, phosphate buffered saline

PEG, polyethylene glycol

PEGDA, polyethylene glycol diacrylate

PMMA, polymethyl methacrylate

RT, room temperature

SEM, scanning electron microscope

Acknowledgements

I would like to sincerely thank and acknowledge some of the many individuals who have contributed tremendously towards the completion of my graduate degree. I would like to first and foremost thank my family, especially my parents Stephen and Heather Seale for always leading by example and for their continued love, support, and encouragement through the toughest of times. Moreover, their hard work and sacrifices have been instrumental in molding me into the person that I am today. Next, I must thank my older siblings Nyasha, Zolani, Jamila, Akilah, Hasani and Damani for paving the way in education, teaching me how to navigate roadblocks and exemplifying that anything is possible. I must also thank my younger siblings Safiya and Akanni, who continue to inspire me with their strength, dedication and will to succeed. I hope that my actions can motivate them to continuously strive for success.

Secondly, I would like to thank my advisor, Dr. Shyni Varghese, for her guidance and support throughout my PhD. Despite the many obligations of her faculty position and running a large lab, she always made herself available, even if that meant coming in on the weekends. Lastly, I would like to thank her for bringing me into this lab. The Varghese lab provided me with a truly unique environment filled with peers and mentors who played an instrumental role in molding my scientific abilities throughout my research career. To this end I must thank Dr. Aereas Aung and Dr. Han Lim and the members of the devices subgroup for always being there to help me to push beyond perceived limitations and expand my scientific curiosities. I would also like to thank Dr. Yuru Shih for helping me with my *in vivo* experiments and for exemplifying the patience, scientific rigor and discipline needed to be a good scientist. I must also thank Dr. Ji Hyun

Ryu for his patience, help and advice pertaining to biomaterials. I would also like to give special thanks to Priya Nayak for helping me with my animal work in the final year of my research. Finally, I would like to thank all the present and the past Varghese lab members, for their camaraderie and help on my journey towards attaining my doctorate degree.

I would also like to thank those who have shaped and molded my scientific abilities throughout my research career. To this end, I would like to thank Dr. Warren Grayson and Dr. Winston Anderson for giving me my first undergraduate research experiences and for instilling in me a sense of scientific discipline. I would also like to thank Dr. Pedro Cabrales for his continued mentorship, understanding and support throughout the years. He has played an integral role in my choosing to study at UCSD and as such I am honored to have him server on my committee. I would also like to thank the rest of my dissertation committee for all of their feedback and guidance along the way.

I would also like to acknowledge the NSF GRFP and the UC-HBCU partnership for financially supporting my Ph.D. career, helping me with career development as well as providing the rare opportunity to meet kind and caring individuals. The UC-HBCU fellows have also provided a safe space, with like-minded individuals who could truly understand my unique struggles faced in graduate school. Their generosity and effort has instilled in me the desire to give back to the community in any way possible.

Last but not least, I must thank my friends for all their support throughout this journey. I must first thank Kwesi Rutledge for his support, patience and understanding throughout the tough times and for believing in me during the times I didn't even believe

in myself. He helped to keep me disciplined and motivated. Next, I must thank my friends from Howard undergrad who have always been there for me to provide me with council and perspective. Many of them have supported me since freshman year and continuously push me to constantly strive for success. I must also thank all the friends that I have made at UCSD, who have gone through similar PhD struggles and can therefore empathize the most with how I feel. They are always there to hear me vent, to support me and to cheer me up on Friday nights after an exhausting workweek.

Chapter 1, in full, is a literature review on the topics discussed within this dissertation and is being prepared for submission for publication. "Concise Review: Engineering biomaterial driven liver cell therapies: from *in vitro* culture to transplantation." Seale NM, Varghese S. The dissertation author was the primary author for this section.

Chapter 2, in full, has been accepted for publication. "Dual Compartment Vascularized device for subcutaneous humanized liver transplantation." Seale NM, Shih Y., Ramaswamy S., Verma I., Varghese S. The dissertation author was the primary investigator and author of this paper.

Chapter 3, in full, is currently being prepared for use in part of a publication for submission. "Modified Chitosan Cell Pouch for allogeneic and xenogeneic hepatocyte transplantation." Seale NM, Ryu JH. , Nayak P., Varghese S. The dissertation author is the primary investigator and author of this material.

Chapter 4, in full, is currently being prepared for use in part of a publication for submission. "Modified Chitosan Cell Pouch for allogeneic and xenogeneic hepatocyte

transplantation." Seale NM, Ryu JH. , Nayak P., Varghese S. The dissertation author is the primary investigator and author of this material.

Vita

2014 Bachelor of Science in Chemical Engineering
Howard University, Washington, DC.

2018 Doctor of Philosophy in Bioengineering,
University of California San Diego, La Jolla, United States

Publications

Seale NM, Varghese S. Biomaterials for pluripotent stem cell engineering: from fate determination to vascularization. Journal of Materials Chemistry B. 2016;4(20):3454-63.

Seale NM, Zeng Y., Varghese S. Biomimetic tissue engineering for Musculoskeletal Tissues. Elsivier. (Accepted)

Seale NM, Shih Y., Ramaswamy S., Verma I., Varghese S. Dual Compartment Vascularized device for subcutaneous humanized liver transplantation. Transplantation. (Accepted)

Seale NM, Ryu JH., Nayak P. , Varghese S. Modified Chitosan Cell Pouch for allogeneic and xenogeneic hepatocyte transplantation. (In preparation)

Seale NM, Varghese S. Concise Review: Engineering biomaterial driven liver cell therapies: from *in vitro* culture to transplantation. (In preparation)

Abstract of the Dissertation

Biomaterial-based devices for liver cell transplantation

by

Nailah Seale

Doctor of Philosophy in Bioengineering

University of California San Diego, 2018

Professor Shyni Varghese, Chair

The liver performs over 500 functions and plays an integral role in maintaining the proper function of the body. Any change to the complex liver structure can disrupt proper function and result in liver diseases or disorders. Approximately 30 million people in the United State have some form of liver disorder. These disorders can be genetic, example hemophilia B, virus based, example hepatitis C, or lifestyle based, example

alcoholic liver disease. Currently, while there may be treatments for some liver disorders, the only long-term cure for all liver disease or disorder is whole or partial organ transplantation. However, there is a significant shortage of transplantable donor organs, which has led to about 27,000 deaths annually attributed to liver disease in the United States alone. To combat this issue researchers are studying different cell therapies to either engineer whole livers as an alternative source for organ transplants; use cell therapies to replace damaged cells and stimulate liver regeneration; or use cell therapy in *ex vivo* devices as a way to extend a patient's life expectancy and bridge the gap until a donor organ is available. In this dissertation, I have engineered novel devices for liver cell transplantation by focusing on optimizing methods for maximizing cell delivery *in vivo* and maintaining long-term function. With these devices I have developed vehicles for autogeneic, allogeneic and xenogeneic liver cell transplantation to provide alternatives or improvements to existing liver therapies.

Chapter 1 is a literature review focusing on the use of biomaterials in hepatocyte culture and transplantation. Specifically, in this chapter, I underscore the role of biomaterials in improving *in vivo* hepatocyte culture techniques to help establish a more reliable and readily available cell source for transplantation therapies. Since primary human hepatocytes have limited availability, I also discuss the role of biomaterials in improving stem cell derived hepatocyte culture. Next, I highlight the most recent advancements in the use of biomaterials for engineering 3D constructs for transplantation. Specifically, I focus on the work that has been done using decellularized liver scaffolds for recellularization and transplantation, and the use of hydrogel based scaffolds for encapsulation and transplantation of cells.

Because the success of cell therapies hinges on the proper delivery, engraftment and long-term function of a large number of cells, in Chapter 2, I engineered transplantable tissues for applications in liver related cell therapies. Firstly, I have developed a dual compartment system for minimally invasive, subcutaneous implantation of 3-D vascularized liver-like tissues. In this system an inner compartment houses large numbers of primary hepatocytes, while the outer porous compartment facilitates vascularization to support sustained hepatocyte function. When implanted into NOD/SCID mice, this system has shown sustained function for at least 1 month *in vivo* as evidenced by human serum albumin secretion and immunostaining.

While the dual compartment system facilitates host cell recruitment for vascularization, making it an intervention better suited for autogeneic, immunosuppressed interventions; it is not suitable for allogeneic or xenogeneic transplants. To address this, in Chapter 3 I developed a biocompatible device that is closed off from host cell infiltration yet still allows flow of necessary nutrients and waste in and out of the implant, through the selectively permeable chitosan membrane. The device was further optimized through surface modification to prevent adhesion of immune cells and fibroblasts and subsequent fibrous capsule formation. While chapter 3 focuses on the development, modification and characterization of the pouch, chapter 4 focuses on the application of the pouch in allogeneic and xenogeneic transplantation. Allogeneic and xenogeneic transplantation success of this device to maintain cell function was shown through ELISA and immunostaining analysis.

Chapter 1: Engineering biomaterial driven liver cell therapies: from *in vitro* culture to transplantation

1.1 Introduction

The liver is the largest internal organ, and with over 500 functions, this metabolically active organ plays an integral role in maintaining the proper function of the body. Disruption to the complex liver structure can alter function and lead to liver disease. Approximately 30 million people in the United State suffer from some form of liver disease(1). While there are over 100 types of liver diseases, they can be categorized into genetic, example alpha-1-antitrypsin deficiency(2), virus based, example hepatitis C(3), or lifestyle based, example alcoholic liver disease(4). While the regenerative capacity of the liver is substantial enough to cure or reverse some lifestyle-based diseases, if addressed early, it does not help in the case genetic disorders (since the genetically defective cell will continue to regenerate). As such, partial or whole organ transplantation (Figure 1.1 A) remains the only long-term cure for most liver diseases, especially those that inevitably lead to acute liver failure (ALF) or end stage liver disease (ESLD). This places a high demand on already limited transplantable donor organs(5). The inability to meet this demand leads to about 27,000 deaths annually in the United States alone(1).

Cell transplantation therapy (Figure 1.1 B-D) is currently being considered as an alternative therapy to help alleviate the demand for donor organs(6). Paramount to the success of any cell therapy is firstly establishing a reliable cell source and secondly maintaining viability and function of these transplanted cells. Currently, human primary

hepatocytes are the most ideal cell source for transplantation therapy, however, they are in limited supply and show limited expansion potential *in vitro*. The advent of stem cell technology promises to provide a potentially unlimited cell source that can be differentiated into liver cells. However, like primary hepatocytes, once differentiated they begin to lose function over time. Additionally, they still suffer from immaturity and impure populations. In an effort to better maintain and expand hepatocytes for transplantation, researchers are focusing on improving their extracellular matrix (ECM) environment. The ECM plays an integral role in maintaining cell function as it provides the necessary structural and biochemical environment for sustained cellular function(7). Not only have biomaterials been employed to improve *in vitro* hepatocyte culture, but they have also played an integral role in liver engineering and transplantation efforts. For example, biomaterials have been manipulated via several approaches (e.g. particle leeching and bio printing) to promote vascular formation in an effort increase the viability and function of transplanted cells(8). In this chapter, we underscore the importance of biomaterials in facilitating successful liver therapy by highlighting the most recent advancements in the use of biomaterials for maintaining functional and viable hepatocytes *in vitro* and improving *in vivo* cell transplantation.

1.2 Biomaterial assisted in vitro hepatocyte culture

The *in vitro* culture of hepatocyte is tasked with providing and maintaining a reliable cell source for transplantation therapies. The quality of *in vivo* therapies depends on the expansion potential, function and viability of the cultured hepatocytes. Early research has shown that hepatocytes cultured on tissue culture plastic undergo changes in

phenotype resulting in reduced function(9). As such, biomaterials like collagen were used to improve hepatocyte culture conditions by providing a more supportive ECM environment (10). Beyond maintaining primary hepatocytes, biomaterial-based technologies have also been extended toward promoting stem cell derived liver differentiation.

1.2.1 Primary hepatocyte culture

Primary human hepatocytes remain the most preferred cell source for transplantation however, when cultured *in vitro*, primary hepatocytes exhibit limited proliferation ability and lose their liver-specific function within days(9). To improve the function of these cells, biomaterials have been employed as an artificial ECM to support 2D and 3D cultures. Collagen type I protein is an abundant component in native liver ECM, and hence is commonly used as a coating to prolong hepatocyte culture and function in vitro. Furthermore, Tuschl et al. found that culturing hepatocytes in collagen sandwich (between two collagen layers) showed even better improvements in morphology, phenotype and gene-expression as compared to monolayer collagen coating(11).

Other biomaterials containing synthetic peptides or linear polysaccharides, like chitosan, have also been used to improve primary hepatocyte culture. Researchers found that seeding cells in 3D hydrogels and polymer scaffolds made further improvements to hepatocyte aggregation and metabolic function*(12, 13)*. Mehta et al. used soft self-assembling synthetic peptide nano-fiber hydrogels to understand how hepatocyte function is affected by ECM tethered growth factors and adhesion ligands. By optimizing this

method they were able to improve hepatocyte metabolic function(13). In another study, Feng et al. demonstrated that in addition to biomaterial composition, architecture also played a role in maintaining hepatocyte cultures (Figure 1.2) (14). Results indicated that mouse hepatocytes cultured on galactosylated chitosan (GC) electrospun nanofibrous scaffolds had higher levels of urea synthesis, albumin secretions and cytochrome P450 enzyme activity, compared to those cultured on GC films(14).

While the incorporation of biomaterials has advanced *in vitro* primary hepatocyte culture, there still remain major issues. Firstly, the universal shortage of donor livers extends to the shortage of livers available for primary hepatocyte isolation. Therefore, hepatocytes are usually harvested from livers not suitable for transplantation, which means the quantity is limited and the quality of the cells varies from donor to donor (15). Exasperating the limited supply of primary human hepatocytes is their limited *in vitro* expansion capacity. While alternative cell sources like primary porcine or murine hepatocytes can be made more readily available, they are unsuitable for transplantation due to xenozoonosis and antibody-mediated rejection concerns. Until these issues are addressed the search for viable alternative cell sources still requires much attention.

1.2.2 Stem Cell Derived Hepatocyte Culture

The inability to source enough primary human cells for transplantation therapies has prompted researchers to explore other cell sources(16). Induced Pluripotent Stem Cell (iPSC) Derived hepatocytes (iHeps) have been suggested as a theoretically unlimited cell source with the potential to produce genetically diverse cells(17-20). The advantages of a genetically diverse population include the development of patient specific cell therapies.

In 2013, Takebe et al were the first to engineer 3D vascularized human liver *in vitro* from hiPSCs . Using a protocol that required the culture of cells on matrigel, they were able to prove that organ bud transplantation could rescue drug induced lethal liver failure models. Since then many studies have used similar protocols and biomaterials like matrigel and or collagen to coat tissue culture plates for cell differentiation on 2D substrates.

Other biomaterials used for differentiation include, alginate, chitin and synthetic polymers. Lau et al used alginate scaffolds to create microcavity hydrogels to induce iPSC colony formation and differentiation into 3D liver micro tissues(21). On the other hand, Du et al used a multistep approach to separately differentiate hiPSCs into endothelial-like cells and hepatocyte-like cells within different chitin based fibres(22). Like alginate, chitin is heavily used in tissue engineering because it possesses characteristics like low cytotoxicity, high biodegradability and high biocompatibility(23). These chitin fibres were later assembled by multi-interfacial polyelectrolyte complexation (MIPC) to form endothelialized liver constructs. Other approaches included culturing the PSCs in 3D spheroids and mixing biomaterials like gelatin-coated poly (l-lactic acid)/poly (DL-lactic-co-glycolic acid) (PLLA/PLGA) within the spheroids to deliver growth factors (24).

While the aforementioned approaches have successfully produced hepatocyte-like cells, they are usually more representative of fetal-stage hepatocytes(25) that only demonstrate short-term or reduced function. As such, recent attempts have been made to use biomaterials to not only induce differentiation, but to also promote maturation of the differentiated cells(26-28). A popular attempt to promote maturation is adopting 3D

culture methods. For example, 3D approaches were used to mature hepatocytes cultured in collagen matrices(27). By adopting this 3D clump format, hepatocytes were more polarized, produced more bile canaliculi and had a longer functional lifetime (75days) compared to traditional 2D culture(27). In another example, during differentiation, cells were aggregated and encapsulated in PEG-diacrylate (PEG-DA) and given FH1 maturation molecules(16). Again, compared to 2D cultures, this 3D configuration produced more functionally mature cells. As a result of these and other maturation attempts, iHeps have been successfully used in drug toxicity prediction studies(29, 30).

1.3 Biomaterials for 3D organ engineering and transplantation

In parallel to establishing a reliable cell source, approaches to improve the delivery and environment of the transplanted cells are also being investigated. A major effort to combat liver disease via cell therapy has been to bioengineer liver surrogates to alleviate the demand for donor organs. Early efforts utilized cell sheets since they would be thin enough to function within the diffusion barrier(31). However, given space constraints, feasibly scaling up this technique would require the stacking of sheets and the incorporation of vascularization. Alternatively, researchers are exploring approaches that use biomaterials as delivery vehicles for cell injections or as structures to house hepatocytes and facilitate integration and engraftment with the host. Some of the more popular biomaterial approaches to engineer livers include the use of natural decellularized liver scaffolds(32-34) or synthetic-hybrid scaffolds(21, 35, 36). These scaffolds are touted to provide the ECM-based cues needed to improve hepatic stem cell differentiation and maintain long-term hepatocyte function.

1.3.1 Decellularized liver matrices

Some of the greatest cell transplantation successes have been achieved through the use of decellularized liver (porcine or rodent)(12, 37, 38) scaffolds. Unlike synthetic scaffolds, these decellularized structures inherently contain the structural support and most of the biochemical components needed to maintain hepatocyte function. Furthermore, they also contain the complex vascular networks, when decellularized as intact structures, needed to support the metabolically demanding liver. In 2010 Uygun et al. successfully decellularized whole rat livers, then recellularized them and transplanted them in rats(37). The recellularized whole liver scaffold displayed normal hepatic function including CYP expression, albumin secretion and urea synthesis as compared to normal livers *in vitro*. Additionally, when transplanted, they exhibited expected viability and function with minimal ischemic damage(37). In 2011 Baptista et al. were able to successfully recellularize a decellularized ferret liver (Figures 1.3) with human fetal liver and endothelial cells to create a transplantable humanized liver(39). Functional analysis indicated that the hepatocytes and endothelial cells engrafted onto the recellularized ferret liver and showed typical function when transplanted into rats. In another example, Mazza et al. decellularized a lobe of human liver, well enough to implant in mice without prompting severe immune attack or rejection. They were then able to successfully recellularize the liver lobe with human cells(34).

Although decellularized liver organs as scaffolds show significant promise, there are still difficulties to overcome in ensuring proper decellularization while preserving the ECM and destroying xenogeneic DNA. While low DNA content (under 50 ng double stranded DNA per mg ECM) may not trigger an immune response in tested animals, it

can still carry the risk of immune rejection in patients(40). As such, this method still requires more development to improve and standardize decellularization techniques, as well as make advancements in properly repopulating the liver and conserving functional vasculature(41). While these issues are being addressed, studying the structure and chemical composition of liver ECM can lead to more breakthroughs in creating more physiochemically relevant alternative systems. Ultimately, it is desirable to use synthetic biomaterials, as they are cost effective, chemically defined and thus can eliminate the problems tied to natural ECM's inconsistent DNA removal process and batch-to-batch variability.

1.3.2 Synthetic or synthetic hybrids Scaffolds

Synthetic or synthetic hybrid scaffolds like hydrogels are the most commonly used scaffolds for tissue engineering. Not only are hydrogels cost effective and chemically defined, but they also have favorable characteristics like high water content and similar viscoelastic properties to soft tissues, which can be a great asset in liver tissue engineering. Hydrogels are commonly used in liver tissue engineering to help maintain cellular function by encapsulating cells within a supportive microenvironment (36). For example, in one study PEDGA hydrogels were functionalized with peptide sequences and used to encapsulate hepatocytes and fibroblasts. Researchers found that this method provided the necessary juxtacrine and paracrine signals necessary to maintain the hepatocyte phenotype prior to and during ectopic transplantation(36). Furthermore, results indicated that the implant integrated with the host vasculature and maintained hepatic function for up to two weeks (Figure 1.4)(36). While these results were promising

since they supported functional cell transplantation without having to damage the host liver, the transplantation still brought up some issues. Firstly, the device still required an invasive procedure to be placed in the kidney capsule. Secondly, the device had to be placed in a heavily vascularized area and remain sufficiently thin in order to stay within the diffusion limitation. This may pose a problem in future scaling up and clinical translation efforts.

In another study PEGDA was used to crosslink hyaluronic acid (HA) to create hyaluronan grafts for human hepatic stem cell delivery(35). HA was used since its chemical structure is conserved across all species, it is non-toxic and does not elicit any immunogenic or inflammatory responses(42). In this study, researchers opted for the delivery of stem cells instead of mature cells, since mature cells have proliferation and viability issues both *in vitro* and *in vivo(35)*. Researchers found that using this hydrogel delivery system resulted in better engraftment of the delivered cells compared to the cells that were injected sans hydrogel.

1.4 Vascularization of Engineered Liver Transplants

Successful, clinically translatable cell transplantation therapies would require the implantation and functional maintenance of billions of cells(43). To properly maintain the function of these transplanted cells, it is essential that they have access to a nutrient rich oxygen supply(8). To achieve this different approaches are being explored to incorporate functional vasculature into the transplantable biomaterial designs. While porous scaffold design has been successfully used thus far in musculoskeletal tissue engineering (44-46), bio printing(43, 47-51) approaches have been applied more towards liver tissue

engineering. For example, Miller et al. used a rapid casting method to 3D print carbohydrate-glass sacrificial vascular networks encapsulated within different cell laden ECM mimics(49). After cell encapsulation, the carbohydrate-glass layer was dissolved, leaving behind a hollow network, which could be subsequently perfused with vascular cells. *In vitro* results showed that upon successful perfusion, vessel sprouting and lumen formation was evident(49). Furthermore, they demonstrated that primary human hepatocytes were more viable and functional in constructs that incorporated these vascular networks (Figure 1.5). Even though *in vivo* analysis was not performed, this study provides a promising approach for pre vascularizing transplantable tissues. In a more recent study, Zhang et al. used a 3D stamping method to create a multi-layer, vascularizable device, termed an AngioChip(51). Like the previous study, once perfused with endothelial cells, vascular sprouting and lumen formation was present *in vitro*. Furthermore, when hepatocytes were incorporated into the device, they showed increased metabolic function and urea production. To further test their design, the group connected the AngioChip to the femoral vessel of the hind limb of Lewis rats to demonstrate both artery-artery and artery-vein anastomosis (Figure 1.6) (51). Results of the anastomosis indicated that blood perfusion was immediate through the AngioChip and that AngioChip lumen were blood clot free after one week *in vivo(51)*. These results show great promise in the right direction towards successfully incorporating vasculature in biomaterials to improve cell transplantation outcomes.

1.5 Conclusion and Perspectives

As lifestyle related liver diseases continue to rise, even more demand is placed on the already limited available donor organs. This chapter highlights the need to improve current or develop more cell transplantation approaches for liver therapies. Thus far, we have highlighted the most promising cell based approaches that are being explored as a potential to alleviate the demand for donor organs. Common to all these attempts is the need to overcome two major hurdles to functional cell therapy success. They are (i) establishing a reliable cell source and (ii) ensuring effective cell delivery for maintaining *in vivo* function. Biomaterial based approaches have been explored to improve both of these areas. However, despite advances made to improve culture conditions, primary hepatocytes and stem cell derived hepatocytes still have limited expansion potential and can lose liver specific function over time. Therefore, more work is needed to establish a reliable cell source for transplantation. Until then, we focus our attentions on the parallel development of transplantation methods that can be adapted for use with different cell types. Again in this arena biomaterials have contributed to major advancements. In earlier research cell injections were heavily used however there were major issues with engraftment. Using biomaterials served as a vehicle to deliver the cells to their intended target and facilitate engraftment. However, despite these improvements, clinical trial results were still inconsistent. Currently, efforts are being focused on using biomaterials to engineer livers or cell carrying devices for cell transplantation. Here we have highlighted the use of natural ECMs (decellularization of animal livers for subsequent recellularization with human cells) as well as the use of synthetic hybrid ECMs (PEG based encapsulations) for cell transplantation efforts. While some short-term successes

have been demonstrated, there are still some improvements that must be made in order to realize long term success, scaling up and clinical translation. One such improvement is the incorporation or facilitation of vascularization. By vascularizing transplanted devices, we can better ensure that the cells are receiving the adequate nutrients necessary to maintain their proper function. As such, we have also highlighted biomaterial fabrication approaches to incorporate vascularization.

1.6 Acknowledgements

Chapter 1, in full, is a literature review on the topics discussed within this dissertation and is being prepared for submission for publication. "Concise Review: Engineering biomaterial driven liver cell therapies: from *in vitro* culture to transplantation." Seale NM, Varghese S. The dissertation author was the primary author for this section.

1.7 Figures

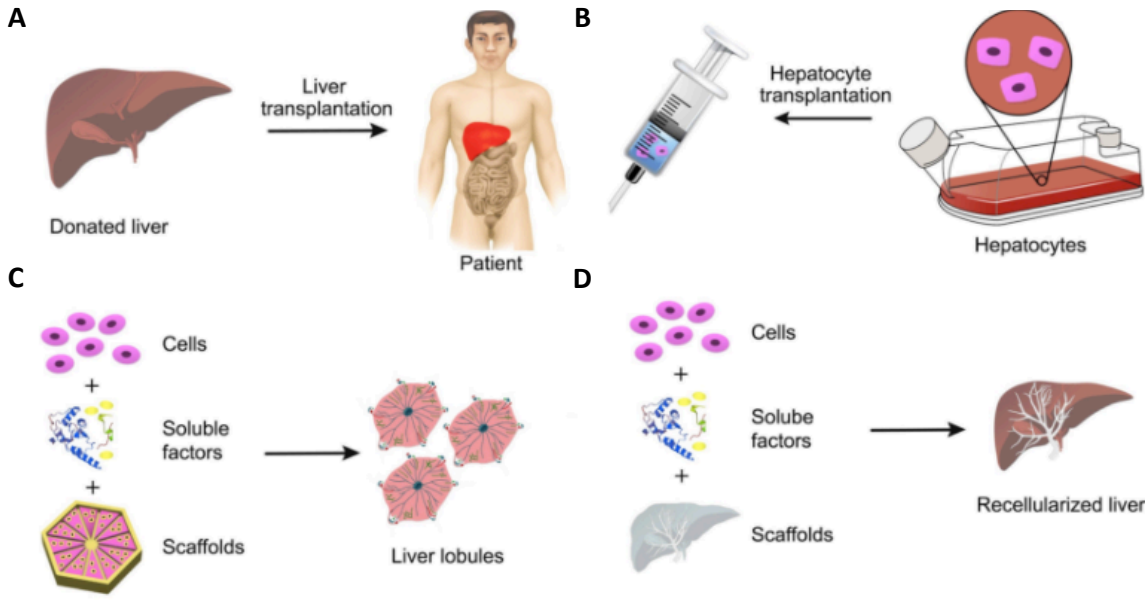

Figure 1. 1: Liver Therapy approaches.

(A) Liver transplantation. (B) Cell transplantation. (C) Bioengineered liver microtissues/organoids. (D) Bioengineered whole liver. Adapted and reprinted from Zhang et al. with permission from Biomaterials(12).

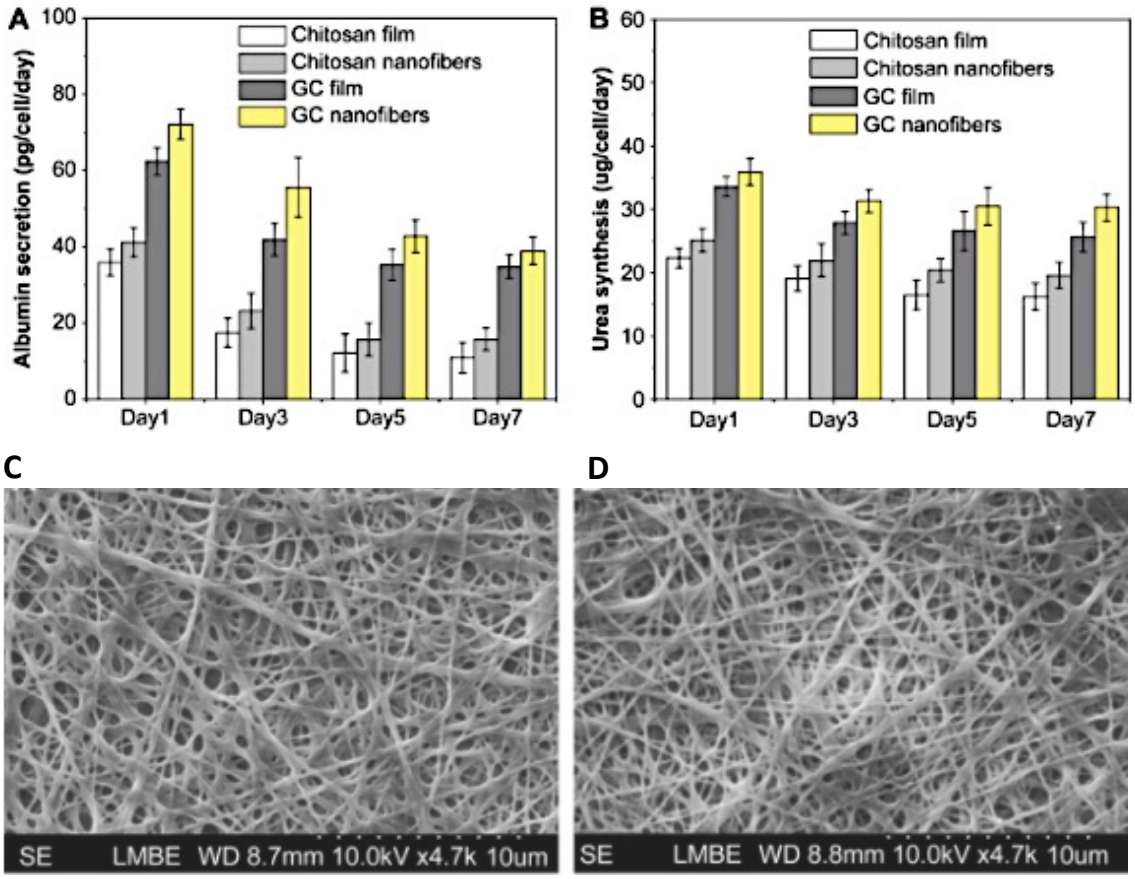

Figure 1. 2: Effect of biomaterial architecture and composition on hepatocyte function

Liver-specific functions of hepatocytes attached on chitosan and GC-based films and nanofibers at various time points during the 7-day culture, including: (A) Albumin secretion; (B) Urea synthesis. SEM images of chitosan nanofibers (C) and GC nanofibers (D) after immersion in PBS solution for 15 days. Adapted and reprinted from Feng et al. with permission from Biomaterials(14).

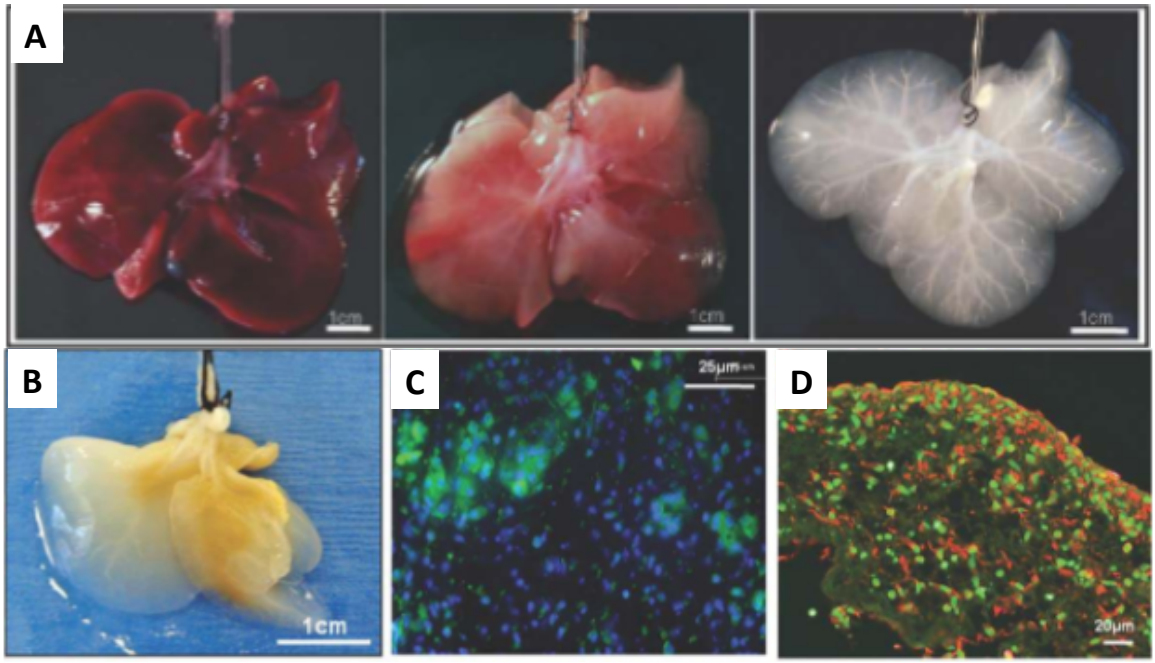

Figure 1. 3: Decellularization and recellularization of a ferret liver
(A) Macroscopic view of a ferret liver at 0, 20, and 120 minutes of the decellularization process. (B) Macroscopic appearance of a right lobe of a ferret liver bioscaffold 7 days after seeding with hFLCs and HUVECS. (C & D) Immunofluorescence staining P450 CYP2A (green) and P450 CYP3A (red), respectively, reveal hFLCs engraftment throughout the liver bioscaffold. Adapted and reprinted from Baptista et al. with permission from Hepatology(39).

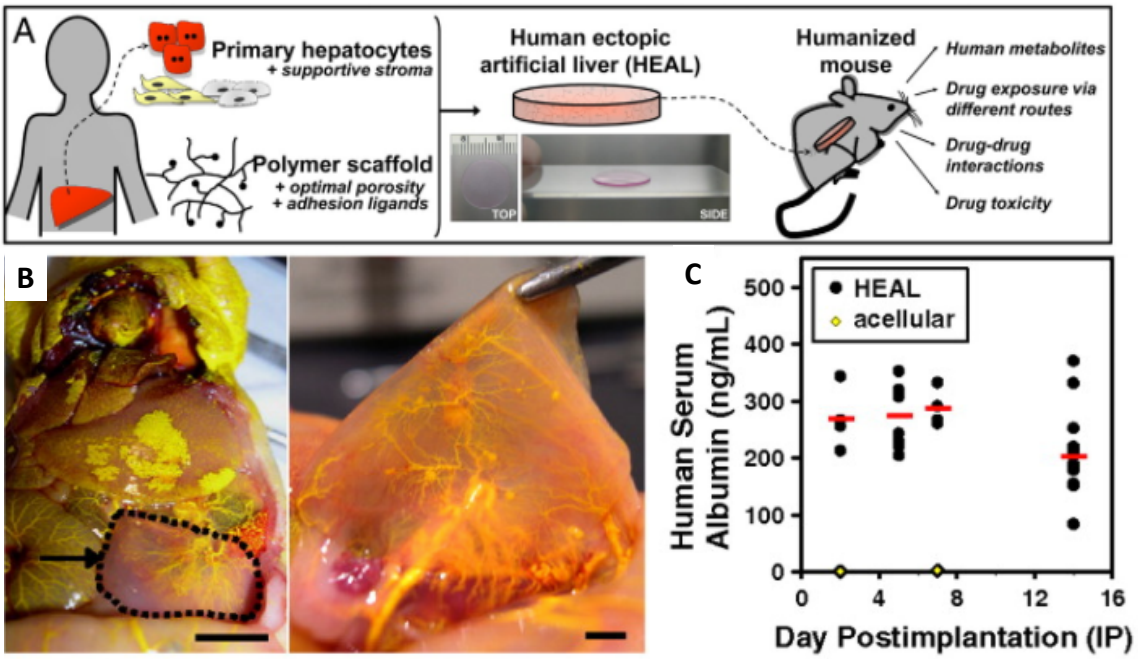

Figure 1. 4: Transplantable Human Ectopic Artificial Liver
(A) Schematic depicting the fabrication, implantation, and utility of HEALs for humanizing mice. Primary hepatocytes are cocultivated with stabilizing stromal fibroblasts on collagen-coated plates, encapsulated with liver endothelial cells in PEG-DA scaffolds derivatized with adhesion peptides. The resulting HEAL is approximately 20-mm diameter and 250-µm thick and comprises ~0.5×10^6 human hepatocytes (inset shows a 10-mm-diameter version from top and side views). After implantation into laboratory mice, engrafted and vascularized HEALs establish humanized models for drug development applications. (B) Mice with HEAL, perfused with yellow Microfil silicone rubber on day 35 after implantation. HEAL is shown pseudooutlined and exposed within peritoneal cavity (arrow; *Left*), and partially dissected (*Right*). (C) Human serum albumin detected in mice humanized with intraperitoneal HEALs. Red bars mark average human serum albumin levels at each timepoint for $n = 6$ to 8 mice. Figure adapted and reprinted from Chen et al. with permission from Proceedings of the National Academy of Sciences of the United States of America(36).

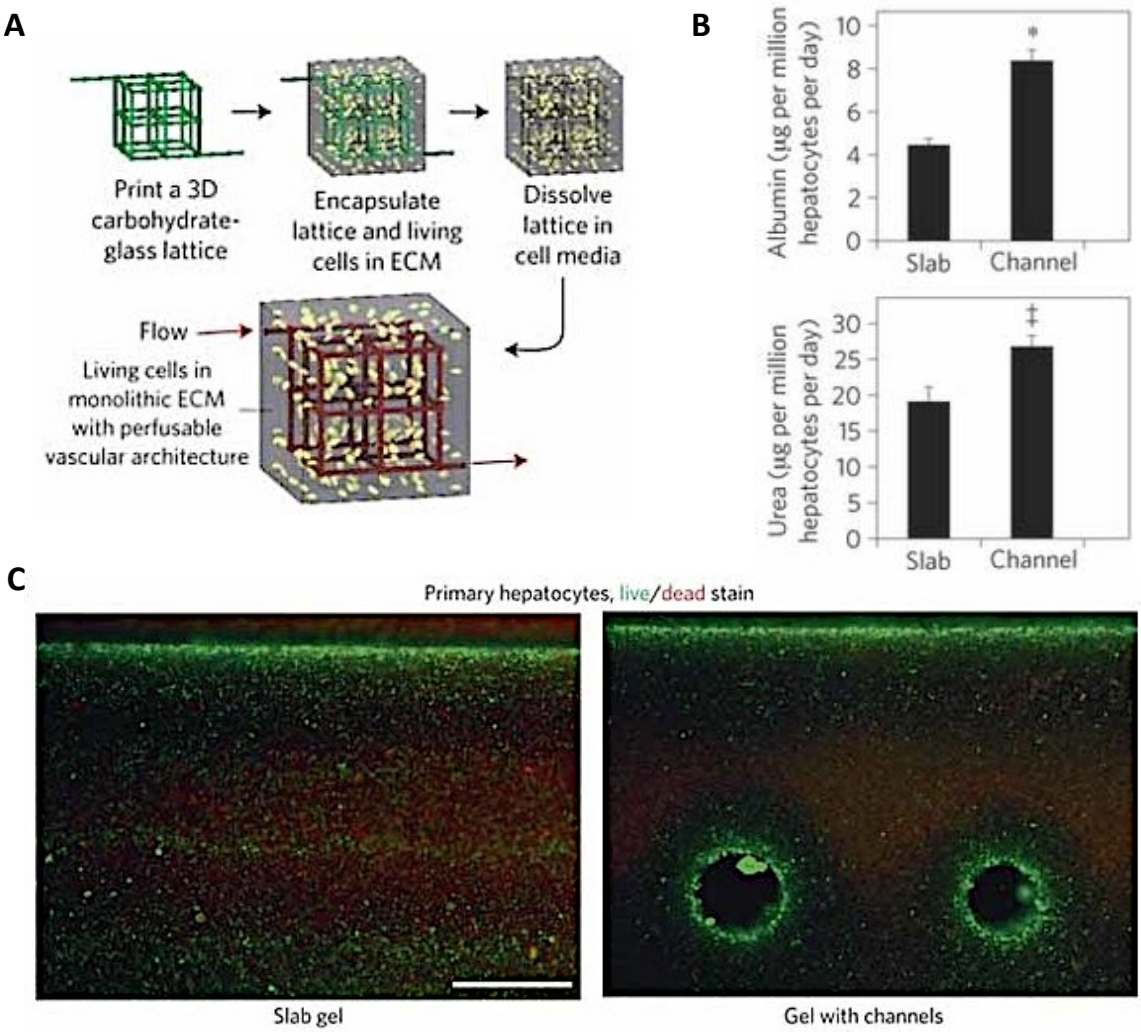

Figure 1. 5: Rapid Casting of patterned vascular networks
(A) Schematic overview of rapid casting sacrificial layer printing and subsequent dissolving. (B) Comparison of the functionality (albumin production and urea synthesis) of engineered constructs with or without vascular channels. (C) Live/dead viability analysis of constructs with or without channels. Scale 1mm. Adapted and reprinted from Miller et al. with permission from Nature Materials(49).

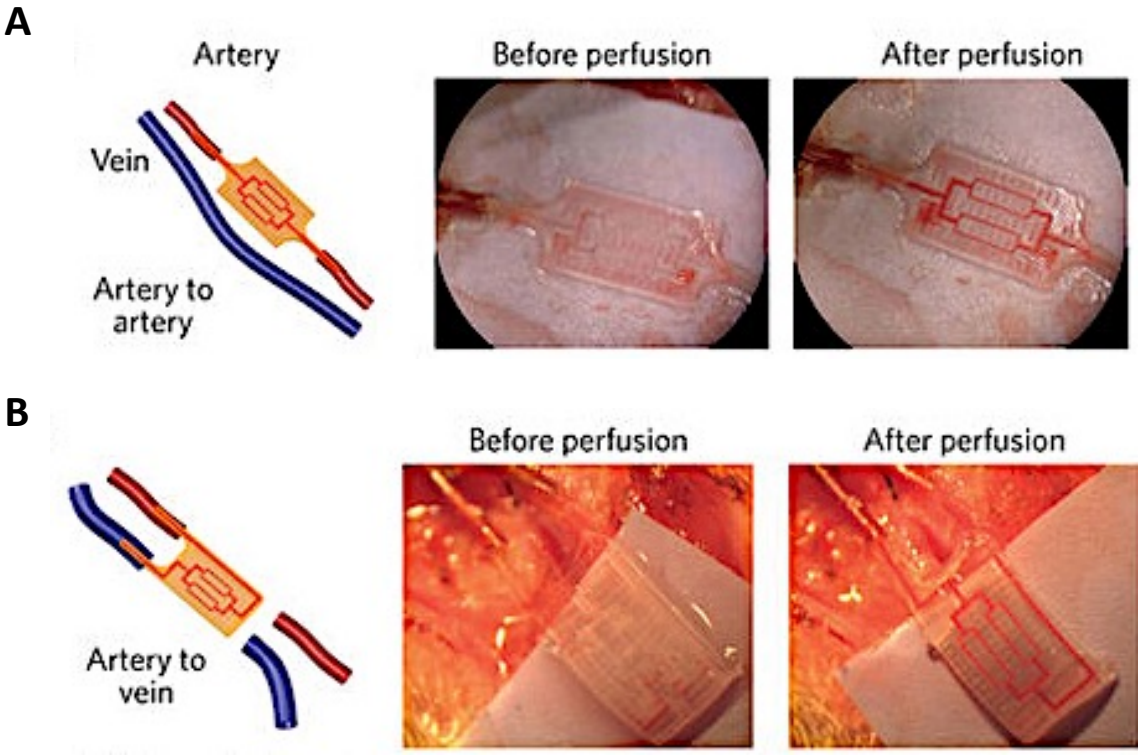

Figure 1. 6: Surgical anastomosis of the AngioChip.
Anastomosis of AngioChip on the rat femoral vessels in the configuration of artery-to-artery graft (A) and artery-to-vein graft (B). Adapted and reprinted from Zhang et al. with permission from Nature Materials(51).

1.8 References

1. Heron MeaDFDfiNVSR, Vol. 57 (Centers for Disease Control and Prevention, Hyattsville, Maryland, 2009).

2. DeMeo DL, Silverman EK. Alpha1-antitrypsin deficiency. 2: genetic aspects of alpha(1)-antitrypsin deficiency: phenotypes and genetic modifiers of emphysema risk. Thorax. 2004;59(3):259-64.

3. Williams R. Global challenges in liver disease. Hepatology (Baltimore, Md). 2006;44(3):521-6.

4. Mandayam S, Jamal MM, Morgan TR. Epidemiology of alcoholic liver disease. Seminars in liver disease. 2004;24(3):217-32.

5. Schramm C, Bubenheim M, Adam R, Karam V, Buckels J, O'Grady JG, Jamieson N, Pollard S, Neuhaus P, Manns MM, Porte R, Castaing D, Paul A, Traynor O, Garden J, Friman S, Ericzon BG, Fischer L, Vitko S, Krawczyk M, Metselaar HJ, Foss A, Kilic M, Rolles K, Burra P, Rogiers X, Lohse AW. Primary liver transplantation for autoimmune hepatitis: a comparative analysis of the European Liver Transplant Registry. Liver Transpl. 2010;16(4):461-9.

6. Nicolas CT, Hickey RD, Chen HS, Mao SA, Lopera Higuita M, Wang Y, Nyberg SL. Concise Review: Liver Regenerative Medicine: From Hepatocyte Transplantation to Bioartificial Livers and Bioengineered Grafts. STEM CELLS. 2017;35(1):42-50.

7. Seale NM, Varghese S. Biomaterials for pluripotent stem cell engineering: from fate determination to vascularization. Journal of Materials Chemistry B. 2016;4(20):3454-63.

8. Seale NM, Varghese S. Biomaterials for pluripotent stem cell engineering: from fate determination to vascularization. Journal of Materials Chemistry B. 2016.

9. Guguen-Guillouzo C, Guillouzo A. General Review on In Vitro Hepatocyte Models and Their Applications. In: Maurel P, editor. Hepatocytes: Methods and Protocols. Totowa, NJ: Humana Press; 2010. p. 1-40.

10. Waring JF, Ciurlionis R, Jolly RA, Heindel M, Gagne G, Fagerland JA, Ulrich RG. Isolated human hepatocytes in culture display markedly different gene expression patterns depending on attachment status. Toxicology in Vitro. 2003;17(5):693-701.

11. Tuschl G, Mueller SO. Effects of cell culture conditions on primary rat hepatocytes-cell morphology and differential gene expression. Toxicology. 2006;218(2-3):205-15.

12. Zhang J, Zhao X, Liang L, Li J, Demirci U, Wang S. A decade of progress in liver

regenerative medicine. Biomaterials. 2018;157:161-76.

13. Mehta G, Williams CM, Alvarez L, Lesniewski M, Kamm RD, Griffith LG. Synergistic effects of tethered growth factors and adhesion ligands on DNA synthesis and function of primary hepatocytes cultured on soft synthetic hydrogels. Biomaterials. 2010;31(17):4657-71.

14. Feng Z-Q, Chu X, Huang N-P, Wang T, Wang Y, Shi X, Ding Y, Gu Z-Z. The effect of nanofibrous galactosylated chitosan scaffolds on the formation of rat primary hepatocyte aggregates and the maintenance of liver function. Biomaterials. 2009;30(14):2753-63.

15. Nicolas CT, Wang Y, Nyberg SL. Cell therapy in chronic liver disease. Current opinion in gastroenterology. 2016;32(3):189-94.

16. Schepers A, Li C, Chhabra A, Seney BT, Bhatia S. Engineering a perfusable 3D human liver platform from iPS cells. Lab on a chip. 2016;16(14):2644-53.

17. Si-Tayeb K, Noto FK, Nagaoka M, Li J, Battle MA, Duris C, North PE, Dalton S, Duncan SA. Highly efficient generation of human hepatocyte-like cells from induced pluripotent stem cells. Hepatology (Baltimore, Md). 2010;51(1):297-305.

18. Song Z, Cai J, Liu Y, Zhao D, Yong J, Duo S, Song X, Guo Y, Zhao Y, Qin H, Yin X, Wu C, Che J, Lu S, Ding M, Deng H. Efficient generation of hepatocyte-like cells from human induced pluripotent stem cells. Cell Res. 2009;19(11):1233-42.

19. Ma X, Duan Y, Tschudy-Seney B, Roll G, Behbahan IS, Ahuja TP, Tolstikov V, Wang C, McGee J, Khoobyari S, Nolta JA, Willenbring H, Zern MA. Highly efficient differentiation of functional hepatocytes from human induced pluripotent stem cells. Stem cells translational medicine. 2013;2(6):409-19.

20. Inoue H, Nagata N, Kurokawa H, Yamanaka S. iPS cells: a game changer for future medicine. Embo j. 2014;33(5):409-17.

21. Lau TT, Ho LW, Wang D-A. Hepatogenesis of murine induced pluripotent stem cells in 3D micro-cavitary hydrogel system for liver regeneration. Biomaterials. 2013;34(28):6659-69.

22. Du C, Narayanan K, Leong MF, Wan ACA. Induced pluripotent stem cell-derived hepatocytes and endothelial cells in multi-component hydrogel fibers for liver tissue engineering. Biomaterials. 2014;35(23):6006-14.

23. Solanas E, Pla-Palacín I, Sainz-Arnal P, Almeida M, Lue A, Serrano T, Baptista PM. Tissue Organoids: Liver. In: Soker S, Skardal A, editors. Tumor Organoids. Cham: Springer International Publishing; 2018. p. 17-33.

24. Heidariyan Z, Ghanian MH, Ashjari M, Farzaneh Z, Najarasl M, Rezaei Larijani

M, Piryaei A, Vosough M, Baharvand H. Efficient and cost-effective generation of hepatocyte-like cells through microparticle-mediated delivery of growth factors in a 3D culture of human pluripotent stem cells. Biomaterials. 2018;159:174-88.

25. Schwartz RE, Fleming HE, Khetani SR, Bhatia SN. Pluripotent stem cell-derived hepatocyte-like cells. Biotechnology advances. 2014;32(2):504-13.

26. Shan J, Schwartz RE, Ross NT, Logan DJ, Thomas D, Duncan SA, North TE, Goessling W, Carpenter AE, Bhatia SN. Identification of small molecules for human hepatocyte expansion and iPS differentiation. Nature chemical biology. 2013;9(8):514-20.

27. Gieseck RL, 3rd, Hannan NR, Bort R, Hanley NA, Drake RA, Cameron GW, Wynn TA, Vallier L. Maturation of induced pluripotent stem cell derived hepatocytes by 3D-culture. PLoS One. 2014;9(1):e86372.

28. Berger DR, Ware BR, Davidson MD, Allsup SR, Khetani SR. Enhancing the functional maturity of induced pluripotent stem cell-derived human hepatocytes by controlled presentation of cell-cell interactions in vitro. Hepatology (Baltimore, Md). 2015;61(4):1370-81.

29. Takayama K, Kawabata K, Nagamoto Y, Kishimoto K, Tashiro K, Sakurai F, Tachibana M, Kanda K, Hayakawa T, Furue MK, Mizuguchi H. 3D spheroid culture of hESC/hiPSC-derived hepatocyte-like cells for drug toxicity testing. Biomaterials. 2013;34(7):1781-9.

30. Ware BR, Berger DR, Khetani SR. Prediction of Drug-Induced Liver Injury in Micropatterned Co-cultures Containing iPSC-Derived Human Hepatocytes. Toxicological sciences : an official journal of the Society of Toxicology. 2015;145(2):252-62.

31. Ohashi K, Yokoyama T, Yamato M, Kuge H, Kanehiro H, Tsutsumi M, Amanuma T, Iwata H, Yang J, Okano T, Nakajima Y. Engineering functional two- and three-dimensional liver systems in vivo using hepatic tissue sheets. Nat Med. 2007;13(7):880-5.

32. Ji R, Zhang N, You N, Li Q, Liu W, Jiang N, Liu J, Zhang H, Wang D, Tao K, Dou K. The differentiation of MSCs into functional hepatocyte-like cells in a liver biomatrix scaffold and their transplantation into liver-fibrotic mice. Biomaterials. 2012;33(35):8995-9008.

33. Kyung-Mee P, Hany HK, Seok-Ho H, Cheol A, Se-Ran Y, Sung-Min P, Oh-Kyeong K, Byeong-Moo K, Heung-Myong W. Decellularized Liver Extracellular Matrix as Promising Tools for Transplantable Bioengineered Liver Promotes Hepatic Lineage Commitments of Induced Pluripotent Stem Cells. Tissue Engineering Part A. 2016;22(5-6):449-60.

34. Mazza G, Rombouts K, Rennie Hall A, Urbani L, Vinh Luong T, Al-Akkad W, Longato L, Brown D, Maghsoudlou P, Dhillon AP, Fuller B, Davidson B, Moore K, Dhar D, De Coppi P, Malago M, Pinzani M. Decellularized human liver as a natural 3D-scaffold for liver bioengineering and transplantation. Scientific reports. 2015;5:13079.

35. Turner RA, Wauthier E, Lozoya O, McClelland R, Bowsher JE, Barbier C, Prestwich G, Hsu E, Gerber DA, Reid LM. Successful transplantation of human hepatic stem cells with restricted localization to liver using hyaluronan grafts†. Hepatology (Baltimore, Md). 2013;57(2):775-84.

36. Chen AA, Thomas DK, Ong LL, Schwartz RE, Golub TR, Bhatia SN. Humanized mice with ectopic artificial liver tissues. Proceedings of the National Academy of Sciences. 2011;108(29):11842-7.

37. Uygun BE, Soto-Gutierrez A, Yagi H, Izamis ML, Guzzardi MA, Shulman C, Milwid J, Kobayashi N, Tilles A, Berthiaume F, Hertl M, Nahmias Y, Yarmush ML, Uygun K. Organ reengineering through development of a transplantable recellularized liver graft using decellularized liver matrix. Nat Med. 2010;16(7):814-20.

38. Barakat O, Abbasi S, Rodriguez G, Rios J, Wood RP, Ozaki C, Holley LS, Gauthier PK. Use of decellularized porcine liver for engineering humanized liver organ. The Journal of surgical research. 2012;173(1):e11-25.

39. Baptista PM, Siddiqui MM, Lozier G, Rodriguez SR, Atala A, Soker S. The use of whole organ decellularization for the generation of a vascularized liver organoid. Hepatology (Baltimore, Md). 2011;53(2):604-17.

40. Leyh RG, Wilhelmi M, Walles T, Kallenbach K, Rebe P, Oberbeck A, Herden T, Haverich A, Mertsching H. Acellularized porcine heart valve scaffolds for heart valve tissue engineering and the risk of cross-species transmission of porcine endogenous retrovirus. J Thorac Cardiovasc Surg. 2003;126(4):1000-4.

41. Ko IK, Peng L, Peloso A, Smith CJ, Dhal A, Deegan DB, Zimmerman C, Clouse C, Zhao W, Shupe TD, Soker S, Yoo JJ, Atala A. Bioengineered transplantable porcine livers with re-endothelialized vasculature. Biomaterials. 2015;40:72-9.

42. Prestwich GD. Hyaluronic acid-based clinical biomaterials derived for cell and molecule delivery in regenerative medicine. Journal of controlled release : official journal of the Controlled Release Society. 2011;155(2):193-9.

43. Miller JS. The Billion Cell Construct: Will Three-Dimensional Printing Get Us There? PLoS Biology. 2014;12(6):e1001882.

44. Druecke D, Langer S, Lamme E, Pieper J, Ugarkovic M, Steinau HU, Homann HH. Neovascularization of poly(ether ester) block-copolymer scaffolds in vivo: long-term investigations using intravital fluorescent microscopy. Journal of biomedical

materials research Part A. 2004;68(1):10-8.

45. Phadke A, Hwang Y, Kim SH, Kim SH, Yamaguchi T, Masuda K, Varghese S. Effect of scaffold microarchitecture on osteogenic differentiation of human mesenchymal stem cells. European cells & materials. 2013;25:114-28; discussion 28-9.

46. Shih Y-R, Kang H, Rao V, Chiu Y-J, Kwon SK, Varghese S. In vivo engineering of bone tissues with hematopoietic functions and mixed chimerism. Proceedings of the National Academy of Sciences. 2017;114(21):5419-24.

47. Chaturvedi RR, Stevens KR, Solorzano RD, Schwartz RE, Eyckmans J, Baranski JD, Stapleton SC, Bhatia SN, Chen CS. Patterning vascular networks in vivo for tissue engineering applications. Tissue engineering Part C, Methods. 2015;21(5):509-17.

48. Culver JC, Hoffmann JC, Poché RA, Slater JH, West JL, Dickinson ME. Three-Dimensional Biomimetic Patterning in Hydrogels to Guide Cellular Organization. Advanced Materials. 2012;24(17):2344-8.

49. Miller JS, Stevens KR, Yang MT, Baker BM, Nguyen D-HT, Cohen DM, Toro E, Chen AA, Galie PA, Yu X, Chaturvedi R, Bhatia SN, Chen CS. Rapid casting of patterned vascular networks for perfusable engineered three-dimensional tissues. Nat Mater. 2012;11(9):768-74.

50. Kolesky DB, Truby RL, Gladman AS, Busbee TA, Homan KA, Lewis JA. 3D Bioprinting of Vascularized, Heterogeneous Cell-Laden Tissue Constructs. Advanced Materials. 2014;26(19):3124-30.

51. Zhang B, Montgomery M, Chamberlain MD, Ogawa S, Korolj A, Pahnke A, Wells Laura A, Massé S, Kim J, Reis L, Momen A, Nunes Sara S, Wheeler AR, Nanthakumar K, Keller G, Sefton Michael V, Radisic M. Biodegradable scaffold with built-in vasculature for organ-on-a-chip engineering and direct surgical anastomosis. Nature Materials. 2016;15:669.

Chapter 2: Macroporous dual compartment hydrogels for minimally invasive transplantation of primary human hepatocytes.

2.1 Abstract

Background:

Given the shortage of available organs for whole or partial liver transplantation, hepatocyte cell transplantation has long been considered a potential strategy to treat patients suffering from various liver diseases. Some of the earliest approaches attempted to deliver hepatocytes via portal vein or spleen with little success due to poor engraftment. More recent efforts include transplantation of cell sheets or thin hepatocyte laden synthetic hydrogels. However, these implants must remain sufficiently thin to ensure that nutrients in surface vasculature can diffuse into the implant.

Methods:

To circumvent these limitations, we investigated the use of a vascularizable dual compartment hydrogel system for minimally invasive transplantation of primary human hepatocytes. The dual compartment system features a macroporous outer Polyethylene glycol diacrylate/ Hyaluronic acid Methacrylate hydrogel compartment for seeding supportive cells and facilitating host cell infiltration and vascularization. It is also contains an inner core that houses the primary human hepatocytes.

Results:

We show that the subcutaneous implantation of these devices in NOD/SCID mice facilitated host cell recruitment and vascular formation. Furthermore, presence of human serum albumin in peripheral blood and immunostaining of excised implants indicated that

the hepatocytes maintained function *in vivo* for at least one month, the longest assayed time point.

Conclusion:

Such cell transplantation devices that assist the anastomosis of implants with the host can be potentially used as a minimally invasive ectopic liver accessory to augment liver specific functions as well as potentially treat various pathologies associated with compromised functions of liver such as hemophilia B or alpha-1 antitrypsin deficiency.

Key Words Primary hepatocyte transplantation; dual-compartment hydrogels; hepatic tissue engineering; subcutaneous implantation; vascularization

2.2 Introduction

Approximately 30 million people in the United State have some form of liver disease (1). Because the only approved cure for end-stage liver disease or acute liver failure is whole or partial organ transplantation, there remains a significant demand on transplantable donor organs(2). This lack of available organs has led to approximately 27,000 deaths annually in the United States alone (1, 3). A number of strategies, ranging from cell(4-8) to engineered liver tissue transplantation, are currently under investigation to help alleviate the demand for donor organs (9-13).

Regardless of the approach, the success of any cell therapy hinges on the long-term survival and function of the transplanted cells. Ectopic transplantation of single and multi-layer sheets of hepatocytes has shown some success in maintaining liver tissue function(14). However, given space constraints, to reasonably scale up this technique,

sheets would have to be stacked. This will inevitably result in the diffusion barrier being breeched, thus necessitating the incorporation of vasculature. Another approach has been to use biomaterials as scaffolds to engineer 3D liver tissues (15). However, for these to function, the implants must be sufficiently thin. Furthermore, studies have shown that such implants function better when placed in a heavily vascularized area(15, 16), which usually requires an invasive surgery.

In an effort to improve the efficacy and function of the engineered tissues, de-cellularized liver organs have been employed as scaffolds(17, 18). De-cellularized livers can provide the structural and biochemical cues necessary to maintain viability and function of primary hepatocytes (19, 20). Furthermore, if used as intact structures, they provide an existing architecture that facilitates vascularization and provides liver specific geometrical cues. In this approach, due to the existing shortage of human organs, porcine or other xenogeneic livers have to be used. It is necessary to ensure proper decellularization to preserve the extracellular matrix (ECM) while ensuring the destruction of xenogeneic deoxyribonucleic acid (DNA). While low DNA content (under 50 ng double stranded DNA per mg ECM) may not have triggered an immune response in tested animals, it can still carry the risk of immune rejection in humans (21, 22).

Bioengineered devices that can facilitate vascularization of the implant while supporting the viability and function of transplanted cells could be a potential solution to improve the outcome of cell transplantation(23). Enabling vascularization of the implant will allow the implant size to be scaled and a large number of cells to be housed within the device, which is necessary to improve the therapeutic outcome. In this study, we describe the use of a dual compartment device for minimally invasive hepatocyte

transplantation. Recently we used such an approach successfully to support bone marrow transplantation (24). Building upon this dual compartment concept, we optimized the biomaterial composition and dimensions to develop constructs with higher cell carrying capacity, capable of maintaining long-term hepatocyte function and promoting vascularization. The dual compartment system consists of an outer interconnected, macroporous solid structure to promote vascularization and/or to house supporting cells and a hollow inner compartment to load the donor cells. When implanted subcutaneously in mice, the hepatocyte-loaded dual compartment device supported cells' viability and sustained function of transplanted primary human hepatocytes (from two different donors) for at least one month (the longest experimental time investigated).

2.3 Materials and Methods

2.3.1 Polyethylene glycol diacrylate (PEGDA) synthesis

PEGDA (Mn=10kDA) oligomer was prepared according to a previously reported method (25). Briefly, 18.0 g of PEG was dissolved in 300 mL of toluene in a 500 mL round bottomed flask in an oil bath heated at 125 °C. The solution was refluxed for 4 h with vigorous stirring. Traces of water in the reaction mixture were removed by azeotropic distillation. Upon cooling the solution to room temperature, 3.262 g (32.2 mmol, 4.493 mL) of triethylamine was added to it with vigorous stirring. Then the flask was moved to an ice bath and stirred for 30 min. 2.918 g (32.2 mmol, 2.452 mL) of acryloyl chloride in 15 mL of anhydrous dichloromethane was then added to the reaction mixture dropwise over 30 min. After keeping the reaction mixture in the ice bath for another 30 min, the flask was heated to 45°C overnight. The reaction mixture was then

cooled to room temperature and the quaternary ammonium salt was removed from the reaction mixture by filtration. The filtrate was condensed using a rotary evaporator and then precipitated in excess diethyl ether. The white precipitate was collected by filtration and vacuum dried at 40 °C for 24 h. The resultant PEGDA oligomer was purified by precipitation followed by column chromatography and dialysis prior to its usage. The purified PEGDA was lyophilized and stored at -20°C.

2.3.2 Hyaluronic acid Methacrylate (HAMA) synthesis

Sodium Hyaluronate (Lifecore Biomedical), Research Grade, 41KDa-65KDa Mw (500 mg) was dissolved in DI water (25 mL). Methacrylate (MA) anhydride (8 mL) was added into the HA solution (drop-by-drop manner), pH was adjusted to 8 and the reaction was carried out at 4°C for 24 hrs. pH was checked frequently and adjusted to 8 as needed. After 24 hrs the resulting mixture was purified using membrane dialysis (3.5-5 kDa) against Milli-Q water for 3 days. After dialysis the mixture was lyophilized.

2.3.3 Porous scaffold formation

The porous scaffolds (either PEGDA alone or PEGDA/HAMA copolymer) were made by the leaching of polymethyl methacrylate (PMMA) beads to create the macroporous structure(26). Briefly, 160 μm PMMA beads were packed in a 10mm diameter by 3mm height mold. 80 μl of 20% acetone solution (in ethanol) was added to the PMMA filled mold before it was placed in a 37°C oven for 10 min. To this PMMA filled mold a PEGDA/HAMA solution (10%/5% w/v mixture in PBS) or a 10% PEGDA (w/v mixture in PBS) containing 0.005% (w/v) Irgacure (*i.e*. a photoinitiator) was added

and UV polymerized for 10 min. Acetone was used to dissolve the PMMA beads to create the macroporous PEGDA/HAMA copolymer hydrogel (Figure 2.1A). The structure was sterilized using multiple ethanol washes, followed by multiple PBS washes.

2.3.4 Dual compartment assembly

A 7 mm punch was used to cut out the center of the porous gels to leave a hollow ring. The 7 mm inner portion that was removed was sliced to make caps for the hollow ring. Both the hollow rings and the caps were sterilized with ethanol then washed multiple times with PBS. Under sterile conditions, the ring and the caps were dried to remove PBS from the pores. Then, supporting cells (some combination of HUVECS, hMSCs or MEFs) were loaded into the pores of the rings and the caps. The primary human hepatocytes were thawed in thawing media (MCHT50; Lonza) and centrifuged for 10 minutes at 100 g. Next, fibrinogen (8 mg/ml) and thrombin (2 U/ml) were added to the cell pellet. Fibrin was allowed to form at 37 °C and the system was maintained at this temperature for up to 30 min. to complete the reaction. Once the gel was formed it was placed into the inner cored out compartment of the porous gel (now consisting of the hollow ring and the bottom cap). The top cap is then placed to seal the dual compartment system. This resulted in a fibrin cell-laden gel inner compartment, encased by a macroporous gel outer compartment (Figure 2.1 B and C). Fibrin was then used around the caps as an added precaution to seal them in place. Each device was loaded with approximately 5 million hepatocytes (or 5-20 million when testing loading capacity) and approximately $5x10^5$ supporting cells. Human Umbilical Vein Endothelial Cells (HUVECS), Human Bone Marrow Stromal Cells (hMSCs) and Mouse embryonic

Fibroblasts (MEFs) were used either alone ($5x10^5$ HUVECS) or in combination ($2.5x10^5$ HUVECS plus $2.5x10^5$ hMSCS or MEFs) as supporting cells. In order to determine the effect of the scaffold to assist *in vivo* vascularization, acellular PEGDA and PEGDA/HAMA constructs were used.

2.3.5 Swelling Ratio

Dual compartment systems made from PEGDA macroporous hydrogels and PEGDA/HAMA macroporous hydrogels were assembled as described above, however, without the inner fibrin compartment. Gels were flash frozen and lyophilized for two days. Then 5 gels for each group were weighed to get the dry weight. Gels were then placed in PBS and weighed periodically over a 48 hour time period to determine the wet weight. The wet weight was divided by the dry weight to get the swelling ratio and swelling kinetics(27).

2.3.6 Scanning Electron Microscopy

The microstructure of the PEGDA/HAMA hydrogels was examined using a scanning electron microscope (SEM). Briefly, samples were thinly sectioned, flash frozen, and lyophilized for two days. Then using a sputter coater (Emitech, K575X), Iridium was coated onto samples for 7 s. The iridium-coated samples were imaged using SEM (Phillips XL30 ESEM). The diameter of interconnected pores was measured using ImageJ from 10 pores selected from each of three different SEM and bright-field images, respectively, and presented as mean ± standard deviation ($n = 30$).

2.3.7 Cell Culture

Primary human hepatocytes from two different donors (Donor 1, HUM4100 and Donor 2 HUM4113) were acquired from LONZA (formerly TRL). The cells were thawed in thawing media (MCHT50, LONZA) and immediately encapsulated into fibrin gel and loaded into scaffolds. The cells encapsulated in fibrin gel were loaded as described above. The cell-laden dual compartment scaffolds were cultured in 4 parts maintenance media (MM250, LONZA) and 1 part HUVEC media (components described below).

Human Umbilical Vein Endothelial Cells (HUVECs) were obtained from ATCC and cultured in HUVEC medium (HM) containing 79% M199 medium (Gibco), 10% FBS (Gibco), 10% endothelial cell growth medium (Cell Application, Inc.), and 1% penicillin/streptomycin (Gibco). HUVECs used in this study were limited to cells between passages 3 and 5.

Mouse embryonic Fibroblasts (MEFs) were cultured in growth medium (GM), composed of Dulbecco's Modified Eagle's high glucose medium (Hyclone) supplemented with 10% fetal bovine serum (FBS, Gibco) and 1% penicillin/streptomycin (Gibco). The cells were grown on 0.1% (w/v) Gelatin coated dishes to 70% confluency.

Human Bone Marrow Stromal Cells (hMSCs) were acquired from the Institute for Regenerative Medicine, Texas A&M University (Donor 8013L). Cells were cultured in GM composed of Dulbecco's Modified Eagle's high glucose medium (Hyclone) supplemented with 16.5% fetal bovine serum (FBS, Gibco) and 1% penicillin/streptomycin (Gibco). The cells were passaged at 70% confluence and used for experiments at passages 4-5.

2.3.8 Subcutaneous implantation of devices

All animal procedures were approved by the Institutional Animal Care and Use Committee of the University of California, San Diego and performed in accordance with the NIH and national and international guidelines for laboratory animal care. Subcutaneous implantation of the cell-laden dual compartment devices was performed 3 days after assembly and culture *in vitro*. Recipient mice were administered with ketamine (100 mg/kg) and xylazine (10 mg/kg), and the fur on the back was shaved. Mice were then placed on a heating pad and a 1 cm-long incision was made in the back of the mice, and one subcutaneous pouch was inserted by blunt dissection using a 1 cm-wide spatula on the left side of the mouse. The process was repeated on the right side. A total of two devices were implanted per mouse. The skin was sutured once the devices were implanted. After the surgery, mice were housed in separated cages.

2.3.9 Albumin measurement

Sandwich enzyme linked immunosorbent assay (ELISA) was performed to assess the albumin production of the implanted cells as a function of time (over 28 days). In short, once a week, blood was collected from the mice via the tail vein using heparinized capillary tubes. The blood was then centrifuged at 14900 g at 4 Degrees Celsius (°C) for 15 min. to separate and extract the serum. The serum was assessed for human albumin by using the Human Albumin ELISA Quantitation Set (Bethyl Labs, Catalogue no. E80-129) according to the manufacturer's protocol.

2.3.10 Vessel quantification

Acellular implants were placed in mice for 3, 7, 14 and 28 days to assess cell infiltration and vascularization over time. At each time point the implants were retrieved and washed with PBS. Then gross images were taken of the implant before fixing for immunostaining. Then number of visible vessels at the top and bottom of the implant that contained blood were counted and divided by the total surface area.

2.3.11 Immunofluorescent staining

Post implantation constructs were retrieved, washed with PBS, then fixed with 4% paraformaldehyde (PFA, Sigma Aldrich) at 4 °C overnight. Samples were then incubated in OCT (Tissue-Tek® O.C.T. Compound; Sakura, Torrance, CA) at 4 °C overnight on a rocker. Samples were transferred to a mold and frozen with 2-methylbutane and liquid nitrogen, and stored at -80°C until sectioning. For cryo-sectioning, frozen tissue blocks were sectioned with a cryotome cryostat (at -20 °C) to 20-µm thicknesses. For immunofluorescent staining, sections were treated with 20 µg/mL proteinase K, permeabilized with 0.5% Triton X-100 [4 min, room temperature (RT)], treated with $NABH_4$ (30 min, RT), blocked with 3% (w/v) bovine serum albumin (BSA; 60 min, RT) in PBS. Sections were stained for either CD31 (platelet endothelial cell adhesion molecule (PECAM-1); 1:100; Santa Cruz) or FITC conjugated human albumin (1:100; Bethyl Labs) or CK18 (R&D Systems) overnight at 4 °C. An appropriate secondary antibody Alexa Fluor 488 (1:200; Thermo Fisher) along with Hoechst 33342 (2 µg/mL; Thermo Fisher) was used to bind primary antibodies for 1 h at RT. Then samples were imaged with a fluorescent microscope.

2.3.12 Statistical analysis

All experiments were independently repeated at least twice with replicate samples as indicated in figure captions. Statistical analysis was performed using one-way ANOVA and Tukey's post hoc test for group comparisons to determine statistical significance ($p < 0.05$). Errors bars represent SEM. GraphPad Prism 5 software was used to determine all statistical analysis.

2.4 Results

2.4.1 Development and characterization of the dual compartment system

The dual compartment device was developed as a cell delivery device to successfully transplant primary human hepatocytes (Figure 2.1A & B). The dual compartment structure consisted of a 3 mm height by 5 mm radius, interconnected macroporous hydrogel (outer compartment), with a 1.5 mm height by 3.5 mm radius hollow interior (inner compartment) for cell loading (Figure 2.1C). Macroporous hydrogels with interconnected pores were fabricated by PMMA templating of PEGDA-co-HAMA crosslinked networks. SEM images were used to verify the presence of an interconnected macroporous network. The SEM images suggest that the gels had both larger pores, which were about 140 microns in diameter, and smaller pores, which were about 85 microns in diameter (Figure 2.2) with an average pore size of 120 microns. We also determined the swelling ratio of the macroporous hydrogels (PEGDA/HAMA and PEGDA) (Figure 2.3). PEGDA/HAMA macroporous hydrogels had a higher swelling

ratio compared to PEGDA alone structures. Similarly, PEGDA/HAMA structures swelled and equilibrated faster compared to PEGDA alone structures.

2.4.2 Porous PEGDA/HAMA facilitates vascular formation

To examine the ability of the macroporous structures to promote vascularization, both PEGDA and PEGDA/HAMA structures were implanted *in vivo* without the presence of any exogenous cells. In addition to the appearance, we used immunofluorescent staining for DAPI (stains nucleus) and CD31 (a vascular marker) to assess host cell infiltration and vascular formation as a function of post-implantation time (3-28 days). Figure 2.5 shows the representative whole-mount images of the excised implants and the staining results. Analyses of the implants after 3 days of implantation showed minimal to no vascularization. While the sections were positive for DAPI staining, indicating that host cells had infiltrated the implant, no positive CD31 was observed. At the next experimental time point, day 7, the presence of vascular structures could be clearly seen in the PEGDA/HAMA constructs. The constructs appeared pink with clearly visible vascular structures filled with blood. The presence of vascular structures was further confirmed by the positive CD31 staining. As the days increased, increased vessel formation (Figure 2.5) as well as more CD31 positive cells was observed (Figure 2.6). By day 14, larger blood vessels filled with blood were observed while multiple smaller vessels filled with blood were seen at day 28. Interestingly, no such vascularization was observed with PEGDA constructs (Figure 2.4). The PEGDA constructs appeared as transparent as before implantation.

2.4.3 Effect of supporting cells on function *in vivo*

Since the supporting cells could play a key role in maintaining hepatocyte function (15, 28), we have compared the effect of i) MEFs plus HUVECs and ii) hMSC plus HUVECs on the functionality of hepatocytes, based on albumin secretions. At one week post-transplantation, both MEFs and hMSCs-supported implants showed similar levels of albumin secretion, which was only slightly higher compared to the HUVECs only group (Figures 2.7 & 2.8). All groups showed significantly higher albumin productions compared to week 1. Amongst the different groups, implants loaded with MEFs or hMSCs produced more albumin than the HUVECs only group. Between the hMSCs and MEFs, the group containing hMSCs produced more albumin than the group containing MEFs. Even though there was no statistically significant difference between the albumin secretions amongst the week 3 hMSCs plus HUVECs group and the MEFs plus HUVECs, all subsequent experiments were carried out using a combination of HUVECs and hMSCs as the supporting cells. In addition to presence of human albumin in the host peripheral blood, we also stained the excised implants and they were positive for human specific albumin (Figure 2.7).

2.4.4 Donor independent function of Dual compartment system *in vivo*

After characterizing and developing the dual compartment system, we wanted to ensure that the device could support cells from multiple donors. To this end, we used the dual compartment systems to transplant cells from two different donors (Table 2.1). The

implant function was assessed for functionality via albumin secretions over a 1-month period post-implantation (Figures 2.9-2.13). Albumin analysis of host serum indicated the presence of human specific albumin in the circulation of the host at day 7 post-implantation. The amount of albumin increased from day 7 to day 15 and remained more or less stable for the rest of the month (Figure 2.10 & 2.11). On day 28 the implants were retrieved and analyzed. The gross picture of both the implants indicated vascular formation (Figure 2.12 & 2.13 column 1). DAPI and albumin staining of the implant (Figure 2.9 and 2.12 & 2.13 column 2) showed that in all implants, the albumin staining was concentrated within the inner compartment. The cells in the inner compartment of the implant were also positive for CK18, another hepatocyte specific marker (Figure 2.12 & 2.13 column 3). The implants were also positive for CD31 staining, which was used to identify vascular cells (Figure 2.12 &2.13 column 4). The staining results corroborated the presence of vascular networks observed earlier by us in the whole-mount images.

2.5 Discussion

This study describes the application of a dual compartment device, containing an outer vascularizable layer and an inner cell-loading compartment, for hepatocyte transplantation. The hollow core structure of the inner compartment enables loading of a large number of cells. At the current dimensions, the inner compartment can be easily loaded with up to 20 million hepatocytes (largest number tested for loading, Supplementary Figure 2). Furthermore, our results demonstrated that the vascularization of the implant in the subcutaneous space supported donor cell function for one month.

The design of the dual compartment system, especially the hydrogel composition and architecture played an integral role in host cell infiltration, and device vascularization. Previously, we have shown that mineralized macroporous hydrogels promote host cell infiltration [24,29]. The findings that the PEGDA macroporous hydrogels were not able to promote vascularization *in vivo* suggest that pore architecture alone is not sufficient to facilitate vascular formation. The addition of HA to the PEGDA allowed cell infiltration and implant vascularization. This could be due to various reasons such as the biological functions of HA and its ability to interact with cell surface receptor CD44[30,31]. Furthermore, the addition of HA could have promoted vascular formation, as studies have shown that HA fragments exhibit pro-angiogenic effects [30,32,33]. While vascularization of the implant enables long-term maintenance of donor cells, the faster swelling-kinetics of the macroporous dual compartment device could be playing an important role in maintaining the viability of the donor cells in the initial days of the implantation (i.e., before the implant was vascularized) through enhanced nutrient transport to the cells. Since these implants are large and thick, to avoid necrotic cores, fast swelling is important to ensure absorption and transport of nutrients throughout the structure.

While the liver has many functions, here we chose to use human serum albumin secretions to characterize the function of the implants. This allowed us to monitor function of the same implant, with minimal interference, over multiple time points. For our proof of concept study, ELISA analysis of albumin secretions for both donors followed the trend of rising after day 7 and then remaining stable for the rest of the

experiment duration. Based on albumin synthesis and secretions, there were no statistically significant differences between the cells from different donors.

Although this proof of concept study used primary hepatocytes, the dual compartment system could be extended towards other cells. The modular assembly of the device allows parallel optimization of the outer and inner compartments to increase overall function of the device. Tuning pore size or material composition to accelerate host cell infiltration and vascularization can optimize the outer compartment. Similarly, the dimensions of the inner compartment could be increased to improve the number of donor cells that can be housed, while maintaining the overall outer dimensions. Increasing the dimensions of the inner compartment without changing the overall dimensions of the device involves decreasing the thickness of the outer compartment, which could improve diffusion of nutrients to the cells in the inner compartments. Further studies are needed to determine the upper cell-loading limit of these devices without compromising their viability or function. It is estimated that a delivery of 1-10 billion functioning cells is needed to achieve therapeutic effects in leu of solid organ transplantation[34]. Even with the vascularization, housing such a large number of cells within a single device could be challenging in its current form. However, since the dimensions of the device can be tuned, it is possible to increase the dimension of the inner compartment to accommodate more cells. If a diffusion limitation is reached leading to death and compromised function of the transplanted cells, then multiple devices can be transplanted. Another key parameter that determines successful cell transplantation is the longevity of the implant. The diminished function of the transplanted cells with time is often thought to be associated with lack of vascularization. Studies have shown that cell transplantation

approaches that incorporated vascularization resulted in improving the viability and function of the transplanted cells. The results described in this study show the viability and function of the transplanted cells for a month. Though the vascularization of the implant suggests the possibility of survival and function of the transplanted cells beyond a month, additional studies involving long-term transplantation are need to assess the potential of the device to support long term viability and function of the transplanted cells. Nonetheless, the dual compartment system described in this study offers a promising tool for cell transplantation. Furthermore, its function can be easily extended for applications in drug screening, personalized medicine and as a platform to screen for key components (e.g., ECM composition, stiffness) of the microenvironment that are necessary to maintain long-term function of donor cells. It can also be used as an *in vivo* experimental tool to study how donor phenotype can affect transplantation success.

2.6 Conclusion

In conclusion, developing successful biomaterial devices for transplantable liver cell therapies requires an approach that can transplant large number of cells and be integrated with the host to facilitate formation of the functional vasculature needed to maintain the viability and function of transplanted cells. To meet these criteria, we have utilized a dual compartment biomaterial device for the transplantation of human primary hepatocytes. This device enabled minimally invasive (subcutaneous implant) cell transplantation and maintained the function of transplanted hepatocytes for at least 1 month. The dual compartment device described here is robust and scalable. Furthermore, the modular assembly of the device can be used as a tool to create and optimize scalable

vascularized 3D liver tissues for extended applications in creating humanized tissue models for investigating disease pathology, drug testing and personalized medicine.

2.7 Acknowledgements

Chapter 2, in full, has been recently accepted for publication in Transplantation. "Dual Compartment Vascularized device for subcutaneous humanized liver transplantation." Seale NM, Shih Y., Ramaswamy S., Verma I., Varghese S. The dissertation author was the primary investigator and author of this paper.

2.8 Figures

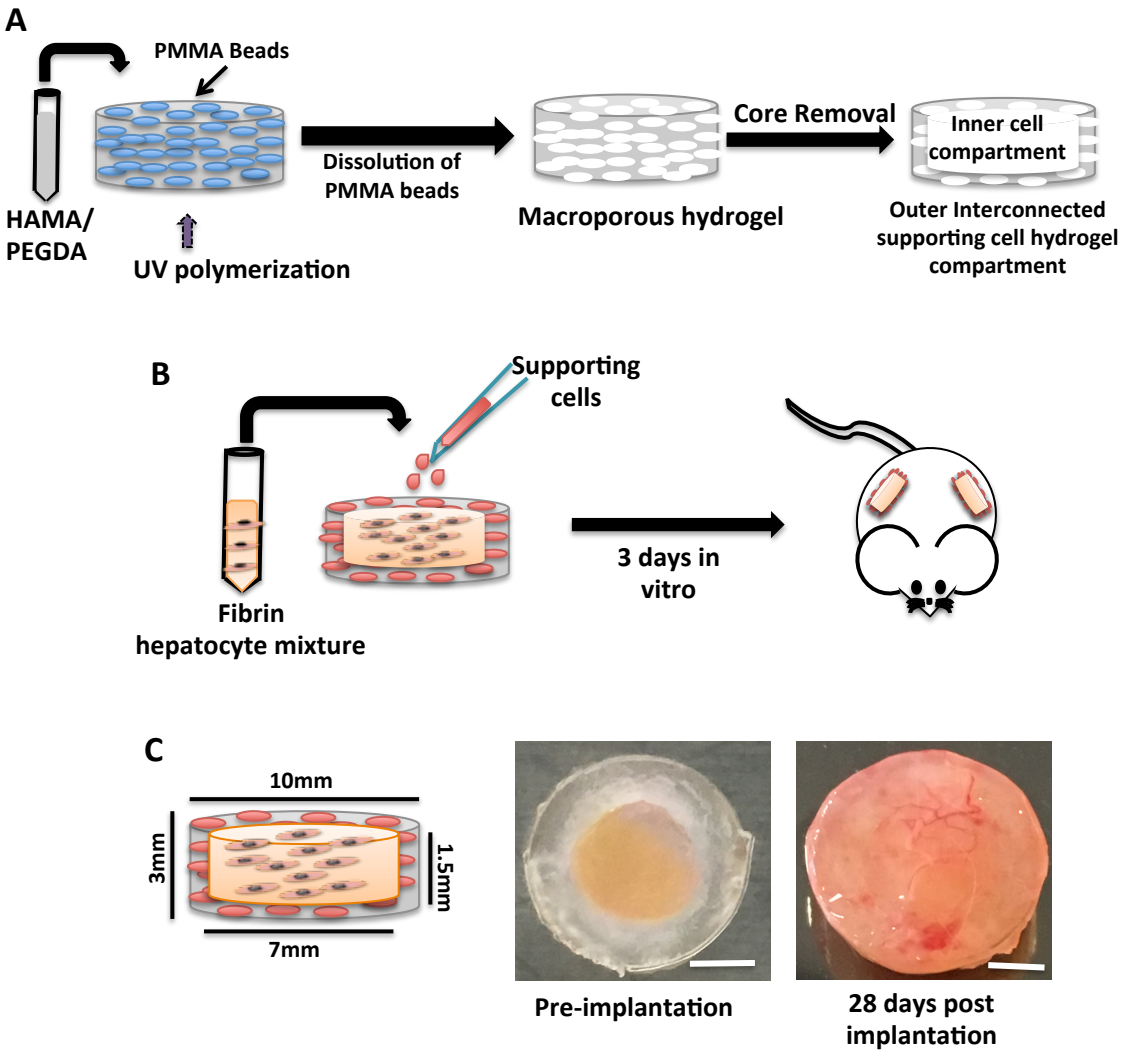

Figure 2. 1: Fabrication of dual compartment device.
A: Creating PEGDA/HAMA outer porous compartment via acetone leeching of PMMA beads. B: Assembly of the dual compartment device. Primary hepatocytes encapsulated in fibrin are loaded into the inner compartment, while supporting cells are seeded into the outer compartment. After 3 days in vitro structures are subcutaneously implanted in NOD/SCID mice. C: Dimensions of the dual compartment device. Gross structure of the device before and 28 days after implantation. Scale 0.25 cm.

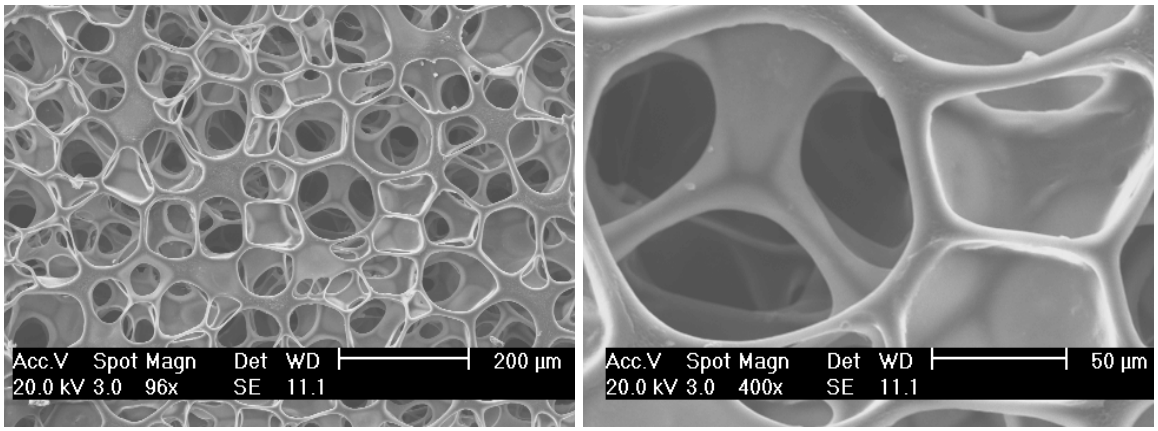

Figure 2. 2: Material Porous network Characterization.
SEM images of porous network in the PEGDA/HAMA outer compartment at two different magnifications.

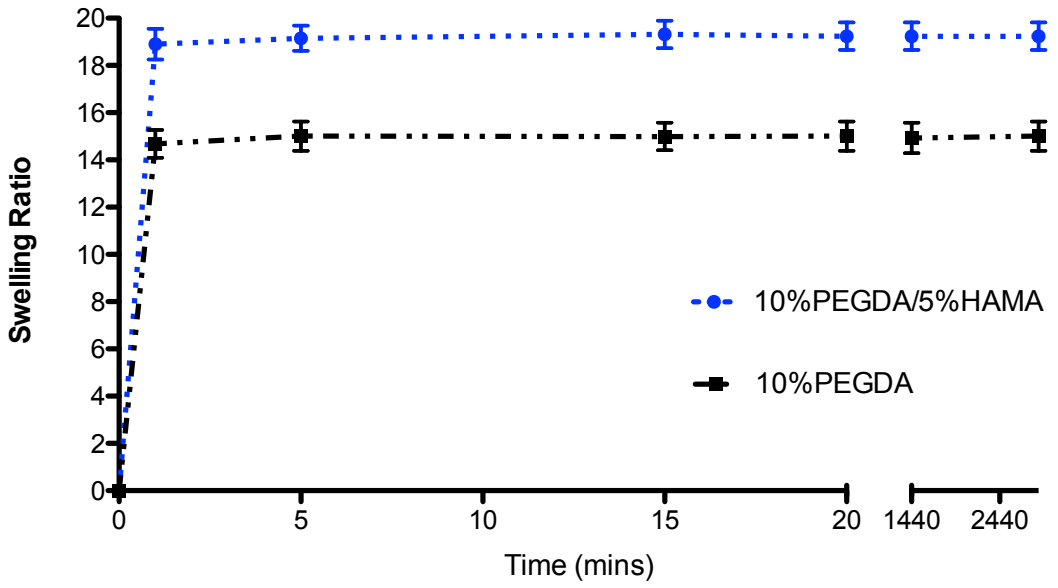

Figure 2. 3: Material Characterization of Swelling Kinetics.
Swelling ratio and kinetics of PEGDA/HAMA porous hydrogel compared to PEGDA porous hydrogel.

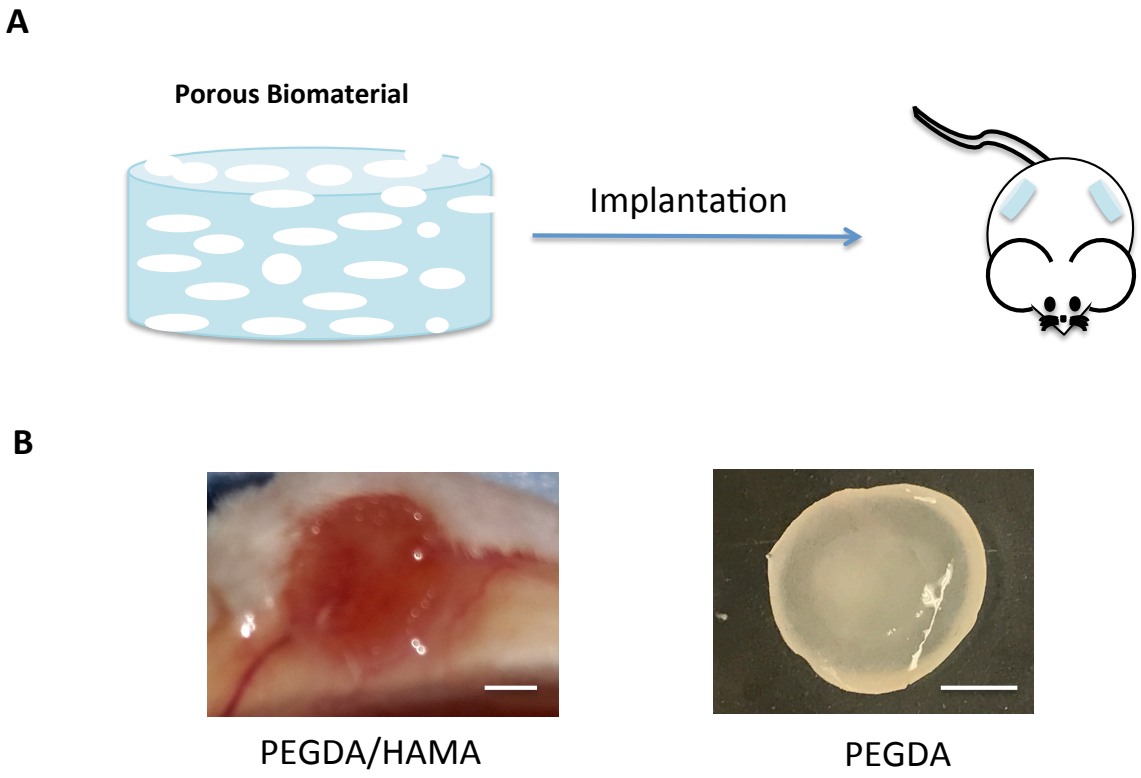

Figure 2. 4: Addition of HAMA to promote vascular formation.
A. Schematic of porous biomaterial implanted into NOD/SCID mice. B. Appearance of HAMA/PEGDA(left) and PEGDA (right) macroporous hydrogels after 2 weeks subcutaneous implantation in NOD/SCID mice. Scale 0.25cm.

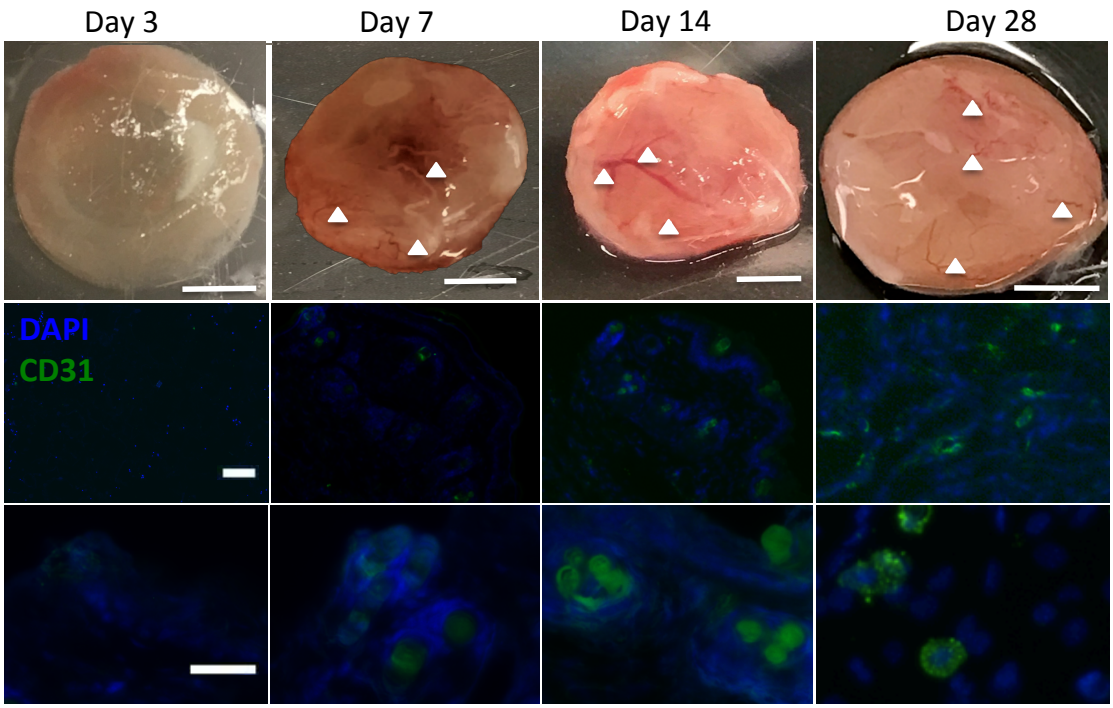

Figure 2. 5: Vascularization of Acellular Structures.
Top Panel: Gross structure of implants after retrieval from subcutaneous implantation in NOD/SCID mice. White arrowheads point to visible vasculature. Scale: 0.25 cm. Middle Panel: CD31 (green) and DAPI (blue) staining to visualize vasculature. Scale: 10μm. Lower panel: Magnified image of DAPI and CD 31 staining. Scale: 10μm. Each time point had n=6 or more constructs.

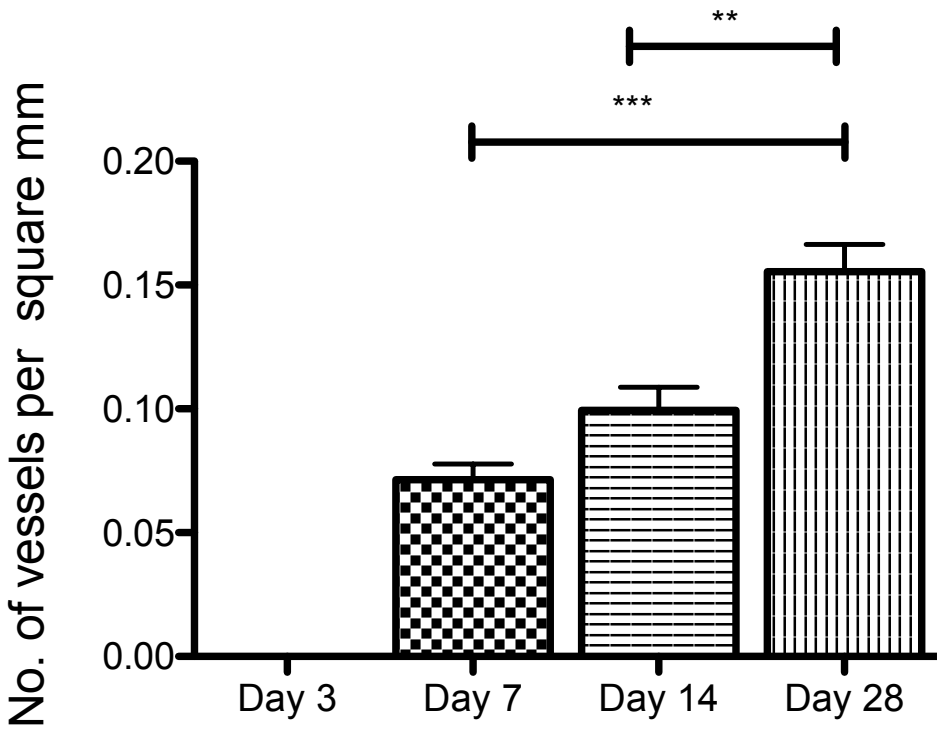

Figure 2. 6: Quantification of blood vessels.
Data are presented as mean ± SE obtained from six engineered constructs ($n = 6$) per group. One-way ANOVA with Tukey post hoc test (on day 7, 14 and 28). ***$P < 0.0001$. **$P < 0.001$

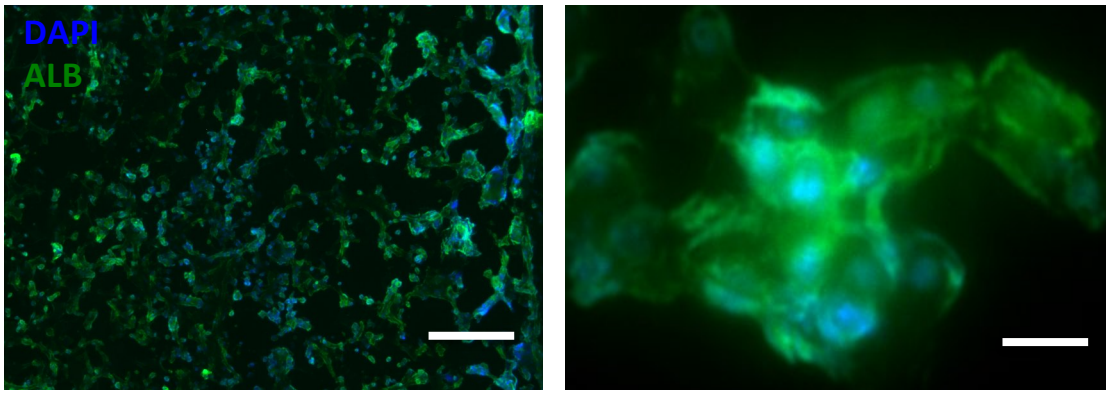

Figure 2. 7: Effect of supporting cells on albumin production.
Albumin staining of scaffolds with hMSCs and HUVECS supporting cells at low and high magnifications. Blue represents DAPI and green represents albumin. Scale: 100μm and 10μm respectively.

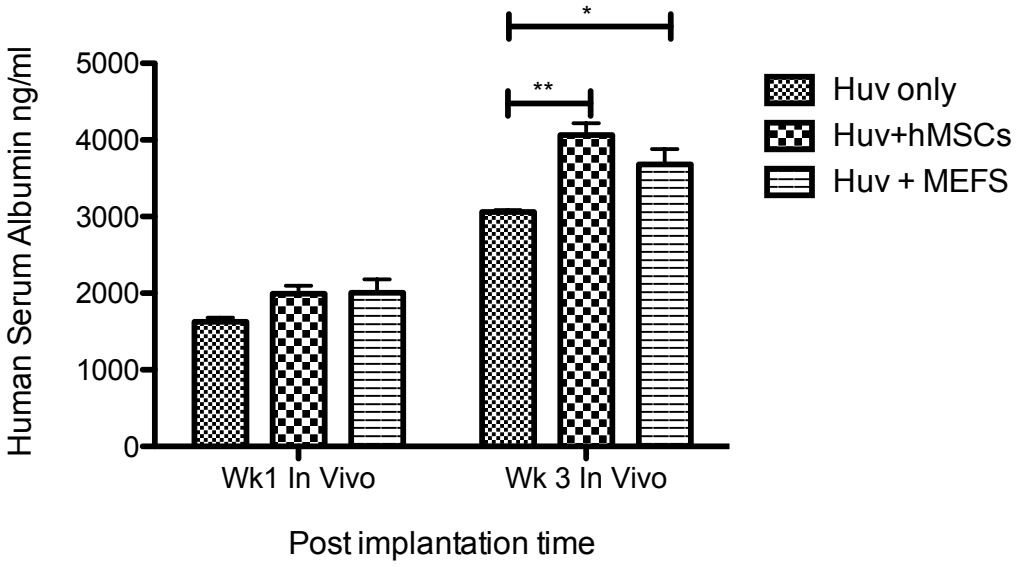

Figure 2. 8: ELISA analysis of the effect of supporting cells on albumin production. Secretion of human serum albumin for supporting cells HUVECS only, HUVECs and hMSCs and HUVECS and MEFs at week 1 and week 3 post implantation. Data are presented as mean ± SE obtained from six engineered constructs ($n = 6$). One-way ANOVA with Tukey post hoc test. *$P < 0.05$. **$P < 0.01$.

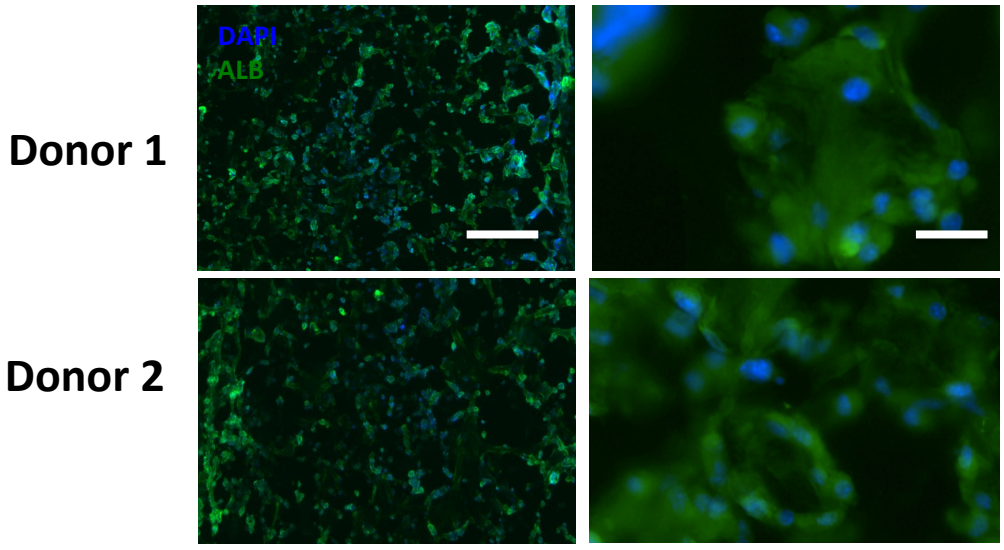

Figure 2. 9: Assessing donor cell function in vivo via human albumin secretion. Albumin staining for donor 1 & 2 after 28 days in vivo. Blue represents DAPI and green represents albumin. Scale: 100μm and 10μm respectively.

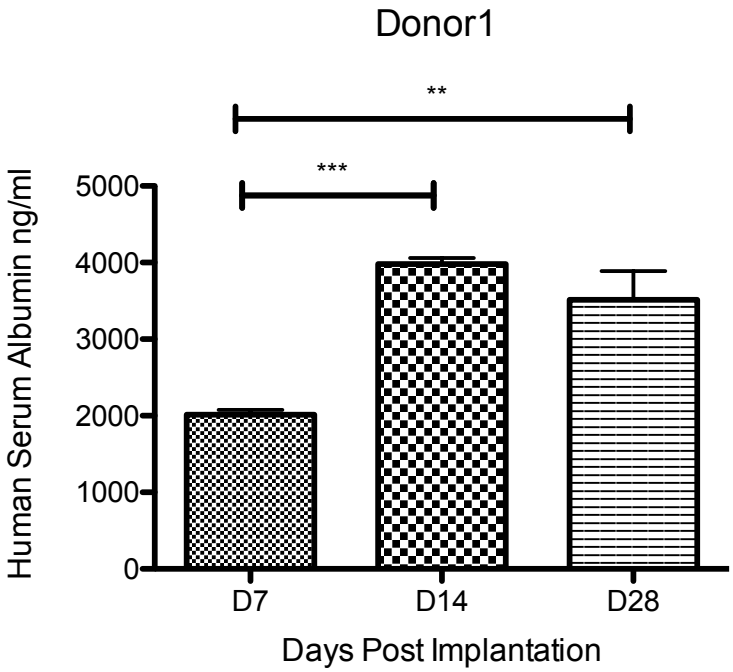

Figure 2. 10: Donor 1 ELISA analysis assessing cell function in vivo via human albumin secretion.

ELISA analysis of human serum albumin secretions of donor 1 in NOD/SCID mice over three time points, day 7, day 15 and day 28. Data are presented as mean ± SE obtained from six engineered constructs ($n = 6$). One-way ANOVA with Tukey post hoc test. *$P < 0.05$. **$P < 0.01$. ***$P < 0.001$

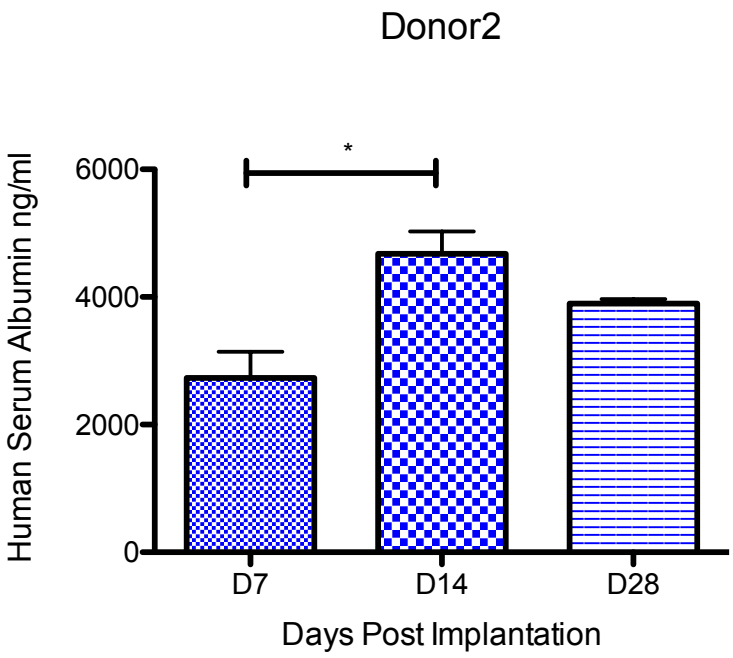

Figure 2. 11: Donor 2 ELISA analysis assessing cell function in vivo via human albumin secretion.
ELISA analysis of human serum albumin secretions of donor 2 in NOD/SCID mice over three time points, day 7, day 15 and day 28. Data are presented as mean ± SE obtained from six engineered constructs ($n = 6$). One-way ANOVA with Tukey post hoc test. *$P <$ 0.05. **$P < 0.01$. ***$P < 0.001$.

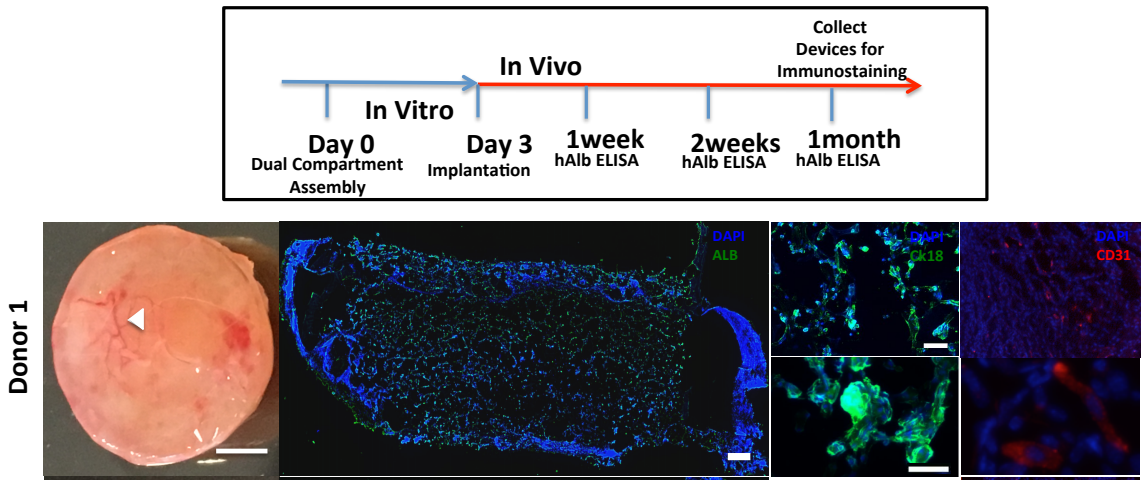

Figure 2. 12: Immunofluorescent staining of donor 1 retrieved implants.
Top panel: Experimental timeline. Bottom Panel: Column 1: Donor 1 gross structure of device 28 days post implantation, with white arrows pointing at visible vascular networks. Scale: 0.25 cm. Column 2: DAPI (blue) and Albumin (green) staining to visualize a slice of the dual compartment system. Scale: 200µm. Column 3: Ck18 (green) and DAPI (blue) staining. Scale: 50µm and 10µm. Column 4: CD31 (red) and DAPI (blue) staining to visualize vasculature. Scale: 50µm and 10µm. At least three mice were used per donor, each containing 2 implants.

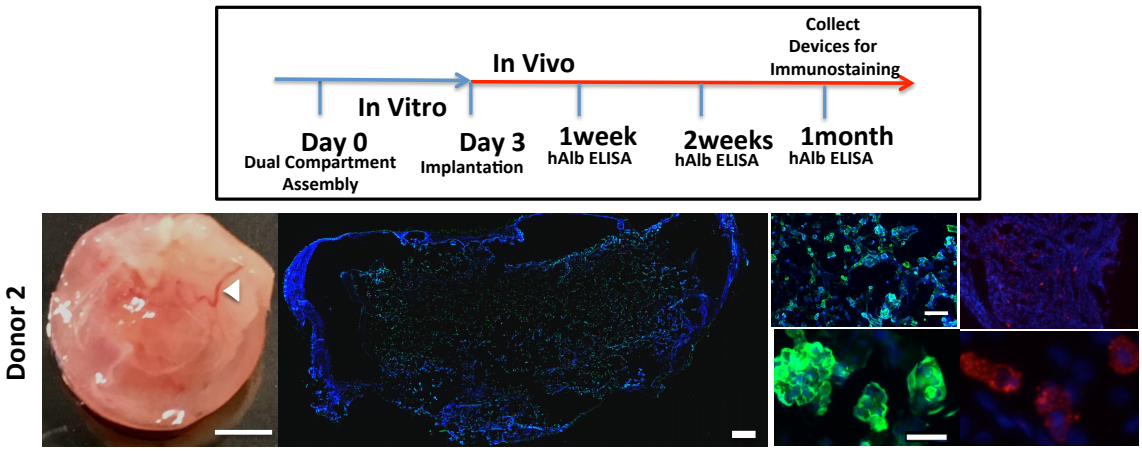

Figure 2. 13: Immunofluorescent staining of donor 2 retrieved implants.
Top panel: Experimental timeline. Bottom Panel: Column 1: Donor 2 gross structure of device 28 days post implantation, with white arrows pointing at visible vascular networks. Scale: 0.25 cm. Column 2: DAPI (blue) and Albumin (green) staining to visualize a slice of the dual compartment system. Scale: 200µm. Column 3: Ck18 (green) and DAPI (blue) staining. Scale: 50µm and 10µm. Column 4: CD31 (red) and DAPI (blue) staining to visualize vasculature. Scale: 50µm and 10µm. At least three mice were used per donor, each containing 2 implants.

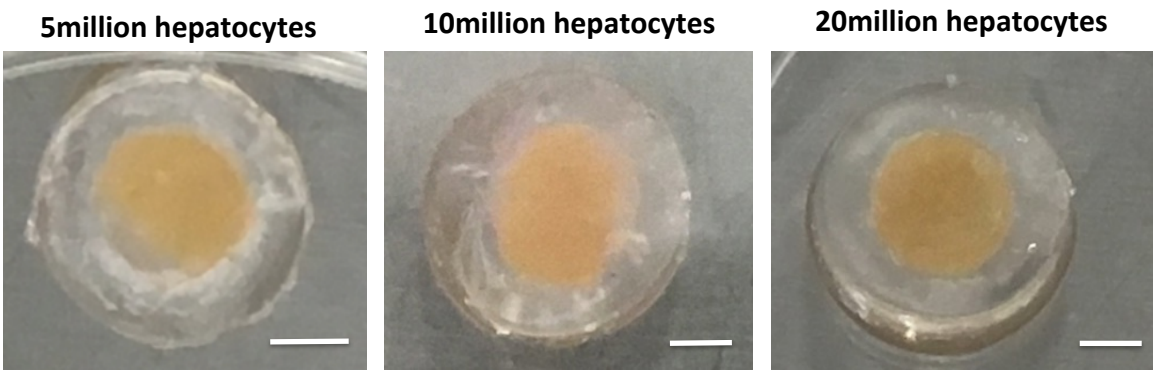

Figure 2. 14: Cell loading.
Gross structure images of dual compartment gels with increasing number of cells (5, 10 and 20 million hepatocytes) loaded in the inner compartment. Scale: 0.25 cm

Table 2. 1: Table of Donor Information.

Demographics, post thaw assessment and fold induction activity for each cell line used.

	Donor Demographics				Post thaw Assessment			Fold Induction (Specific Activity)			Fold Induction (mRNA)		
Lot #	Gender	Race	Age	BMI	Viability	Yield (million cells/vial)	24-Well Monolayer Confluency	CYP1A2	CYP2B6	CYP3A4	CYP1A2	CYP2B6	CYP3A4
HUM4113	Male	Caucasian	29	28	90%	9.5	95%	21.4	21.9	29.5	89.5	18.8	158.4
HUM4100	Female	Caucasian	8 Months	18	86%	9.2	100%	54.2	13.8	12	58.3	10	8.3

2.9 References

1. Heron MeaDFDfiNVSR, Vol. 57 (Centers for Disease Control and Prevention, Hyattsville, Maryland, 2009).

2. Schramm C, Bubenheim M, Adam R, Karam V, Buckels J, O'Grady JG, Jamieson N, Pollard S, Neuhaus P, Manns MM, Porte R, Castaing D, Paul A, Traynor O, Garden J, Friman S, Ericzon BG, Fischer L, Vitko S, Krawczyk M, Metselaar HJ, Foss A, Kilic M, Rolles K, Burra P, Rogiers X, Lohse AW. Primary liver transplantation for autoimmune hepatitis: a comparative analysis of the European Liver Transplant Registry. Liver Transpl. 2010;16(4):461-9.

3. Heron M, Hoyert DL, Murphy SL, Xu J, Kochanek KD, Tejada-Vera B. Deaths: final data for 2006. National vital statistics reports : from the Centers for Disease Control and Prevention, National Center for Health Statistics, National Vital Statistics System. 2009;57(14):1-134.

4. Ambrosino G, Varotto S, Strom SC, Guariso G, Franchin E, Miotto D, Caenazzo L, Basso S, Carraro P, Valente ML, D'amico D, Zancan L, D'antiga L. Isolated Hepatocyte Transplantation for Crigler-Najjar Syndrome Type 1. Cell transplantation. 2005;14(2-3):151-7.

5. Fox IJ, Chowdhury JR, Kaufman SS, Goertzen TC, Chowdhury NR, Warkentin PI, Dorko K, Sauter BV, Strom SC. Treatment of the Crigler–Najjar Syndrome Type I with Hepatocyte Transplantation. New England Journal of Medicine. 1998;338(20):1422-7.

6. Lysy PA, Najimi M, Stephenne X, Bourgois A, Smets F, Sokal EM. Liver cell transplantation for Crigler-Najjar syndrome type I: update and perspectives. World J Gastroenterol. 2008;14(22):3464-70.

7. Jorns C, Ellis EC, Nowak G, Fischler B, Nemeth A, Strom SC, Ericzon BG. Hepatocyte transplantation for inherited metabolic diseases of the liver. Journal of Internal Medicine. 2012;272(3):201-23.

8. Dhawan A, Puppi J, Hughes RD, Mitry RR. Human hepatocyte transplantation: current experience and future challenges. Nature Reviews Gastroenterology &Amp; Hepatology. 2010;7:288.

9. Nicolas CT, Wang Y, Nyberg SL. Cell therapy in chronic liver disease. Current opinion in gastroenterology. 2016;32(3):189-94.

10. Mazza G, Rombouts K, Rennie Hall A, Urbani L, Vinh Luong T, Al-Akkad W, Longato L, Brown D, Maghsoudlou P, Dhillon AP, Fuller B, Davidson B, Moore K, Dhar

D, De Coppi P, Malago M, Pinzani M. Decellularized human liver as a natural 3D-scaffold for liver bioengineering and transplantation. Scientific reports. 2015;5:13079.

11. Zhang J, Zhao X, Liang L, Li J, Demirci U, Wang S. A decade of progress in liver regenerative medicine. Biomaterials. 2018;157:161-76.

12. Dhawan A, Puppi J, Hughes RD, Mitry RR. Human hepatocyte transplantation: current experience and future challenges. Nature reviews Gastroenterology & hepatology. 2010;7(5):288-98.

13. Fox IJ, Chowdhury JR. Hepatocyte transplantation. American journal of transplantation : official journal of the American Society of Transplantation and the American Society of Transplant Surgeons. 2004;4 Suppl 6:7-13.

14. Ohashi K, Yokoyama T, Yamato M, Kuge H, Kanehiro H, Tsutsumi M, Amanuma T, Iwata H, Yang J, Okano T, Nakajima Y. Engineering functional two- and three-dimensional liver systems in vivo using hepatic tissue sheets. Nat Med. 2007;13(7):880-5.

15. Chen AA, Thomas DK, Ong LL, Schwartz RE, Golub TR, Bhatia SN. Humanized mice with ectopic artificial liver tissues. Proceedings of the National Academy of Sciences. 2011;108(29):11842-7.

16. Ohashi K, Tatsumi K, Utoh R, Takagi S, Shima M, Okano T. Engineering liver tissues under the kidney capsule site provides therapeutic effects to hemophilia B mice. Cell transplantation. 2010;19(6):807-13.

17. Baptista PM, Siddiqui MM, Lozier G, Rodriguez SR, Atala A, Soker S. The use of whole organ decellularization for the generation of a vascularized liver organoid. Hepatology (Baltimore, Md). 2011;53(2):604-17.

18. Badylak SF, Weiss DJ, Caplan A, Macchiarini P. Engineered whole organs and complex tissues. The Lancet. 2012;379(9819):943-52.

19. Barakat O, Abbasi S, Rodriguez G, Rios J, Wood RP, Ozaki C, Holley LS, Gauthier PK. Use of decellularized porcine liver for engineering humanized liver organ. The Journal of surgical research. 2012;173(1):e11-25.

20. Bernard MP, Myers JC, Chu ML, Ramirez F, Eikenberry EF, Prockop DJ. Structure of a cDNA for the pro.alpha.2 chain of human type I procollagen. Comparison with chick cDNA for pro.alpha.2(I) identifies structurally conserved features of the protein and the gene. Biochemistry. 1983;22(5):1139-45.

21. Leyh RG, Wilhelmi M, Walles T, Kallenbach K, Rebe P, Oberbeck A, Herden T, Haverich A, Mertsching H. Acellularized porcine heart valve scaffolds for heart valve tissue engineering and the risk of cross-species transmission of porcine endogenous

retrovirus. J Thorac Cardiovasc Surg. 2003;126(4):1000-4.

22. Ko IK, Peng L, Peloso A, Smith CJ, Dhal A, Deegan DB, Zimmerman C, Clouse C, Zhao W, Shupe TD, Soker S, Yoo JJ, Atala A. Bioengineered transplantable porcine livers with re-endothelialized vasculature. Biomaterials. 2015;40:72-9.

23. Seale NM, Varghese S. Biomaterials for pluripotent stem cell engineering: from fate determination to vascularization. Journal of Materials Chemistry B. 2016;4(20):3454-63.

24. Shih Y-R, Kang H, Rao V, Chiu Y-J, Kwon SK, Varghese S. In vivo engineering of bone tissues with hematopoietic functions and mixed chimerism. Proceedings of the National Academy of Sciences. 2017;114(21):5419-24.

25. Zhang C, Aung A, Liao L, Varghese S. A novel single precursor-based biodegradable hydrogel with enhanced mechanical properties. Soft Matter. 2009;5(20):3831-4.

26. Kang H, Shih Y-RV, Hwang Y, Wen C, Rao V, Seo T, Varghese S. Mineralized gelatin methacrylate-based matrices induce osteogenic differentiation of human induced pluripotent stem cells. Acta Biomaterialia. 2014;10(12):4961-70.

27. Hwang Y, Zhang C, Varghese S. Poly(ethylene glycol) cryogels as potential cell scaffolds: effect of polymerization conditions on cryogel microstructure and properties. Journal of Materials Chemistry. 2010;20(2):345-51.

28. Takebe T, Sekine K, Enomura M, Koike H, Kimura M, Ogaeri T, Zhang R-R, Ueno Y, Zheng Y-W, Koike N, Aoyama S, Adachi Y, Taniguchi H. Vascularized and functional human liver from an iPSC-derived organ bud transplant. Nature. 2013;499(7459):481-4.

29. Phadke A, Hwang Y, Kim SH, Kim SH, Yamaguchi T, Masuda K, Varghese S. Effect of scaffold microarchitecture on osteogenic differentiation of human mesenchymal stem cells. European cells & materials. 2013;25:114-29.

30. Park D, Kim Y, Kim H, Kim k, Lee Y-S, Choe J, Hahn J-H, Lee H, Jeon J, Choi C, Kim Y-M, Jeoung D. Hyaluronic Acid Promotes Angiogenesis by Inducing RHAMM-TGFβ Receptor Interaction via CD44-PKCδ. Molecules and Cells. 2012;33(6):563-74.

31. Turner RA, Wauthier E, Lozoya O, McClelland R, Bowsher JE, Barbier C, Prestwich G, Hsu E, Gerber DA, Reid LM. Successful transplantation of human hepatic stem cells with restricted localization to liver using hyaluronan grafts†. Hepatology (Baltimore, Md). 2013;57(2):775-84.

32. Montesano R, Kumar S, Orci L, Pepper MS. Synergistic effect of hyaluronan oligosaccharides and vascular endothelial growth factor on angiogenesis in vitro.

Laboratory investigation; a journal of technical methods and pathology. 1996;75(2):249-62.

33. Van Hove AH, Benoit DSW. Depot-Based Delivery Systems for Pro-Angiogenic Peptides: A Review. Frontiers in Bioengineering and Biotechnology. 2015;3:102.

34. Miller JS. The Billion Cell Construct: Will Three-Dimensional Printing Get Us There? PLoS Biology. 2014;12(6):e1001882.

Chapter 3: Development and modification of chitosan pouches for hepatocyte transplantation in immune-competent mice

3.1 Abstract

The foreign body response to transplanted biomaterial-based cell devices threatens the success and clinical translation of promising liver therapies. Even though immunosuppressive therapy is heavily utilized to reduce the impact of foreign body rejection, it has been associated with many side effects including renal dysfunction and infections. To address these issues more emphasis is being placed on developing biomaterial strategies suitable for immune competent systems. Here we demonstrate one such attempt by investigating the use of chitosan as a hepatocyte carrier for transplantation in immune competent mice. We showed that surface modification of the chitosan pouch reduced the impact of the foreign body response by hindering the attachment of immune cells and fibroblasts. More importantly, we demonstrated that the device supported hepatocyte viability and function in immune competent mice for at least one month, the longest experimental time point. Such devices can be used for a minimally invasive approach to augment specific liver function to treat various compromised liver function pathologies. It can also be extended for the transplantation of other cell types (not just liver cells) in immune competent systems and even provide a new protein fouling resistant material for developing medical devices.

Key words Chitosan; chitosan pouch; immune competent; hepatocyte transplantation; subcutaneous implantation

3.2 Introduction

One of the biggest challenges impeding the clinical success of transplanted biomaterial based cell therapies is the foreign body response(1-5). This immune-mediated reaction can lead to rejection of the implants and recipient complications(6-8). To mitigate the issue of implant rejection most researchers and clinicians rely on lifelong immunosuppressive therapy(9, 10). While immunosuppression is currently one of the best available options, lifelong suppression has been associated with many side effects including renal dysfunction, hypertension, infections and malignancies(8). To avoid the need for immunosuppression, more efforts are being focused on developing biomaterial based cell therapies suitable for immune competent systems(5, 11).

Chitosan is a linear polysaccharide (Figure 3.1) that can be commercially obtained from shellfish sources(12). This biopolymer has already been heavily researched for applications ranging from wound healing and tissue engineering to drug delivery and gene delivery(12, 13). Already shown to have an intrinsic antibacterial nature and to elicit minimal foreign body response(13), chitosan holds great promise as a potential biomaterial for therapies in immune competent recipients. Chitosan based materials have already been used to improve hepatocyte function(14). Furthermore, *in vitro* experiments using alginate-chitosan microcapsules pointed to their ability to protect encapsulated cells from lymphocytes(15). While these results are promising, no evidence has been provided for the successful chitosan based transplantation of hepatocytes in immune competent mice.

Here we show the development and modification of a chitosan cell pouch for hepatocyte transplantation in immune competent mice. In previous work we have shown

that surface modifications can affect cell adhesion(16). Leveraging this knowledge, we hypothesized that modifying the chitosan could mitigate the foreign body response (Figure 3.2) by reducing macrophage and fibroblast cell attachment. To this end we have developed an 11-aminoundecanoic acid modified chitosan transplantation pouch that resists cell attachment *in vitro* and *in vivo*. Furthermore, once loaded with hepatocytes and implanted subcutaneously, the chitosan pouch supported cell viability and function for one month (the longest experimental time-point investigated). To our knowledge this is the first demonstration of successful biomaterial based transplantation of hepatocytes in immune competent mice.

3.3 Methods and Materials

3.3.1 Preparation of Chitosan solution

8g Chitosan (medium molecular weight, Sigma), 40ml glacial acetic acid and 360ml Milli-Q water were added in that order to a 500mL glass beaker. The mixture was stirred overnight. After mixing the solution was transferred into 50ml tubes and centrifuged at 3000rpm for 10minutes to allow any unmixed particles to settle. The chitosan solution was separated from the unmixed particles and stored for future use.

3.3.2 Chitosan pouch development

The first layer was cast by pouring 15ml of the chitosan solution into a 10cm glass petri dish. The dish was heated at 50 °C for 3hrs or until cured. To create the space for cell loading, either paraffin or polytetrafluoroethylene (PTFE) tubing molds were used. The paraffin mold was made by attaching (with hot paraffin as the “glue”) either

PTFE tubing (SWTT-18-C, Zeuss) or needle to a 100μm thin by 1cm width by 1cm length paraffin sheet. The PTFE mold was made by cutting 18 Gauge PTFE tubing into 1cm pieces. The molds were placed on the cured layer. Another layer was cast by pouring 15ml (or the amount necessary to fully cover the mold and previous layer) of chitosan solution over the mold and the previous layer. This layer was heated and cured overnight at 37 °C to avoid melting the paraffin mold. Once fully cured, the chitosan was neutralized by adding 2.5M NaOH to the dish for at least 10 minutes. The NaOH was then replaced with PBS for 15minutes. Then a spatula was used to carefully lift the chitosan structures off of the petri dish. The pouches were then cut out, the tubing was removed and the paraffin mold was dissolved out (through the channel left by the tubing) in a water bath at 60 Celsius. The pouch was then sterilized by multiple ethanol washes followed by multiple sterile PBS washes to remove ethanol. The final sterilization wash was done with penstrep/PBS (5%v/v).

3.3.3 Tuning pouch thickness

The thickness of the couch can be manipulated by varying the volume of chitosan solution used to cast each layer. For imaging purposes 1% wt/v of 200 nm diameter green fluorescent particles were added to the chitosan solution used to make each chitosan film. In each well of a 6 well plate either 3ml, 2ml or 1ml of chitosan solution was poured. The solution was allowed to cure, then the chitosan film layer was neutralized with NaOH followed by washing with PBS. The films (i.e walls of the chitosan pouch) were then immersed transferred to a mold filled with OCT and frozen with 2-methylbutane and liquid nitrogen, and stored at -80°C until sectioning. For cryosectioning, frozen tissue

blocks were sectioned with a cryotome cryostat (at -20 °C) to 20-μm thicknesses.

3.3.4 Cell loading of the chitosan pouch

Primary human hepatocytes (HUM 4100, Lonza) were thawed in thawing media (MCHT50; Lonza) and centrifuged for 10 minutes at 100 g. Next, thrombin (2 U/ml) was added to the cell pellet. Next, a 5%(v/v) solution of collagen type I (rat tail, Corning) in endothelial growth media (containing 79% M199 medium (Gibco), 10% FBS (Gibco), 10% endothelial cell growth medium (Cell Application, Inc.), and 1% penicillin/streptomycin (Gibco)) solution was added to the pellet. The cell mixture containing 5 million hepatocytes was then added to a syringe and infused into the pouch. Immediately, fibrinogen 8mg/mL was added to the outside of the pouch, and allowed to diffuse in to form a gel with the thrombin. Finally, the pouch was sealed with an acrylate-based glue (allowed to fully dry) and incubated with maintenance media (MM250, LONZA) until ready for use. As indicated by the figure captions, in some cases the pouch was filled with HepG2 cells.

3.3.5 HepG2 Cell culture

HepG2 cells were cultured in growth medium (GM), composed of Dulbecco's Modified Eagle's high glucose medium (Hyclone) supplemented with 10% fetal bovine serum (FBS, Gibco) and 1% penicillin/streptomycin (Gibco). The cells were grown on 10mm cell culture dishes to 70% confluency before being passaged for use.

3.3.6 Subcutaneous implantation of Chitosan Pouch or film

All animal procedures were approved by the Institutional Animal Care and Use Committee of the University of California, San Diego and performed in accordance with the NIH and national and international guidelines for laboratory animal care. Subcutaneous implantation of the cell-laden chitosan pouch or aceelular chitosan film (one cured layer of chitosan) was performed 1 day after loading and culture *in vitro*. Recipient mice (NOD/SCID) were administered with ketamine (100 mg/kg) and xylazine (10 mg/kg), and the fur on the back was shaved. Mice were then placed on a heating pad and a 1 cm-long incision was made in the back of the mice, and one subcutaneous pouch was inserted by blunt dissection using a 1 cm-wide spatula on the left side of the mouse. The skin was sutured once the pouch or film was implanted.

3.3.7 Live dead

A Live/Dead assay was performed to evaluate the cell viability after 24 h of cell loading and again after 7days post implantation. Briefly, cell-laden pouches were incubated with the Live/Dead assay dye solution (Molecular Probes, Cat# L-3224), which contained 0.5 μL of Calcein-AM and 2 μL of ethidium homodimer-1 in 1 mL of DMEM (more live-dead solution was used as necessary to ensure that pouch was fully submerged) . After 30 min of incubation, the pouch was rinsed with PBS and images were obtained using fluorescence microscopy.

3.3.8 Chitosan Modification

After making the chitosan pouch or chitosan film, the outer surface was modified with the following: C1: Glycine (Fisher Scientific); C5: 6-aminocaproic acid (Acros

Organics); C10: 11-aminoundecanoic acid (Aldrich). First, hydroxyl groups were activated by immersing pouch in DMSO containing 1,1'-carbonyldiimidazole CDI (80mg/ml) for 2hrs. Then, the chitosan was washed vigorously with DMSO (x3). C1 or C5 or C10 was then dissolved in pH8 PBS (2mg/mL). The chitosan was soaked in this solution overnight. After the modification process was complete the pouch was rinsed in PBS then sterilized by a series of ethanol washes and subsequent PBS washes. The final wash was performed using PenStrep PBS.

3.3.9 *In vitro* Cell attachment and Proliferation Quantification

Unmodified chitosan, C1, C5 and C10 modified chitosan were prepared in different wells of a 12 well plate. All previous chitosan film preparation and modification procedures were followed, except, the chitosan film was allowed to remain attached to the well where it was cured. Following the modification of the attached films, sterilization was carried out as usual and the films were allowed to incubate with growth media (Dulbecco's Modified Eagle's high glucose medium (Hyclone) supplemented with 10% fetal bovine serum (FBS, Gibco) and 1% penicillin/streptomycin (Gibco)) for 24hrs. Then, either NIH/3t3 cells or RAW 264.7 cells were plated (25,000 cells per 3.8cm^2 well) on each film. After 24hrs or 7days, cells were trypsonized and counted to assess cell attachment and cell proliferation, respectively.

3.3.10 Albumin measurement

Sandwich enzyme linked immunosorbent assay (ELISA) was performed to assess the albumin production of the implanted cells. All animal procedures were approved by the Institutional Animal Care and Use Committee of the University of California, San Diego

and performed in accordance with the NIH and national and international guidelines for laboratory animal care. In short, on the day of implant retrieval, blood was collected from the heart of the mice. The blood was then centrifuged at 14900 g at 4 Degrees Celsius (°C) for 15 min. to separate and extract the serum. The serum was assessed for human albumin by using the Human Albumin ELISA Quantitation Set (Bethyl Labs, Catalogue no. E80-129) according to the manufacturer's protocol.

3.3.11 Immunostaining

Post implantation constructs were retrieved and cells were replated for 24hours. Next, cells were washed with PBS, then fixed with 4% paraformaldehyde (PFA, Sigma Aldrich) at 4 °C overnight. For immunofluorescent staining, cells were blocked with blocking buffer containing 3% (w/v) bovine serum albumin (BSA; 60 min, RT) and 0.1% Triton X-100 (v/v) in PBS. Cells were stained with FITC conjugated human albumin (1:500; Bethyl Labs) overnight at 4 °C. Then Hoechst 33342 (2 µg/mL; Thermo Fisher) was used to stain the nuclei for 1 h at RT. Then samples were washed with PBS and imaged with fluorescent microscopy.

3.3.12 Statistical analysis

All experiments were independently repeated at least twice with replicate samples as indicated in figure captions. Statistical analysis was performed using one-way ANOVA and Tukey's post hoc test for group comparisons to determine statistical significance ($p < 0.05$). Errors bars represent SEM. GraphPad Prism 5 software was used to determine all statistical analysis.

3.4 Results

3.4.1 Development of Chitosan Pouch

The chitosan pouch was developed as a transplantation device for liver cells (Figure 3.3). Using a simple process, the pouch was created by casting two layers of chitosan around a desired mold (Figure 3.3). If a paraffin mold was used in creating the pouch, an additional step to fully remove the paraffin to make room for cell loading was required (Figure 3.4). Placing the pouch in a 60 °C water bath was enough to melt and remove all of the chitosan (Figure 3.4). To manipulate the cell carrying capacity of the pouch molds with different dimensions could be used. In unmodified chitosan studies a paraffin mold measuring 1cm length x 1cm width x 100μm height was used to prepare pouches. Throughout the preparation process the height of the pouch expanded to 0.5mm due to air pockets forming between the mold and the second layer. For hepG2 studies the chitosan pouch was prepared with a PTFE mold measuring 1cm length by 2.5mm Diameter. Measurements were conserved when using PTFE as a mold. In addition to changing the size of the pouch, we also manipulated the thickness of the walls of the pouch. By manipulating the volume of chitosan used to cast each layer, we showed that the thickness could be controlled (Figure 3.5). Using this technique we showed that thicknesses between 220 and 25μm could be achieved (Figure 3.5).

After development of the chitosan pouch design, it was loaded with cells to ensure that the material was biocompatible. After paraffin removal and pouch sterilization, the pouch was loaded with 5 million hepatocytes, fibrin and collagen ECM (Figure 3.6). Live dead analysis indicated that the majority of the cells (at least 80%) were viable after being loaded into the chitosan pouch (Figure 3.6). Moreover, results indicated that even if

the chitosan pouch had any residual paraffin left in it; that did not majorly affect the viability of the cells.

3.4.2 Implantation of Unmodified Chitosan Cell Pouch

To assess the effect of cell transplantation on cell viability, we performed live dead analysis on cells 1week post implantation in immunosuppressed mice. We first observed that even in immunosuppressed mice the pouches were encased in a fibrous capsule, and when they were finally retrieved they appeared to have white cell or ECM deposits on them. Live dead indicated that over 50% of cells were dead (Figure 3.7). To further investigate this phenomenon we implanted chitosan films in the same mice for a longer time period (Figure 3.8). After 1 month the films were retrieved and appeared to have even more white ECM/cell deposits than the 1-week samples. There were even visible vascular formations (Figure 3.8).

3.4.3 Modification of Chitosan Cell Pouch to mitigate the foreign body response in immune competent mice

Because ECM deposition was taking place in immunosuppressed mice, we inferred that it would most likely be even more prevalent in immune competent mice. Thus, pouch modification was carried out to mitigate this occurrence. The surface of the chitosan pouch was modified (Figure 3.9) with C1 (glycine), C5 (6 aminocaporic acid) or C10 (11-aminoundecanoic acid). To determine whether the modification yielded a successful outcome, *in vitro* cell attachment and proliferation experiments were carried out. For these experiments NIH 3T3, a murine fibroblast cell line and RAW 264.7, a

murine macrophage cell line, were seeded onto the films and monitored. For both cell lines, more cells appeared to attach to the unmodified chitosan and the C5 modified chitosan group (Figure 3.10). Quantification of the cell attachment indicated that for both cell lines, all groups had significantly higher cell attachment than the C10 modified group (Figure 3.11). In proliferation studies, a similar trend was observed (Figure 3.12). After 7 days *in vitro* all groups had significantly higher proliferation as compared to the C10 group. To determine whether the trend would be similar *in vivo*, chitosan with different modifications were implanted in immune competent mice (C57BL/6) for two weeks. Upon retrieval, pouches appeared to exhibit a similar trend in cell and ECM attachment as seen *in vitro*. Unmodified, C1 and C5 groups had the most deposition of cell/ECM (Figure 3.13). However, little to no deposition was seen on the C10 modified group as evidenced by its transparent appearance (Figure 3.13). Based on these *in vitro* and *in vivo* results, C10 modified chitosan was used in all subsequent experiments.

3.4.4 HepG2 transplantation in immune-competent mice

After development, modification and *in vitro* testing of the chitosan pouch, we needed to test its intended potential as a transplantation device in immune-competent mice. As such, we used the C10 modified pouch to transport HepG2 cells, in CD1 mice. 5 million cells in fibrin and collagen ECM were successfully transplanted subcutaneously in the cell pouch. The contents of the pre-implanted pouch appear pink due to the color of the media they were loaded with and cultured in before implantation. At the week 1 time point, implants were retrieved to assess viability. Live dead analysis indicated that at least 85% of cells were viable (Figure 3.14). Furthermore, the appearance of the excised

implant, was similar to the pre implanted pouch, and seemed to have little to no visible cells or ECM deposition (Figure 3.14). Once viability was confirmed, C10 modified pouches were transplanted for one month to assess function. Albumin ELISA performed on the CD1 mice serum indicated that human albumin from the HepG2 cells was present in mouse circulation (Figure 3.15). Albumin staining of the excised chitosan pouch confirmed the presence of albumin. Additionally, as in the case of the 1week time point, the 1month excised pouch appeared to have little to no visible cell or ECM deposition (Figures 3.14 and 3.15).

3.5 Discussion

This study describes the development and modification of a chitosan cell pouch for the transplantation of hepatocytes in immune competent mice. The chitosan pouch is easy to assemble and can be scaled up by simply changing the shape and size of the mold used to create the cell loading cavity. Additionally, we demonstrated the manipulation of thickness of the chitosan pouch by simply tuning the volume used to cast each layer (Figure 3.5). This can reduce the diffusive distance and potentially speed up the diffusion of nutrients and secreted products through the pouch. We also demonstrated that the surface modification of chitosan could be performed to mitigate foreign body rejection in immune competent mice. The modified pouch exhibited little to no detrimental foreign body rejection characteristics and was capable of supporting hepatocyte viability and function for one month.

When chitosan or any other biomaterial is introduced into the body, a series of events occur in the surrounding tissue that elicits a foreign body reaction(17). To recreate

aspects of this phenomenon *in vitro* and determine whether chitosan could be modified to mitigate the foreign body response; we studied the interaction between chitosan films and RAW 264.7, a macrophage cell line, and NIH/3T3 cells, a fibroblast cell line. Although we have previously demonstrated that surface modifications can mitigate stem cell attachment(16), in this study we show that this can also be extended to the cell attachment and proliferation of macrophages and fibroblasts (Figures 3.11 and 3.12). These findings are of significance since macrophages have been shown to adhere to the implant surfaces and can trigger events that promote implant degradation(18-21). Furthermore, macrophages can also be activated to secrete pro-fibrogenic factors that stimulate fibroblast fibrogenesis and ultimately lead to fibrous capsule formation(17, 22, 23). Thus, our results demonstrated that the C10 modification of chitosan was sufficient to significantly reduce certain foreign body effects. To fully validate this claim we implanted the chitosan in CD1 immune competent mice. Similar to the *in vitro* results, when compared to all other groups, the C10 modified chitosan resisted the immune response as evidenced by the lack of cell or ECM attachment (Figure 3.13).

Although this proof of concept study used the HepG2, a carcinoma cell line, the C10 chitosan cell pouch can be extended for use with primary liver cells and even other cell types. While primary hepatocytes may be considered the most ideal cell source, their limited availability and loss of liver specific function during culture still provides hurdles for their application in bioartificial liver (BAL) engineering(24). As such, we chose to use HepG2 cells, a carcinoma cell line that is still widely used in liver engineering and toxicity study research(25), as a model cell source to investigate the potential of our chitosan pouch. Results indicated that the HepG2 cells remained protected in the chitosan

cell pouch and did not elicit any visible immune response (Figures 3.14 and 3.15). If further testing suggests that the hepG2 cells can remain contained in the pouch, without immune rejection or negatively impacting the mice (forming hematomas) then this device has the potential to be clinically translated without needing to incorporate primary cells. HepG2 cells have the advantage of easy culture and providing a theoretically unlimited cell source(24, 26) that would make scaling up and mass production much more feasible compared to primary hepatocyte use. One area of concern for using HepG2 cells is that they have reduced liver specific functions compared to primary hepatocytes, however, researchers are rectifying this by genetically engineering HepG2 cells to have improved functions(27, 28). Therefore, the development of the C10 chitosan pouch combined with emerging technology to genetically enhance HepG2 functions can have major applications in developing liver therapy devices that can augment specific liver functions to provide therapies for disorders like hemophilia B or alpha-1-antitrypsin deficiency, but it can also be used as a BAL device to bridge the gap until an organ becomes available for transplantation.

3.6 Conclusion

While many scientists explore the development of successful biomaterial devices for liver cell therapies, not enough efforts are focused on developing approaches that could work in immune competent systems. To our knowledge, no previous study has evaluated the potential of modified chitosan to be used as a cell transplantation tool in immune competent mice. To address this issue we have developed a chitosan pouch for cell transplantation. We have modified the surface of the pouch with 11-

aminoundecanoic acid (C10) to mitigate the foreign body reaction in mice. This C10 modified chitosan cell pouch was capable of minimally invasive xenogeneic transplantation of HepG2 cells in immune competent CD1 mice. Furthermore, the transplanted device maintained function for 1month, the longest assayed time point. The C-10 chitosan device described here is simple, robust and scalable. These characteristics lend the device to be used as a tool to further investigate long term allogeneic and xenogeneic transplantation in immune competent systems. Moreover, the chitosan pouch can be extended for investigating drug testing, personalized medicine and disease pathology of the liver and even other organs such as the pancreas.

3.7 Acknowledgements

Chapter 3, in full, is currently being prepared for use in part of a publication for submission. “Modified Chitosan Cell Pouch for allogeneic and xenogeneic hepatocyte transplantation.” Seale NM, Ryu JH. , Nayak P., Varghese S. The dissertation author is the primary investigator and author of this material.

3.8 Figures

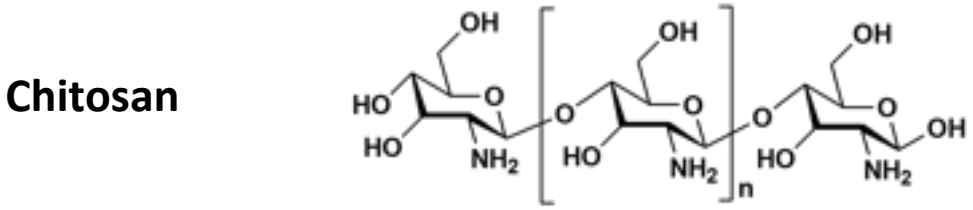

Figure 3. 1: Chemical structure of chitosan.
Linear polysaccharide structure of chitosan composed of randomly acetylated (N-acetyl-D-glucosamine) and deacetylated untis (D-glucosamine).

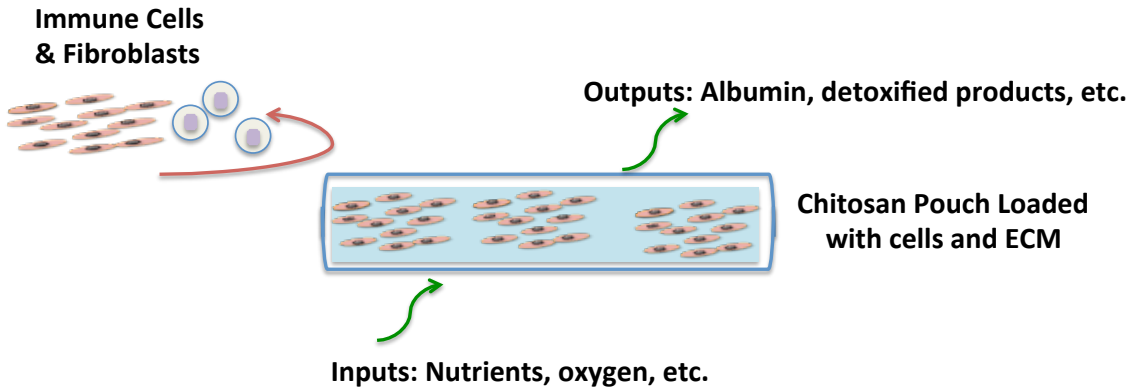

Figure 3. 2: Schematic of Chitosan Pouch foreign body response mitigation
The chitosan cell pouch (blue) is engineered to mitigate the foreign body response in immune competent mice. The pouch acts as a selectively permeable membrane that allows nutrients to diffuse in and cell secreted products to diffuse out (green arrows). The pouch membrane also acts as a protective barrier to keep transplanted cells inside and host cells outside. To mitigate the foreign body response to the pouch, the pouch would resist immune cell and fibroblast attachment (red curved arrow).

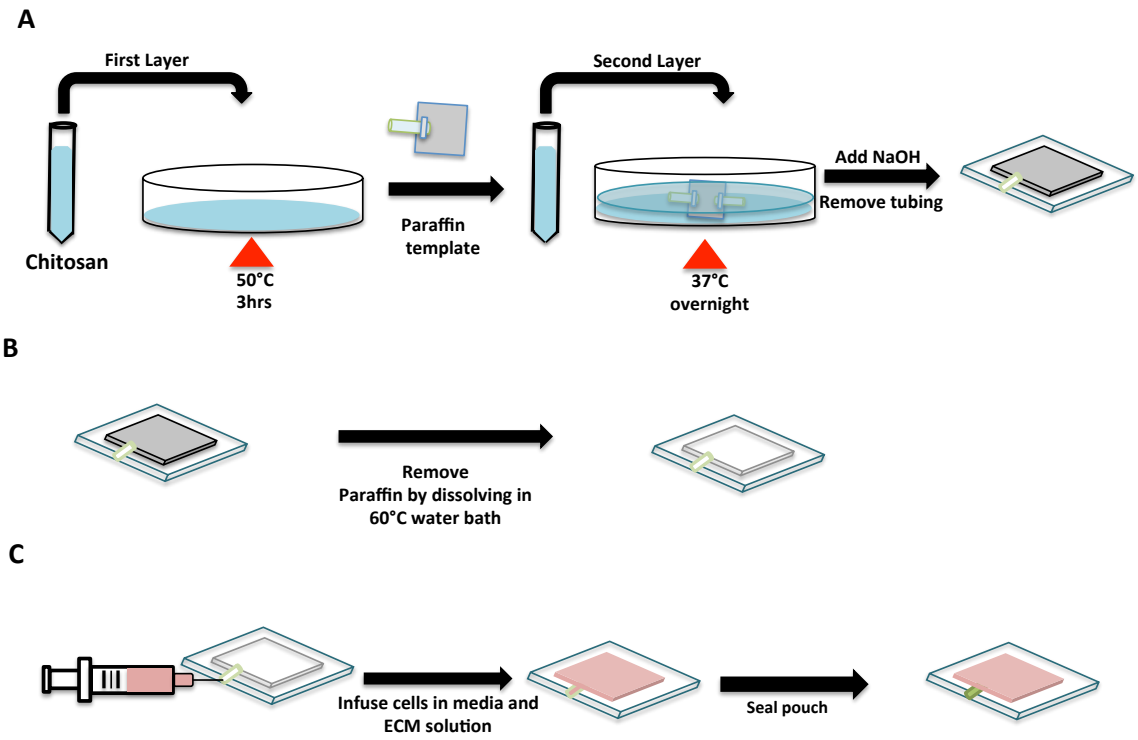

Figure 3. 3: Chitosan Pouch Assembly
A. Chitosan solution is poured into a glass petri dish and heated until the layer is cured. A paraffin template is placed on top of the 1st layer. The second layer is poured and cured at a reduced temperature to avoid melting the paraffin. NaOH is then used to neutralize the chitosan pouch and lift it off of the petri dish. B. The paraffin is dissolved out of the pouch. C. A syringe is used to load the cells and ECM into the pouch. Then the pouch is sealed using an acrylate-based glue.

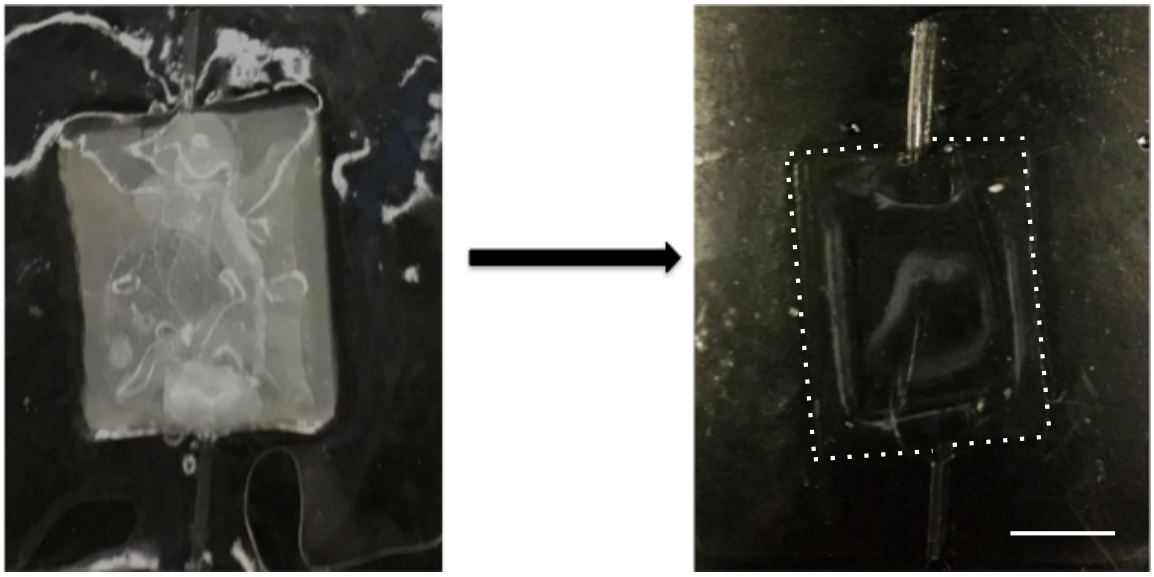

Figure 3. 4: Paraffin mold removal
Paraffin was removed from the inside of the pouch (left) by placing the pouch in a 60°C water bath. The dissolved paraffin exits the pouch leaving an empty cavity (right) for cell loading. Scale 0.5cm.

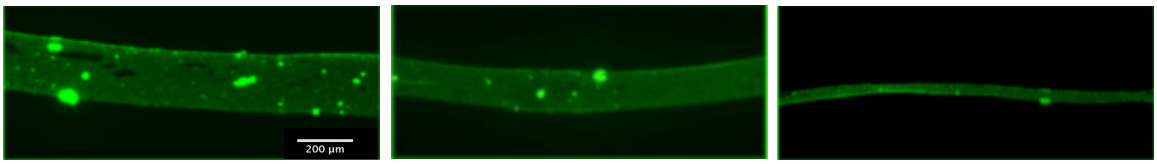

Figure 3. 5: Tuning the thickness of the chitosan pouch membrane.
The thickness of the chitosan pouch membrane was tuned by manipulating the volume of chitosan used to cast each layer. In each well of a 6-well plate, 3ml, 2ml or 1ml of chitosan mixed with green fluorescent beads was poured. Images show the thickness of resulting the chitosan layers. Scale 200µm

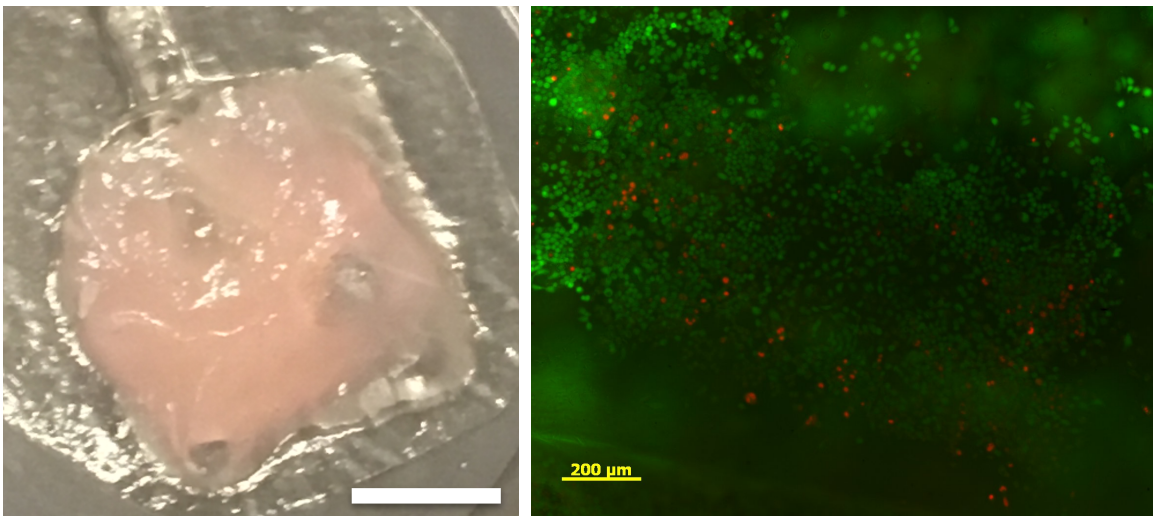

Figure 3. 6: Cell Viability of loaded cell pouch
Left: Cell pouch immediately after loading with primary hepatocytes, fibrin and collagen. Scale 0.5cm. Right. Cell viability of primary hepatocytes inside the chitosan cell pouch after 24hours in vitro. Green indicates live cells and red indicates dead cells. Scale 200µm.

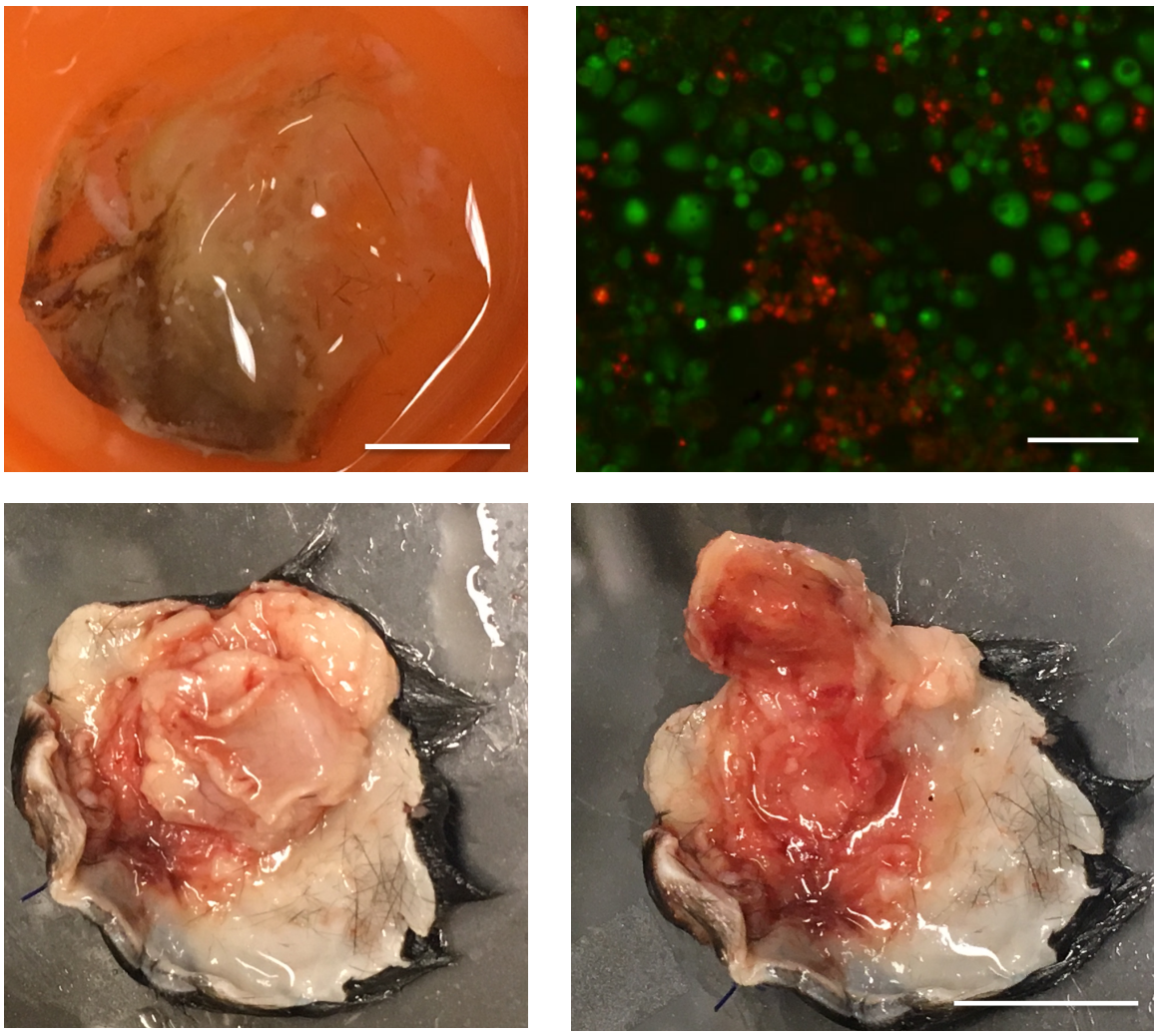

Figure 3. 7: Cell viability of cell pouch post implantation
Top Left. Cell pouch after one week implantation in immunosuppressed mice. Scale 0.5cm. Top Right. Cell viability of primary hepatocytes inside the chitosan cell pouch after one week implantation. Green indicates live cells and red indicates dead cells. Scale 100µm. Top Left and Right show the fibrous capsule that the pouch was retrieved from. Scale 1cm.

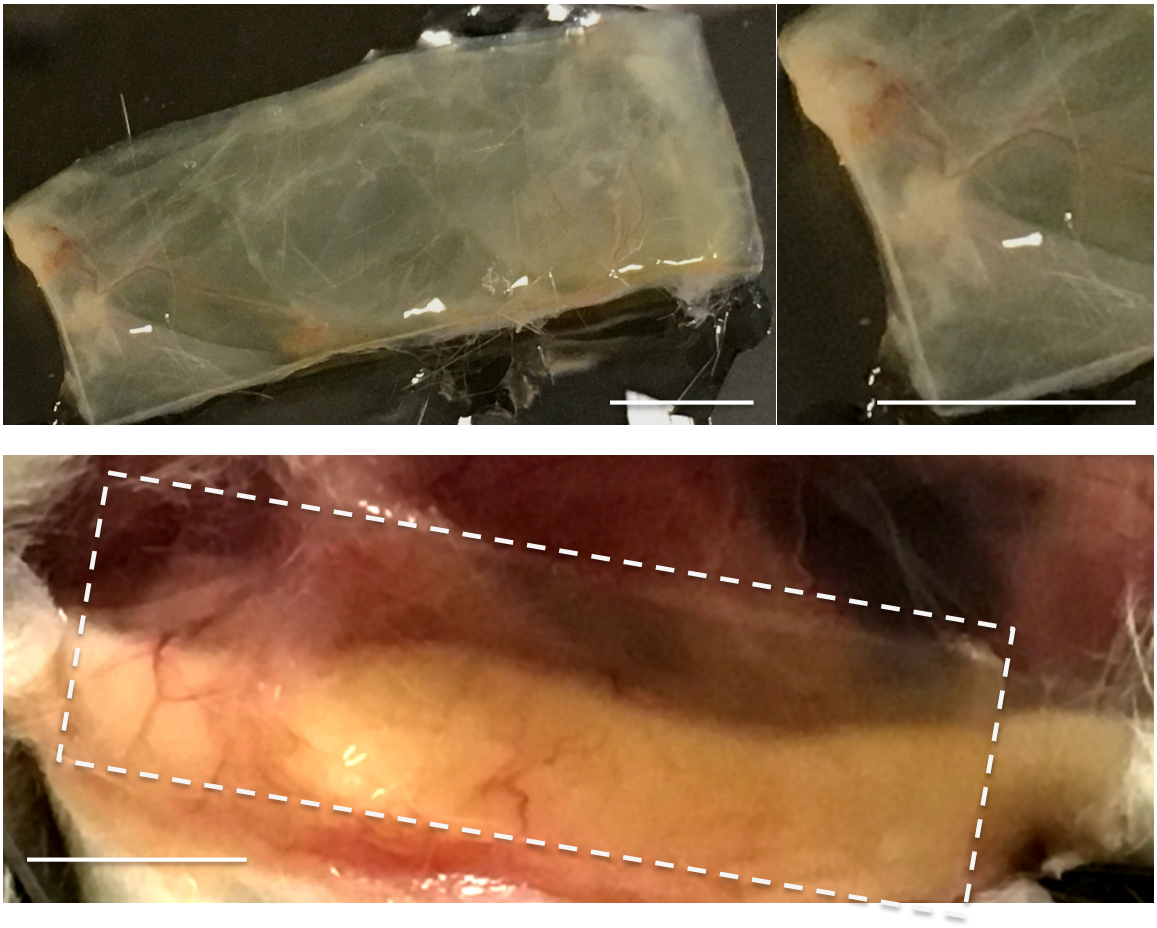

Figure 3. 8: Chitosan film 1 month post implantation in immunosuppressed mice. Top Left. Appearance of chitosan film after 1month implantation in NOD/SCID mice. ECM and blood vessels appear to have attached to the surface of the chitosan film. Top Right. Zoomed in look at the blood vessel formation on the surface of the chitosan film. Scale 0.25cm Bottom. Chitosan film immediately before retrieval from the NOD/SCID mouse. White dotted lines indicate the location of the film. Scale 0.25cm

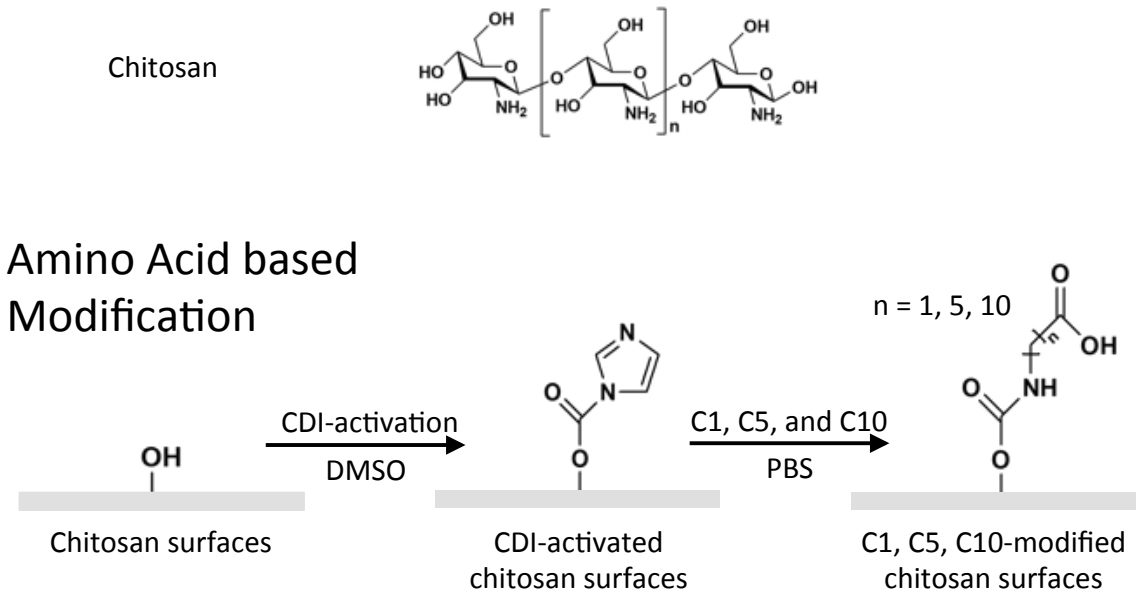

Figure 3. 9: Amino acid surface modification of the Chitosan Pouch
The surface of the chitosan pouch was modified with either C1 (glycine), C5 (6 aminocaporic acid) or C10 (11-aminoundecanoic acid). First the surface was activated using Carbonyldiimidizole (CDI). Then the respective amino acid was added to the CDI-activated chitosan surface.

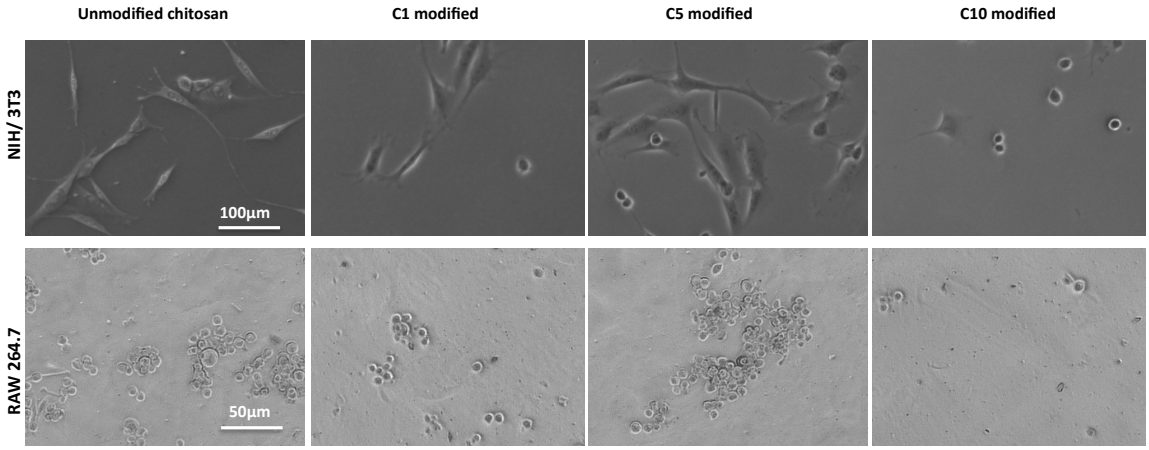

Figure 3. 10: Attachment of NIH/3T3 and RAW 264.7 cells on modified chitosan surfaces

Top panel. Bright-field images of NIH/3T3 cells plated on chitosan films with different surface modifications (unmodified, C1, C5 or C10 modified). Scale 100µm. Bottom panel. Bright-field images of RAW 264.7 cells plated on chitosan films with different surface modifications (unmodified, C1, C5 or C10 modified). Scale 50µm.

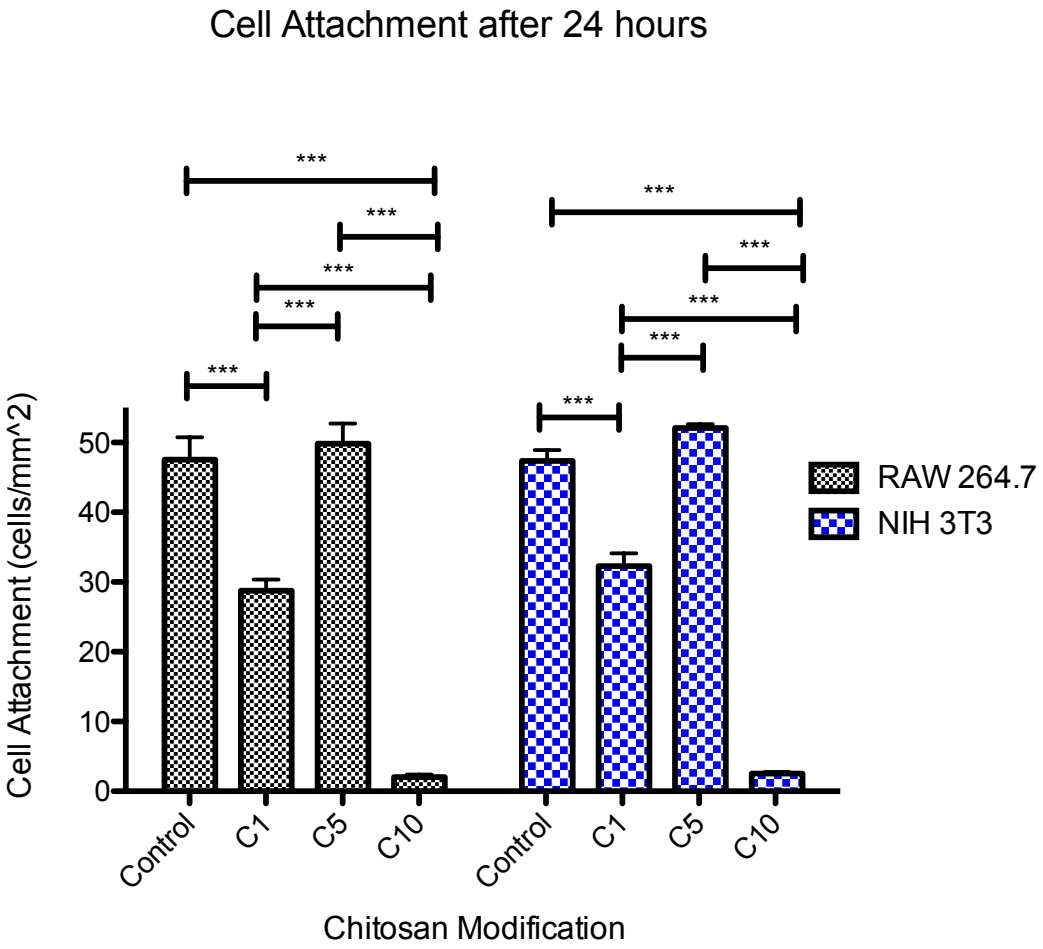

Figure 3. 11: Chitosan modification affects cell attachment
The graph shows the influence chitosan surface modification has on RAW 264.7 (grey) and NIH/3T3 (blue) cell attachment. The control group represents unmodified chitosan. Each group had at least n=6 films. Data are presented as mean ± SE. One-way ANOVA with Tukey post hoc test. ***P<0.0001.

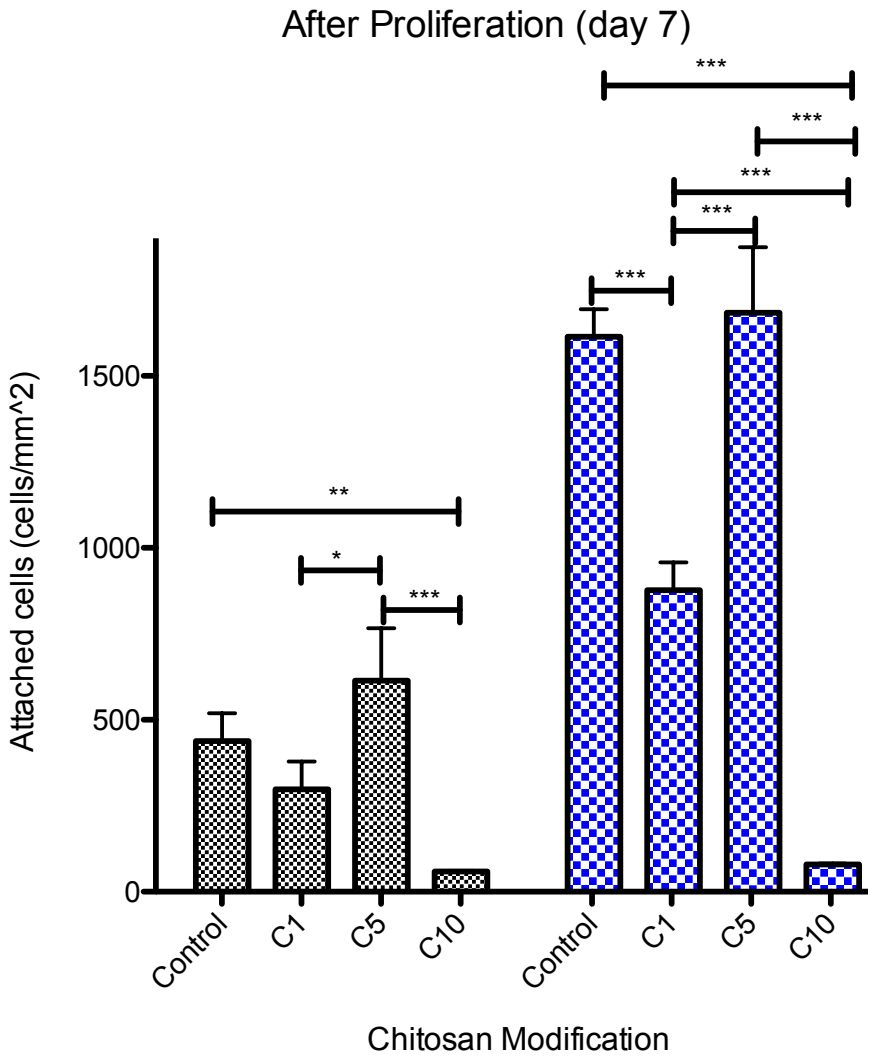

Figure 3. 12: Chitosan modification affects cell proliferation
The graph shows the influence chitosan surface modification has on RAW 264.7 (grey) and NIH/3T3 (blue) cell proliferation. The control group represents unmodified chitosan. Each group had at least n=6 films. Data are presented as mean ± SE. One way ANOVA with Tukey post hoc test. ***P<0.0001. **P<.001. *P<0.01.

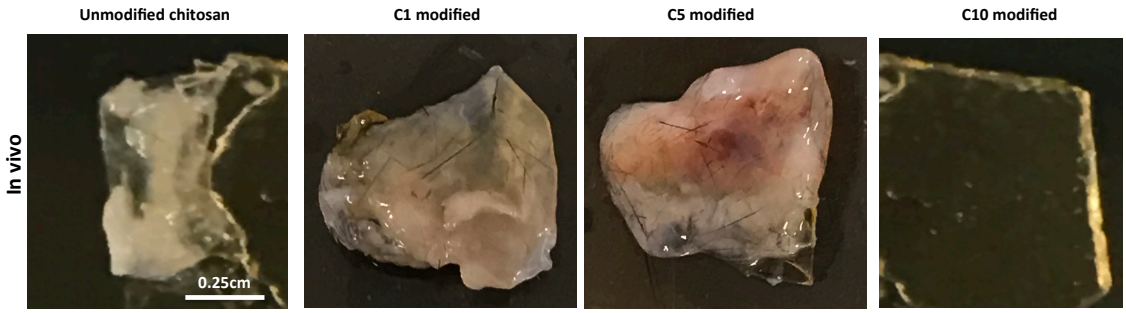

Figure 3. 13: Affect of surface modification on chitosan in vivo
Appearance of chitosan film with different modifications after 2weeks implantation in immune competent mice. Unmodified, C1 and C5 groups appear to have ECM and or cell attachment while the C10 group appears to have little to no deposition. Scale 0.25cm.

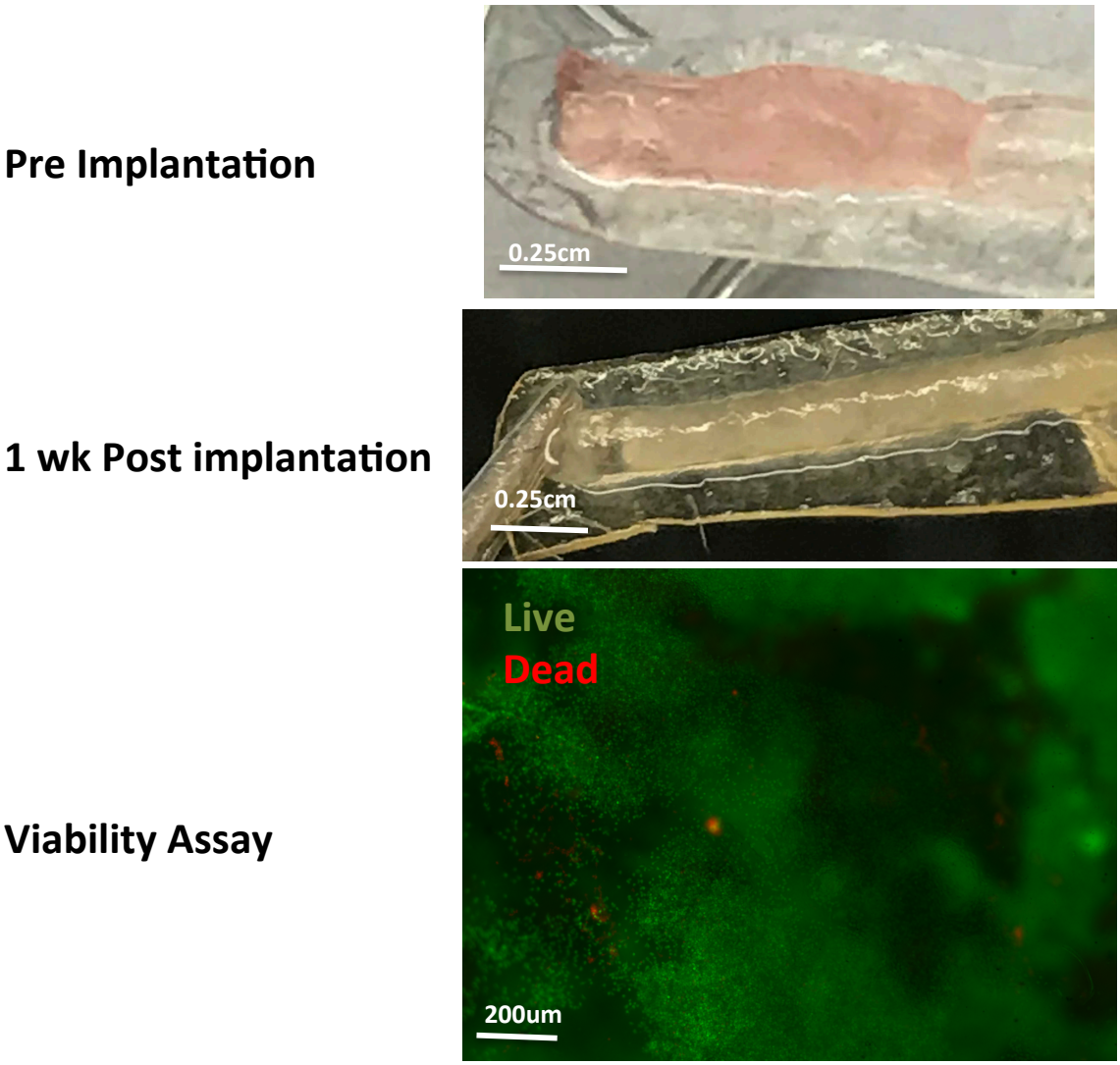

Figure 3. 14: HepG2 viability after 1week transplantation in immune competent mice

Top Panel. C10 modified chitosan cell pouch loaded with 5 million HepG2 cells, fibrin and collagen right before subcutaneous implantation in CD1 immune competent mice. Scale 0.25cm. Middle Panel. 1 week post implantation image of the C10 modified pouch after retrieval from the CD1 mice. Scale 0.25cm. Bottom panel. Live dead analysis of 1 week post implantation HepG2 cells. Green indicated live cells while red indicates dead. Scale 200μm.

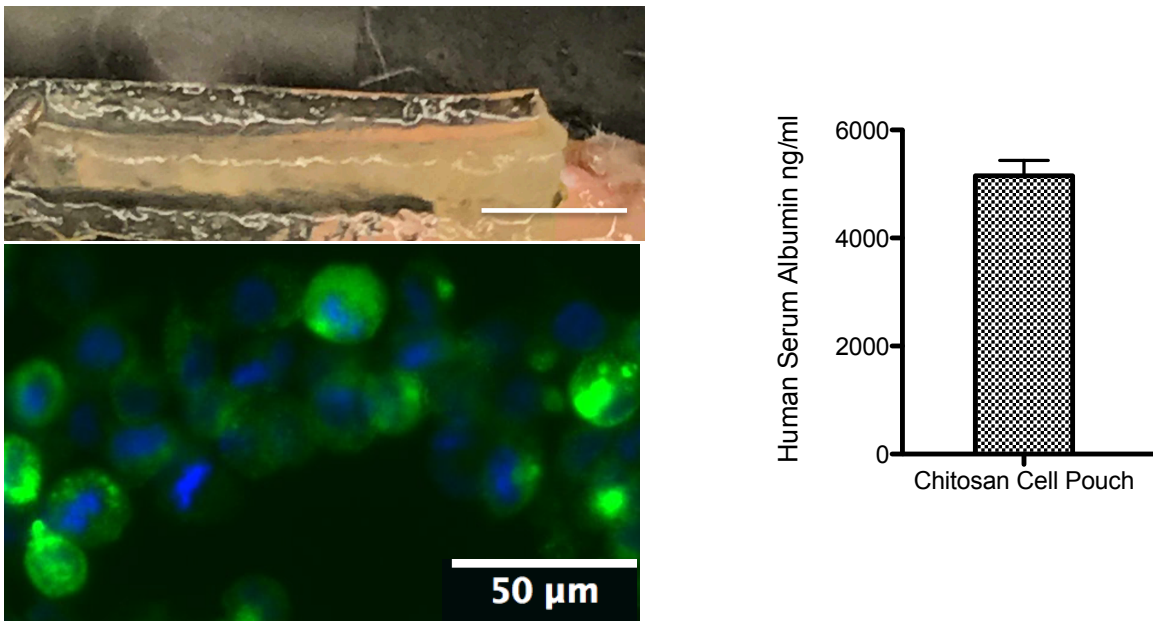

Figure 3. 15: HepG2 albumin secretions after 1month transplantation in immune competent mice

Top Left Panel. C10 modified chitosan cell pouch loaded with 5 million HepG2 cells, fibrin and collagen right after retrieval from the CD1 mice, 1 month post implantation in. Scale 0.25cm. Bottom Left panel. Immunostaining of albumin secreted by HepG2 mice 1 month post implantation. Green indicates presence of albumin. Blue indicates presence of DAPI. Scale 50µm. Right panel. Human Albumin ELISA was used to quantify the albumin present in the mouse serum.

3.9 References

1. Anderson JM, Rodriguez A, Chang DT. Foreign body reaction to biomaterials. Semin Immunol. 2008;20(2):86-100.

2. Langer R. Perspectives and challenges in tissue engineering and regenerative medicine. Advanced materials (Deerfield Beach, Fla). 2009;21(32-33):3235-6.

3. Kenneth Ward W. A review of the foreign-body response to subcutaneously-implanted devices: the role of macrophages and cytokines in biofouling and fibrosis. Journal of diabetes science and technology. 2008;2(5):768-77.

4. Harding JL, Reynolds MM. Combating medical device fouling. Trends Biotechnol. 2014;32(3):140-6.

5. Vegas AJ, Veiseh O, Gurtler M, Millman JR, Pagliuca FW, Bader AR, Doloff JC, Li J, Chen M, Olejnik K, Tam HH, Jhunjhunwala S, Langan E, Aresta-Dasilva S, Gandham S, McGarrigle JJ, Bochenek MA, Hollister-Lock J, Oberholzer J, Greiner DL, Weir GC, Melton DA, Langer R, Anderson DG. Long-term glycemic control using polymer-encapsulated human stem cell-derived beta cells in immune-competent mice. Nat Med. 2016;22(3):306-11.

6. Marks SD. New immunosuppressants in pediatric solid organ transplantation. Current opinion in organ transplantation. 2012;17(5):503-8.

7. Webber A, Hirose R, Vincenti F. Novel strategies in immunosuppression: issues in perspective. Transplantation. 2011;91(10):1057-64.

8. Girlanda R. Complications of Post-Transplant Immunosuppression. In: Andrades JA, editor. Regenerative Medicine and Tissue Engineering. Rijeka: InTech; 2013. p. Ch. 33.

9. Petersen J, Dandri M, Gupta S, Rogler CE. Liver repopulation with xenogenic hepatocytes in B and T cell-deficient mice leads to chronic hepadnavirus infection and clonal growth of hepatocellular carcinoma. Proc Natl Acad Sci U S A. 1998;95(1):310-5.

10. Mazariegos GV, Reyes J, Marino I, Flynn B, Fung JJ, Starzl TE. Risks and Benefits of Weaning Immunosuppression in Liver Transplant Recipients: Long-Term Follow-up. Transplantation proceedings. 1997;29(1-2):1174-7.

11. Vegas AJ, Veiseh O, Doloff JC, Ma M, Tam HH, Bratlie K, Li J, Bader AR, Langan E, Olejnik K, Fenton P, Kang JW, Hollister-Locke J, Bochenek MA, Chiu A, Siebert S, Tang K, Jhunjhunwala S, Aresta-Dasilva S, Dholakia N, Thakrar R, Vietti T, Chen M, Cohen J, Siniakowicz K, Qi M, McGarrigle J, Graham AC, Lyle S, Harlan DM, Greiner DL, Oberholzer J, Weir GC, Langer R, Anderson DG. Combinatorial hydrogel

library enables identification of materials that mitigate the foreign body response in primates. Nature Biotechnology. 2016;34:345.

12. Khor E, Lim LY. Implantable applications of chitin and chitosan. Biomaterials. 2003;24(13):2339-49.

13. Di Martino A, Sittinger M, Risbud MV. Chitosan: A versatile biopolymer for orthopaedic tissue-engineering. Biomaterials. 2005;26(30):5983-90.

14. Feng Z-Q, Chu X, Huang N-P, Wang T, Wang Y, Shi X, Ding Y, Gu Z-Z. The effect of nanofibrous galactosylated chitosan scaffolds on the formation of rat primary hepatocyte aggregates and the maintenance of liver function. Biomaterials. 2009;30(14):2753-63.

15. Haque T, Chen H, Ouyang W, Martoni C, Lawuyi B, Urbanska AM, Prakash S. In vitro study of alginate–chitosan microcapsules: an alternative to liver cell transplants for the treatment of liver failure. Biotechnology Letters. 2005;27(5):317-22.

16. Ayala R, Zhang C, Yang D, Hwang Y, Aung A, Shroff SS, Arce FT, Lal R, Arya G, Varghese S. Engineering the cell–material interface for controlling stem cell adhesion, migration, and differentiation. Biomaterials. 2011;32(15):3700-11.

17. Anderson JM, Rodriguez A, Chang DT. FOREIGN BODY REACTION TO BIOMATERIALS. Seminars in immunology. 2008;20(2):86-100.

18. Zhao QH, McNally AK, Rubin KR, Renier M, Wu Y, Rose-Caprara V, Anderson JM, Hiltner A, Urbanski P, Stokes K. Human plasma alpha 2-macroglobulin promotes in vitro oxidative stress cracking of Pellethane 2363-80A: in vivo and in vitro correlations. J Biomed Mater Res. 1993;27(3):379-88.

19. Christenson EM, Anderson JM, Hiltner A. Oxidative mechanisms of poly(carbonate urethane) and poly(ether urethane) biodegradation: in vivo and in vitro correlations. Journal of biomedical materials research Part A. 2004;70(2):245-55.

20. Kao WJ, Zhao QH, Hiltner A, Anderson JM. Theoretical analysis of in vivo macrophage adhesion and foreign body giant cell formation on polydimethylsiloxane, low density polyethylene, and polyetherurethanes. J Biomed Mater Res. 1994;28(1):73-9.

21. Wiggins MJ, Wilkoff B, Anderson JM, Hiltner A. Biodegradation of polyether polyurethane inner insulation in bipolar pacemaker leads. J Biomed Mater Res. 2001;58(3):302-7.

22. Song E, Ouyang N, Horbelt M, Antus B, Wang M, Exton MS. Influence of alternatively and classically activated macrophages on fibrogenic activities of human fibroblasts. Cellular immunology. 2000;204(1):19-28.

23. Gretzer C, Emanuelsson L, Liljensten E, Thomsen P. The inflammatory cell influx and cytokines changes during transition from acute inflammation to fibrous repair around implanted materials. Journal of biomaterials science Polymer edition. 2006;17(6):669-87.

24. Zhang J, Zhao X, Liang L, Li J, Demirci U, Wang S. A decade of progress in liver regenerative medicine. Biomaterials. 2018;157:161-76.

25. Starokozhko V, Hemmingsen M, Larsen L, Mohanty S, Merema M, Pimentel RC, Wolff A, Emnéus J, Aspegren A, Groothuis G, Dufva M. Differentiation of human-induced pluripotent stem cell under flow conditions to mature hepatocytes for liver tissue engineering. Journal of Tissue Engineering and Regenerative Medicine.0(0).

26. Solanas E, Pla-Palacín I, Sainz-Arnal P, Almeida M, Lue A, Serrano T, Baptista PM. Tissue Organoids: Liver. In: Soker S, Skardal A, editors. Tumor Organoids. Cham: Springer International Publishing; 2018. p. 17-33.

27. Enosawa S, Miyashita T, Suzuki S, Li XK, Tsunoda M, Amemiya H, Yamanaka M, Hiramatsu S, Tanimura N, Omasa T, Suga K, Matsumura T. Long-term culture of glutamine synthetase-transfected HepG2 cells in circulatory flow bioreactor for development of a bioartificial liver. Cell transplantation. 2000;9(5):711-5.

28. Wang N, Tsuruoka S, Yamamoto H, Enosawa S, Omasa T, Sata N, Matsumura T, Nagai H, Fujimura A. The bioreactor with CYP3A4- and glutamine synthetase-introduced HepG2 cells: treatment of hepatic failure dog with diazepam overdosage. Artificial organs. 2005;29(8):681-4.

Chapter 4: Modified Chitosan pouches for allogeneic and xenogeneic transplantation of primary hepatocytes

4.1 Abstract

The ectopic transplantation of primary hepatocytes has the potential to provide a minimally invasive treatment for genetic liver disorders, like hemophilia B and alpha-1-antitrypsin deficiency, by providing a source of healthy hepatocytes to produce the deficient liver proteins. Current research attempts to transport primary hepatocytes have been invasive and conducted in immunosuppressed systems. While immunosuppression is a common clinical practice to help reduce organ rejection, patients are still plagued by adverse effects resulting from a lifetime of immunosuppressive therapy. To address these issues, more research is being done to provide solutions for transplantation in immune competent systems. Here we describe the minimally invasive, ectopic transplantation of primary hepatocytes in immune competent mice. We demonstrated that the C-10 modified chitosan pouch was capable of facilitating both allogeneic and xenogeneic transplantation of primary hepatocytes in CD1 mice. The allogeneic transplantation of C57BL/6J primary hepatocytes was successful as the cells remained functional and produced albumin up to 1 month post transplantation. The xenogeneic transplantation of primary human hepatocytes was also successful as evidenced by the presence of human albumin and human alpha-1-antitrypsin in the CD1 mice serum up to 1 month post transplantation (the longest experimental time-point investigated).

Key words Chitosan pouch; immune competent; xenogeneic: allogeneic; primary hepatocyte transplantation; subcutaneous implantation: minimally invasive

4.2 Introduction

Liver diseases/disorders affect over 30 million people in United states alone(1). These diseases can be further categorized into genetic, example alpha-1-antitrypsin deficiency(2), virus based, example hepatitis C(3), or lifestyle based, example alcoholic liver disease(4). Even though the regenerative nature of the liver may be substantial enough to cure or reverse some lifestyle-based diseases, it does not help in the case of genetic disorders, since the genetically defective cells will continue to regenerate. Therefore genetic disorders like alpha-1 antitrypsin deficiency(2) or hemophilia B(5, 6) would require either whole or partial organ transplantation to be cured(7-9), or lifelong protein supplements to be treated(5, 10). Since donor organs are limited, transplantation is usually reserved for diseases leading to acute liver failure (ALF) or end stage liver disease (ESLD), and patients with genetic disorders usually have to settle for a lifetime of protein supplement therapy. Such therapies are usually very costly and can become complicated if the patient develops inhibitory antibody complications(11).

Cell transplantation is currently being considered as a therapeutic approach to treat genetic liver disorders(5, 12, 13). While a recent study successfully demonstrated the treatment of a monogenetic liver disorder by transplanting primary liver cells to the host liver(5); like other cell therapy approaches before it, the transplantation was invasive, suffered from engraftment issues and was conducted in immunosuppressed animals(5). The development of biomaterial-based solutions may be the key to improving such cell therapy approaches. Firstly, biomaterials can incorporate ECM components that provide the necessary structural and biochemical environment for improved cellular function(14). Secondly, biomaterials can overcome the need for immunosuppression by

encapsulating transplanted cells and protecting them from rejection by the host immune system(15, 16).

In Chapter 3 we determined that the 11-aminoundecanoic acid (C-10) surface modification of the chitosan cell pouch was capable of mitigating the immune response by reducing the attachment of immune cells, fibroblasts and ECM. Furthermore, the C-10 pouch facilitated the successful transplantation of HepG2 cells in immune competent mice. Here we showcased the potential of the pouch to facilitate the subcutaneous allogeneic and xenogeneic transplantation of primary hepatocytes. Our results demonstrated that the C-10 chitosan pouch was capable of supporting and maintaining the allogeneic and xenogeneic transplantation of primary hepatocytes. To our knowledge this is the first demonstration of successful biomaterial based, minimally invasive transplantation of primary hepatocytes in immune competent mice. Based on this success, these devices can be potentially used as therapeutic tools to treat genetic liver disorders.

4.3 Methods and Materials

4.3.1 Preparation of Chitosan solution

8g Chitosan (medium molecular weight, Sigma), 40ml glacial acetic acid and 360ml Milli-Q water were added in that order to a 500mL glass beaker. The mixture was stirred overnight. After mixing the solution was transferred into 50ml tubes and centrifuged at 3000rpm for 10minutes to allow any unmixed particles to settle. The chitosan solution was separated from the unmixed particles and stored for future use.

4.3.2 Chitosan pouch development

The first layer was cast by pouring 15ml of the chitosan solution into a 10cm

glass petri dish. The dish was heated at 50 °C for 3hrs or until cured. 18 Gauge PTFE tubing (SWTT-18-C, Zeuss) cut into 1cm pieces were used as a mold to create the cell pouch. The molds were placed on the cured layer. Another layer was cast by pouring 15ml (or the amount necessary to fully cover the mold and previous layer) of chitosan solution over the mold and the previous layer. This layer was heated and cured at 50 °C for 3hrs. Once fully cured, the chitosan was neutralized by adding 2.5M NaOH to the dish for at least 10 minutes. The NaOH was then replaced with PBS for 15minutes. Then a spatula was used to carefully lift the chitosan structures off of the petri dish. The pouches were then cut out and the tubing was removed. The pouch was then modified.

4.3.3 Chitosan Modification

After making the chitosan pouch, the outer surface was modified with the C10: 11-aminoundecanoic acid (Aldrich). First, hydroxyl groups were activated by immersing pouch in DMSO containing 1,1'-carbonyldiimidazole CDI (80mg/ml) for 2hrs. Then, the chitosan was washed vigorously with DMSO (x3). C10 was then dissolved in pH8 PBS (2mg/mL). The chitosan was soaked in this solution overnight. After the modification process was complete the pouch was rinsed in PBS then sterilized by a series of ethanol washes and subsequent PBS washes. The final wash was performed using Pen Strep PBS.

4.3.4 Primary mouse hepatocyte isolation and culture

Cells were isolated based on a previously described method(17). All animal procedures were approved by the Institutional Animal Care and Use Committee of the University of California, San Diego and performed in accordance with the NIH and

national and international guidelines for laboratory animal care. Briefly, mice (2-4 month old wild type C57BL/6J) were euthanized and the livers were removed. Livers were washed with PBS then suspended in a collagenase solution and incubated for 20 minutes to break down ECM. Then the livers were transferred to a petri dish containing DMEM. The liver sack was sliced and moved back and forth vigorously to release cells. The cells were collected, centrifuged and then plated on a collagen I-coated 6-well plate. Albumin immunostaining was performed to ensure that the isolated cell mixture contained hepatocytes. We were not concerned with achieving 100% cell purity since the supporting cells could help improve the function of the primary hepatocytes. Cells were cultured for 24 hours in maintenance media (MM250, LONZA) before being loaded into the pouch.

4.3.4. ECM Decellularization

The ECM of the livers was prepared using a previously established protocol(18). Briefly, on day 1 the intact livers were removed from the mice, cut into smaller pieces and washed with PBS (1X) for 24 hours to remove blood residues. PBS was continuously changes throughout the 24hrs as needed. On day 2 livers were transferred to a 1% solution of Triton X-100. The solution was continuously changed throughout the day as needed. On day 3, the livers were transferred to 0.1% Triton X-100 solutions for washing for the first 12 hours. In the second twelve hours the livers were washed in PBS. All washing took place on a shaker at 4°C. The resulting decellularized ECM was then frozen and stored at -80°C until ready for milling. Samples were milled using 6875 Freezer/ Mill (SPEX SamplePrep) High capacity sample grinder then lyophilized and stored at -20°C.

4.3.5 Cell loading

Primary human hepatocytes (HUM 4113, Lonza) were thawed in thawing media (MCHT50; Lonza) and centrifuged for 10 minutes at 100 g. Next, thrombin (2 U/ml) was added to the cell pellet. Next, a 5%(v/v) solution of collagen type I (rat tail, Corning) in endothelial growth media solution was added to the pellet. Decellularized ECM (1mg/ml) was then added. The cell mixture containing 6 million hepatocytes and ECM was then added to a syringe and infused into the pouch. Immediately, fibrinogen 8mg/mL was added to the outside of the pouch, and allowed to diffuse in to form a gel with the thrombin. Finally, the pouch was sealed with an acrylate-based glue (allowed to fully dry) and incubated with maintenance media (MM250, LONZA) until ready for use. As indicated by the figure captions, in some cases the pouch was filled with primary mouse hepatocytes instead of primary human hepatocytes. Additionally, in allogeneic studies to compare ECM, some groups contained no decellularized ECM.

4.3.7 Subcutaneous implantation of Chitosan Pouch

All animal procedures were approved by the Institutional Animal Care and Use Committee of the University of California, San Diego and performed in accordance with the NIH and national and international guidelines for laboratory animal care. Subcutaneous implantation of the cell-laden chitosan pouch was performed 1 day after loading and culture *in vitro*. Recipient mice (CD1 wild type, 3-4month old) were administered with ketamine (100 mg/kg) and xylazine (10 mg/kg), and the fur on the back was shaved. Mice were then placed on a heating pad and a 1 cm-long incision was

made in the back of the mice, and one subcutaneous pouch was inserted by blunt dissection using a 1 cm-wide spatula on the left side of the mouse. The skin was sutured once the pouch was implanted.

4.3.8 Albumin measurement

Enzyme linked immunosorbent assay (ELISA) was performed to assess the albumin production of the implanted cells. All animal procedures were approved by the Institutional Animal Care and Use Committee of the University of California, San Diego and performed in accordance with the NIH and national and international guidelines for laboratory animal care. In short, for xenogeneic groups, on the day of implant retrieval, blood was collected from the heart of the mice. The blood was then centrifuged at 14900 g at 4 Degrees Celsius (°C) for 15 min. to separate and extract the serum. The serum was assessed for human albumin by using the Human Albumin ELISA Quantitation Set (Bethyl Labs, Catalogue no. E80-129) according to the manufacturer's protocol. For allogeneic groups blood analysis was not possible since it would be difficult to distinguish the albumin of the implanted cells versus host cells. Thus, the implanted cells were retrieved from the implant and replated unto collagen coated tissue culture plastic dishes. After 24 hours the media was collected and used for albumin analysis.

4.3.9 Alpha-1-antitrypsin assay

Enzyme linked immunosorbent assay (ELISA) was performed to assess the human alpha-1-antitrypsin (hA1AT) production of the implanted cells. All animal procedures were approved by the Institutional Animal Care and Use Committee of the

University of California, San Diego and performed in accordance with the NIH and national and international guidelines for laboratory animal care. In short, for xenogeneic groups, on the day of implant retrieval, blood was collected from the heart of the mice. The blood was then centrifuged at 14900 g at 4 Degrees Celsius (°C) for 15 min. to separate and extract the serum. The serum was assessed for hA1AT by using the Human alpha-1-antitrypsin ELISA Quantitation Set (Bethyl Labs, Catalogue no. E88-122) according to the manufacturer's protocol.

4.3.10 Immunostaining

Post implantation constructs were retrieved and cells were replated for 24hours. Next, cells were washed with PBS, then fixed with 4% paraformaldehyde (PFA, Sigma Aldrich) at 4 °C overnight. For immunofluorescent staining, cells were blocked with blocking buffer containing 3% (w/v) bovine serum albumin (BSA; 60 min, RT) and 0.1% Triton X-100 (v/v) in PBS. Cells were stained for either FITC conjugated human albumin (1:500; Bethyl Labs) or CK18 (1:500; R&D Systems) or CYP 3A4 (1:500; Invitrogen) or Cyp 1A2 (1:500; Santa Cruz) overnight at 4 °C. An appropriate secondary antibody Alexa Fluor 488 (1:200; Thermo Fisher) along with Hoechst 33342 (2 µg/mL; Thermo Fisher) was used to bind primary antibodies for 1 h at RT. Then samples were imaged with fluorescent microscopy.

4.3.11 Statistics

All experiments were independently repeated at least twice with replicate samples as indicated in figure captions. Statistical analysis was performed using one-way

ANOVA and Tukey's post hoc test or a t test for group comparisons to determine statistical significance ($p < 0.05$). Errors bars represent SEM. GraphPad Prism 5 software was used to determine all statistical analysis.

4.4 Results

4.4.1 Effect of varying ECM composition on the function of transplanted cells

The chitosan cell pouch was successfully prepared and modified according to figure 4.1. After the appropriate sterilization, the C-10 modified chitosan pouch was loaded with 6 million hepatocytes isolated from C57BL/6J mice. Then we varied the ECM environment of the cells in the pouch by loading them with either i) collagen, fibrin, decellularized liver ECM or ii) fibrin and collagen (Figure 4.2). The resulting positive albumin staining of the cells indicated that the isolation process was successful and primary mouse hepatocytes were indeed amongst the cells loaded into the pouch (Figure 4.3). One month after subcutaneous transplantation, chitosan pouches with the varying ECMs were retrieved and re plated for albumin analysis. ELISA results indicated that the pouches containing added decellularized liver ECM produced more albumin than the pouches containing just collagen and fibrin alone (Figure 4.4). Given this statistically significant difference, all subsequent transplantations were performed with pouches loaded with decellularized ECM, fibrin and collagen.

4.4.2 Allogeneic transplantation of C57BL/6J primary mouse hepatocytes in CD1 immune-competent mice

To study the success of allogeneic transplantation of primary mouse hepatocytes in immune competent mice, subcutaneously transplanted pouches were retrieved for analysis at 1 week and 1 month time points. Because the albumin from the transplanted mice cells cannot be distinguished from the albumin produced by host liver cells, albumin had to be measured from the transplanted cells after they were retrieved and re-plated. Albumin ELISA results (Figure 4.5) indicated that the cells retrieved at 1 week and 1 month secreted albumin and were therefore still functional. Even though cells retrieved from 1 month explants produced slightly less albumin than the 1 week explants, it was not a statistically significant difference. Week 1 and 1 month cells were also compared to freshly plated hepatocytes. The freshly plated hepatocytes produced more albumin than the other groups. This may be because the excised hepatocytes were being moved to a new environment and needed more time to acclimatize to stabilize their function. Albumin staining of the excised chitosan pouch (Figure 4.6) further confirmed that the transplanted cells were functional and that the allogeneic primary mouse hepatocyte transplantation was successful.

4.4.3 Xenogeneic transplantation of primary human hepatocytes in immune competent mice

To study the success of xenogeneic transplantation of primary human hepatocytes in immune competent mice, subcutaneously transplanted pouches were retrieved for analysis at week 1 and week 4 time points. The contents of the pouches appeared to be

brown, the color of the densely packed primary human hepatocytes in colorless media and ECM (Figure 4.7). The pouches retrieved at week 4 appear to be more shrunken and dry compared to those retrieved at week 1. This may indicate that the pouch may require additional modification in the future to help maintain its moisture and prevent shrinking. The pouches were also stained for human specific hepatocyte markers Ck18 and albumin to ensure that cells were viable and functional. At both time points cells were positive for both hepatocyte markers and appeared to be clumped (Figure 4.8). To quantify the function of the hepatocytes, serum from the mice were analyzed for human albumin secretion and hA1AT. A similar trend was observed for both functional markers, in that the function of the hepatocytes increased between the week 1 and week 4 time points (Figure 4.9 and 4.10).

4.5 Discussion

This study describes the successful use of the C-10 modified chitosan cell pouch for the allogeneic and xenogeneic transplantation of primary mouse and primary human hepatocytes, respectively, in immune competent mice. We first used the pouch to demonstrate that the ECM composition does have an affect on the function of the transplanted primary hepatocytes. Then we demonstrated that the chitosan cell pouch could successfully transplant and maintain the function of primary mouse hepatocytes and primary human hepatocytes in immune competent CD1 mice. Both the allogeneic and xenogeneic transplants exhibited little to no detrimental foreign body rejection characteristics and were capable of supporting hepatocyte viability and function, as

evidenced by the secretion of albumin (and hA1AT, in the case of human hepatocytes), for one month (the longest experimental time point).

In chapter three, we demonstrated the successful transplantation of HepG2 cells using the C-10 modified chitosan cell pouch. However, because HepG2 cells are a cancer cell line, they are more robust and are less sensitive to their culture environment as compared to primary cells. Therefore, in order to demonstrate the full potential of the pouch, it was important to validate that it was capable of transplanting primary hepatocytes, which have been known to be especially sensitive to their environment(19, 20). Such sensitivity can result in reduced viability and function of hepatocytes. Therefore, it stands to reason that when hepatocytes are transplanted ectopically, recreating an ECM environment similar to the native liver may be the key to improving cell transplantation outcomes. Therefore, we used the chitosan cell pouch as a tool to validate that the composition of the environment for the transplantation of primary mouse hepatocytes does indeed impact function. Results indicated that the addition of decellularized liver ECM significantly improved the albumin secretion of primary mouse hepatocytes (Figure 4.4). This is most likely because the decellularized ECM is more complex in both composition and structure than just collagen and fibrin alone. The decellularized ECM most likely contains other liver ECM components like laminin, fibronectin, collagen III and collagen IV, among other things(21, 22). These ECM components may be capable of sequestering growth factors like hepatocyte growth factor that plays an instrumental role in liver regeneration and repair(23, 24).

In addition to looking at albumin secretions to measure hepatic function, in the case of the primary human hepatocytes, we also chose to assay for hA1AT. hA1AT is a

protease inhibitor produced by the liver(2). Patients who have hA1AT deficiency can develop lung disease or liver disease(25). Therefore, the ability of the transplanted cells to produce this protein can provide preliminary evidence to prompt research into the use of the chitosan pouch to treat this genetic disorder. A cell therapy treatment for hA1AT and other genetic liver disorders can dramatically improve the quality of life of patients. Moreover, providing a cell therapy that does not require immune suppression would eliminate the need for lifelong immunosuppression therapy and the adverse affects that usually come along with it. While further extensive studies are necessary to validate the potential of this therapy in immune competent systems, findings in this area can have a significant impact on the future of not just liver cell transplantation therapies but on cell transplantation therapies in general.

4.6 Conclusion

Cell transplantation is a promising approach to providing better treatments and improvements to the quality of life of people with genetic liver disorders. The incorporation of biomaterials can improve the outcomes of cell transplantation by not only increasing cell viability and maintaining cell function, but also by facilitating successful transplantation without the need for immunosuppression. To our knowledge, no previous study has evaluated the potential of modified chitosan pouches to be used as an allogeneic and xenogeneic primary hepatocyte transplantation device in immune competent mice. To address this issue we have demonstrated that a C10 modified chitosan cell pouch was capable of minimally invasive allogeneic and xenogeneic transplantation of primary hepatocytes in immune competent CD1 mice. Furthermore, results show that the transplanted cells maintained function for 1month, the longest

assayed time point. Though results are preliminary and proof of concept, promising findings suggest that this device may be a useful tool in treating liver deficiencies. The presence of hA1AT, indicates that the transplanted cells can successfully produce this protein. The next steps would be to test out the device in A1AT animal models, to determine whether the A1AT produced is enough to reverse the phenotype.

4.7 Acknowledgements

Chapter 4, in full, is currently being prepared for use in part of a publication for submission. "Modified Chitosan Cell Pouch for allogeneic and xenogeneic hepatocyte transplantation." Seale NM, Ryu JH. , Nayak P., Varghese S. The dissertation author is the primary investigator and author of this material. I would also like to acknowledge Zulfar Ghulam-Jelani for helping in the milling the decellularized ECM.

4.8 Figures

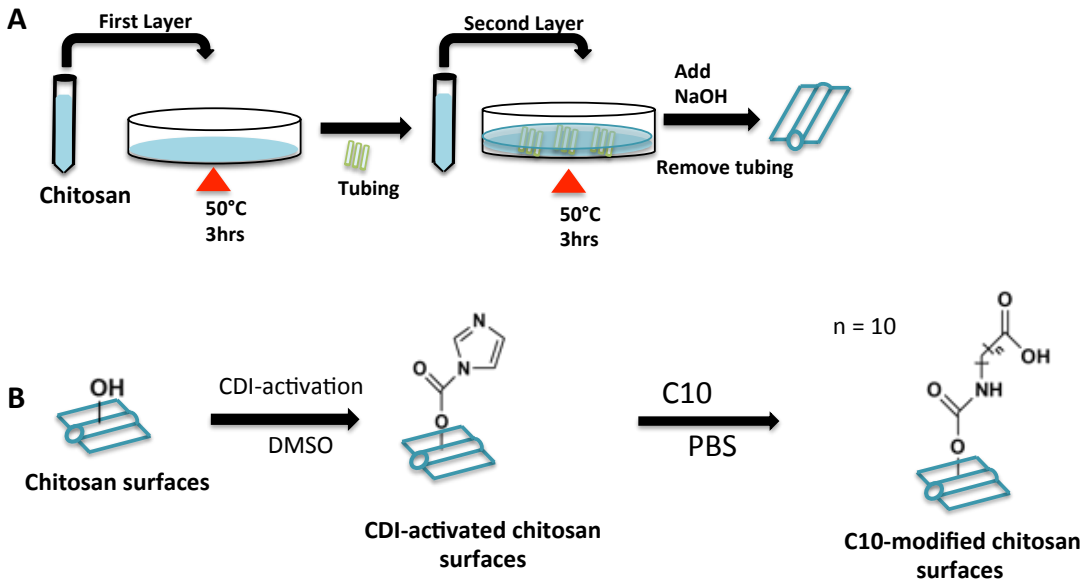

Figure 4. 1 Schematic of C-10 modified chitosan cell pouch fabrication

A. Chitosan pouch is first fabricated by curing two layers of chitosan around a PTFE tubing mold. B. The surface of the chitosan pouch is modified by first performing CDI activation, then conjugating with the C10 amino acid chains.

Figure 4. 2 Modified chitosan cell pouch loaded with primary mouse hepatocytes

C-10 modified cell pouch containing primary mouse hepatocytes. Contents of the pouch appear to be pink, the color of the culture media and fibrin used in loading the pouch. Pouch dimensions are 1cm internal length and 2.5mm internal diameter. Scale 0.25cm.

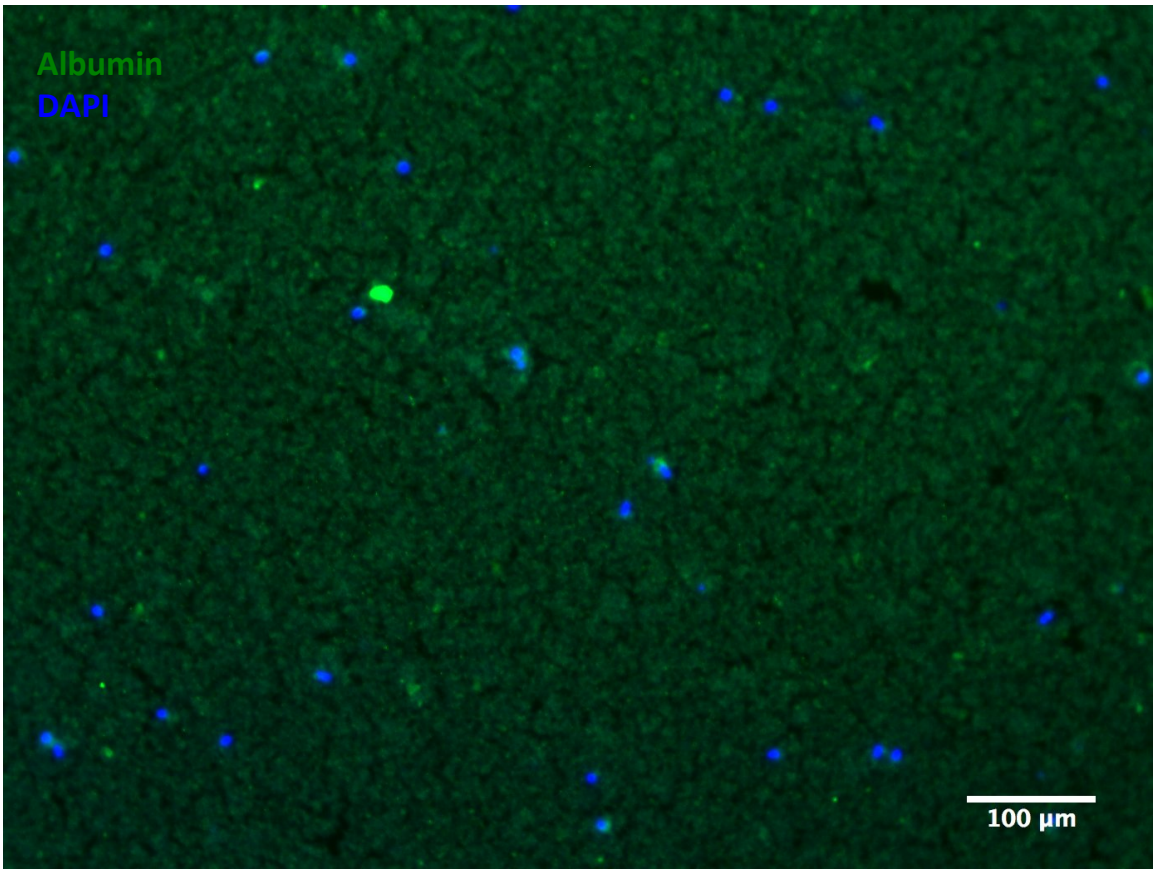

Figure 4. 3 Immunostaining of isolated primary mouse hepatocytes

Albumin staining was performed on the hepatocytes isolated from the C57BL/6J mice livers. Positive Albumin (green) and DAPI (blue) staining indicates that the cells loaded into the pouches for use in the allogeneic transplantation experiments contained primary mouse hepatocytes. Scale 100µm.

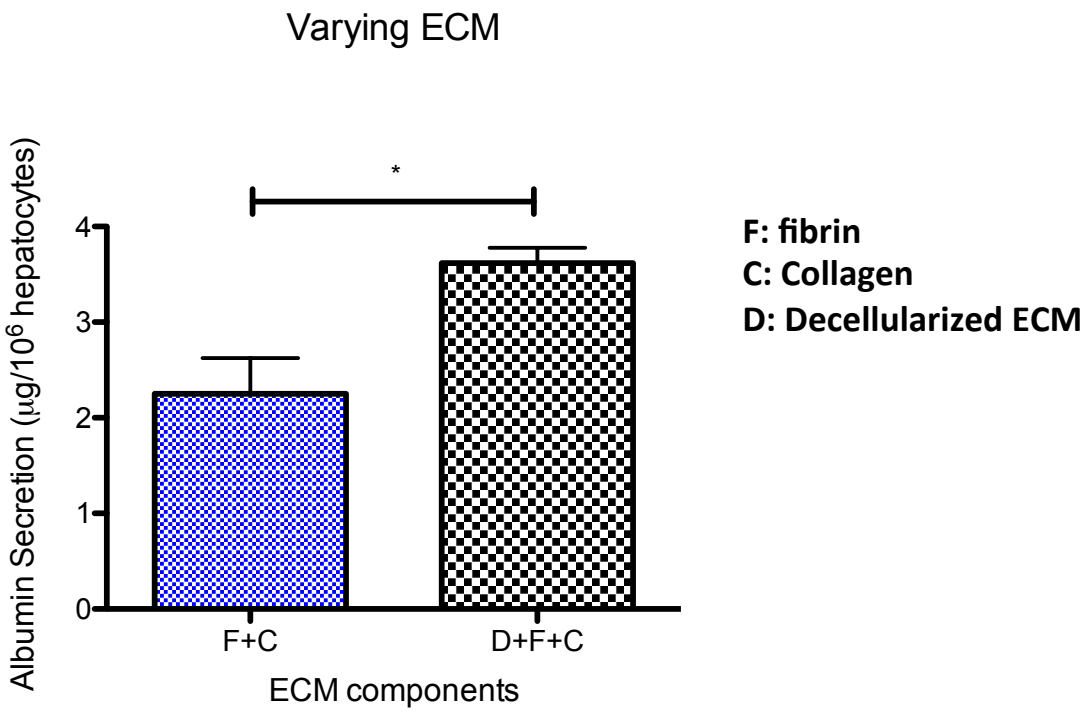

Figure 4. 4 The affect of ECM composition on the function of transplanted primary mouse hepatocytes

Primary mouse hepatocytes (C57BL/6J) were loaded with different ECM components and transplanted in CD1 immune competent mice for one month. Albumin ELISA was done to assess the function of the cells after this period. The graph indicates that the addition of decellularized ECM resulted in significantly higher albumin production. Data are presented as mean ± SE. Number of samples for each group equals 4. A t test was performed. *P<0.0279

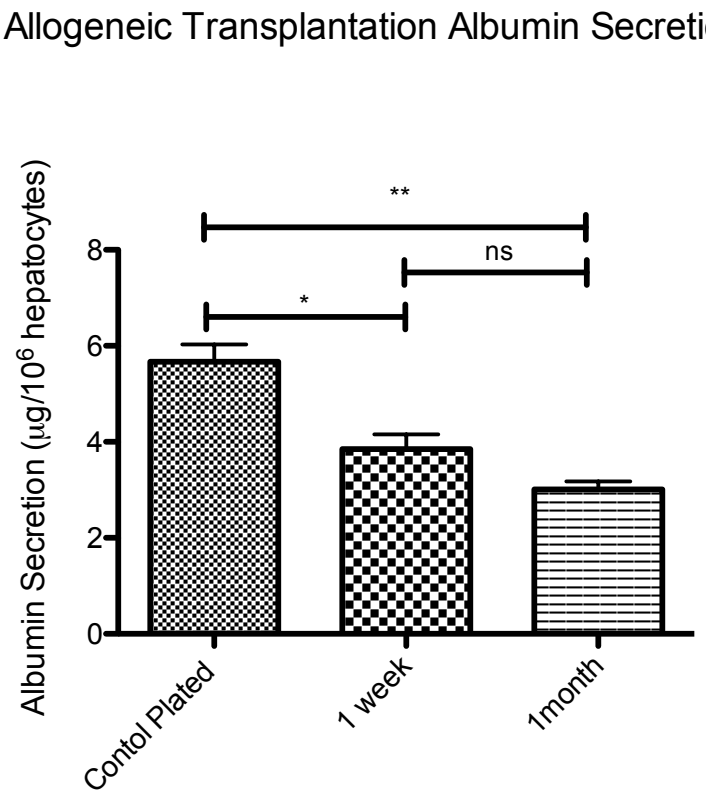

Figure 4. 5 Albumin secretions of Allogeneic Transplanted primary mouse hepatocytes

Secretion of mouse albumin for control plated cells and replated cells that were retrieved 1 week and 1 month post implantation. Data are presented as mean ± SE obtained from 3 engineered constructs ($n = 3$). One-way ANOVA with Tukey post hoc test. *$P < 0.05$. **$P < 0.01$.

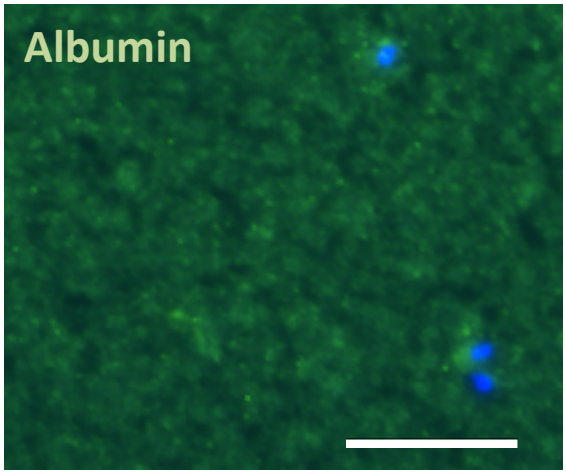

Figure 4. 6 Albumin Immunosaining of primary mouse hepatocytes 1 month post implantation.

Cells retrieved from 1month explants were re-plated and stained for albumin (green). Positive albumin staining corroborates the ELISA analysis and proves that the cells were able to survive and remain functional even after 1 month of transplantation in immune competent mice. Scale 100μm.

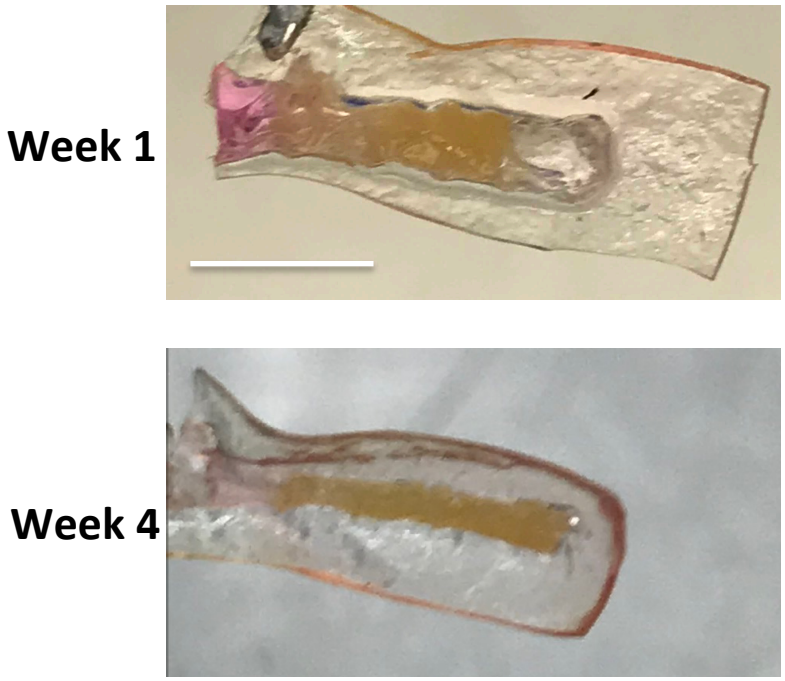

Figure 4. 7 Xenogeneic primary human hepatocyte excised chitosan cell pouches

Whole mount images of chitosan cell pouches at week 1 and week 4 post implantation. Contents of the pouch appear brown, the color of the human hepatocytes. The size of the week 4 pouch appears more shrunken indicating that some drying of the pouch may have occurred. Scale 0.5cm.

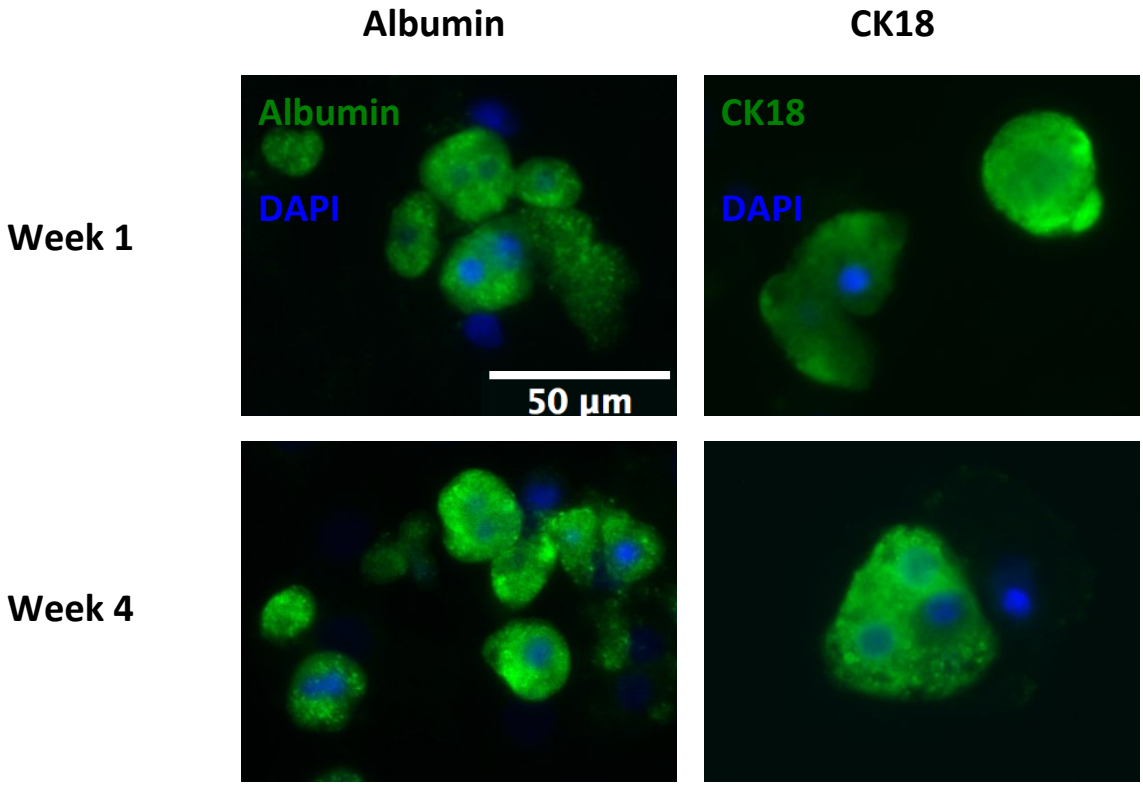

Figure 4. 8 Immunostaining of primary human hepatocytes post xenogeneic transplantation

Immunostaining of hepatocyte functional markers albumin (left panel, green) and CK18 (right panel, green) at week 1 and week 4 post transplantation. At both time points cells were positive for both hepatocyte markers. Scale 50µm.

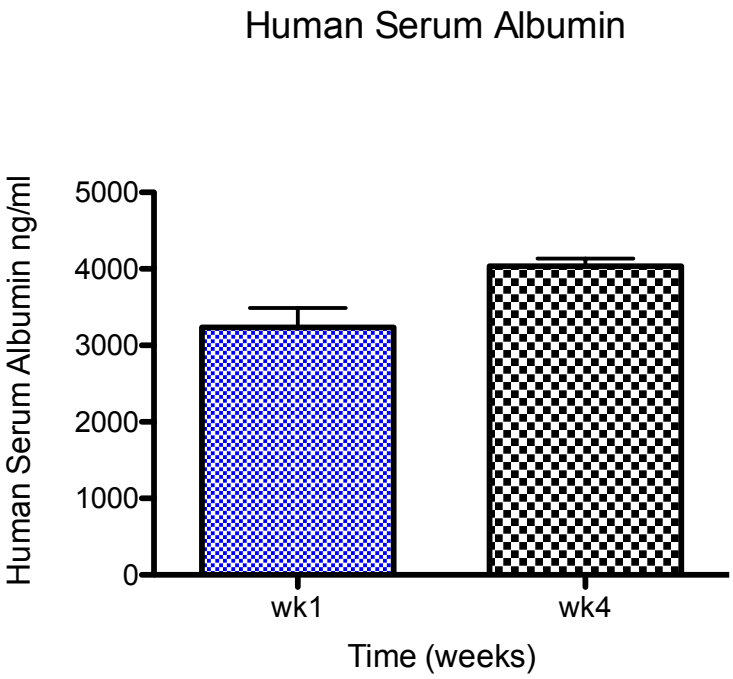

Figure 4. 9 Quantification of human serum albumin

Quantification of the human albumin present in the serum of the CD1 mice at 1 week and 4weeks post implantation. Data are presented as mean ± SE obtained from 4 engineered constructs ($n = 4$). The t test performed indicated that there was no significant difference between week 1 and week 4 albumin secretions.

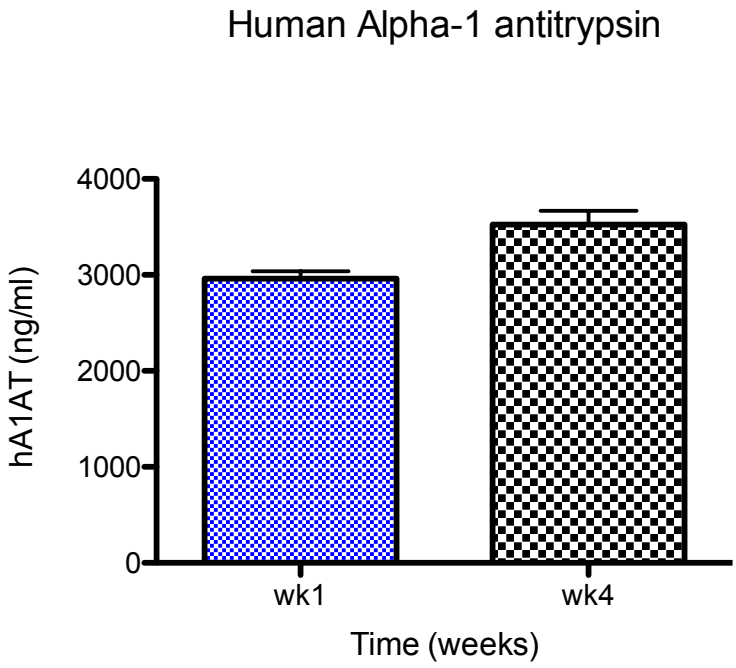

Figure 4. 10 Quantification of human alpha-1-antitrypsin

Quantification of the human alpha-1-antitrypsin (hA1AT) present in the serum of the CD1 mice at 1 week and 4weeks post implantation. Data are presented as mean ± SE obtained from 4 engineered constructs ($n = 4$). The t test performed indicated that there was no significant difference between week 1 and week 4 hA1AT production.

4.9 References

1. Heron MeaDFDfiNVSR, Vol. 57 (Centers for Disease Control and Prevention, Hyattsville, Maryland, 2009).

2. DeMeo DL, Silverman EK. Alpha1-antitrypsin deficiency. 2: genetic aspects of alpha(1)-antitrypsin deficiency: phenotypes and genetic modifiers of emphysema risk. Thorax. 2004;59(3):259-64.

3. Williams R. Global challenges in liver disease. Hepatology (Baltimore, Md). 2006;44(3):521-6.

4. Mandayam S, Jamal MM, Morgan TR. Epidemiology of alcoholic liver disease. Seminars in liver disease. 2004;24(3):217-32.

5. Ramaswamy S, Tonnu N, Menon T, Lewis BM, Green KT, Wampler D, Monahan PE, Verma IM. Autologous and Heterologous Cell Therapy for Hemophilia B toward Functional Restoration of Factor IX. Cell Reports. 2018;23(5):1565-80.

6. Ramaswamy S, Tonnu N, Tachikawa K, Limphong P, Vega JB, Karmali PP, Chivukula P, Verma IM. Systemic delivery of factor IX messenger RNA for protein replacement therapy. Proceedings of the National Academy of Sciences. 2017;114(10):E1941-E50.

7. A. DM, C. AP, David G, N. GC, R. WI, J. WW. Orthotopic liver transplantation in a patient with combined hemophilia A and B. American Journal of Hematology. 1990;33(2):136-8.

8. Merion RM, Delius RE, Campbell DA, Jr., Turcotte JG. Orthotopic liver transplantation totally corrects factor IX deficiency in hemophilia B. Surgery. 1988;104(5):929-31.

9. Gibas A, Dienstag JL, Schafer AI, Delmonico F, Bynum TE, Schooley R, Rubin RH, Cosimi AB. Cure of hemophilia A by orthotopic liver transplantation. Gastroenterology. 1988;95(1):192-4.

10. Liras A, Segovia C, Gabán AS. Advanced therapies for the treatment of hemophilia: future perspectives. Orphanet Journal of Rare Diseases. 2012;7:97-.

11. Chen SL. Economic costs of hemophilia and the impact of prophylactic treatment on patient management. The American journal of managed care. 2016;22(5 Suppl):s126-33.

12. Ohashi K, Tatsumi K, Utoh R, Takagi S, Shima M, Okano T. Engineering liver tissues under the kidney capsule site provides therapeutic effects to hemophilia B mice. Cell transplantation. 2010;19(6):807-13.

13. Tatsumi K, Ohashi K, Shima M, Nakajima Y, Okano T, Yoshioka A. Therapeutic effects of hepatocyte transplantation on hemophilia B. Transplantation. 2008;86(1):167-70.

14. Seale NM, Varghese S. Biomaterials for pluripotent stem cell engineering: from fate determination to vascularization. Journal of Materials Chemistry B. 2016;4(20):3454-63.

15. Vegas AJ, Veiseh O, Gurtler M, Millman JR, Pagliuca FW, Bader AR, Doloff JC, Li J, Chen M, Olejnik K, Tam HH, Jhunjhunwala S, Langan E, Aresta-Dasilva S, Gandham S, McGarrigle JJ, Bochenek MA, Hollister-Lock J, Oberholzer J, Greiner DL, Weir GC, Melton DA, Langer R, Anderson DG. Long-term glycemic control using polymer-encapsulated human stem cell-derived beta cells in immune-competent mice. Nat Med. 2016;22(3):306-11.

16. Vegas AJ, Veiseh O, Doloff JC, Ma M, Tam HH, Bratlie K, Li J, Bader AR, Langan E, Olejnik K, Fenton P, Kang JW, Hollister-Locke J, Bochenek MA, Chiu A, Siebert S, Tang K, Jhunjhunwala S, Aresta-Dasilva S, Dholakia N, Thakrar R, Vietti T, Chen M, Cohen J, Siniakowicz K, Qi M, McGarrigle J, Graham AC, Lyle S, Harlan DM, Greiner DL, Oberholzer J, Weir GC, Langer R, Anderson DG. Combinatorial hydrogel library enables identification of materials that mitigate the foreign body response in primates. Nature Biotechnology. 2016;34:345.

17. Severgnini M, Sherman J, Sehgal A, Jayaprakash NK, Aubin J, Wang G, Zhang L, Peng CG, Yucius K, Butler J, Fitzgerald K. A rapid two-step method for isolation of functional primary mouse hepatocytes: cell characterization and asialoglycoprotein receptor based assay development. Cytotechnology. 2012;64(2):187-95.

18. Mattei G, Di Patria V, Tirella A, Alaimo A, Elia G, Corti A, Paolicchi A, Ahluwalia A. Mechanostructure and composition of highly reproducible decellularized liver matrices. Acta Biomater. 2014;10(2):875-82.

19. Solanas E, Pla-Palacín I, Sainz-Arnal P, Almeida M, Lue A, Serrano T, Baptista PM. Tissue Organoids: Liver. In: Soker S, Skardal A, editors. Tumor Organoids. Cham: Springer International Publishing; 2018. p. 17-33.

20. Guguen-Guillouzo C, Guillouzo A. General Review on In Vitro Hepatocyte Models and Their Applications. In: Maurel P, editor. Hepatocytes: Methods and Protocols. Totowa, NJ: Humana Press; 2010. p. 1-40.

21. Flaim CJ, Chien S, Bhatia SN. An extracellular matrix microarray for probing cellular differentiation. Nat Meth. 2005;2(2):119-25.

22. Martinez-Hernandez A, Amenta PS. The hepatic extracellular matrix. I. Components and distribution in normal liver. Virchows Archiv A, Pathological anatomy and histopathology. 1993;423(1):1-11.

23. Matsumoto K, Nakamura T. Hepatocyte growth factor: molecular structure, roles in liver regeneration, and other biological functions. Crit Rev Oncog. 1992;3(1-2):27-54.

24. Huh C-G, Factor VM, Sánchez A, Uchida K, Conner EA, Thorgeirsson SS. Hepatocyte growth factor/c-met signaling pathway is required for efficient liver regeneration and repair. Proceedings of the National Academy of Sciences of the United States of America. 2004;101(13):4477-82.

25. Lascano JE, Campos MA. The important role of primary care providers in the detection of alpha-1 antitrypsin deficiency. Postgraduate medicine. 2017;129(8):889-95.

Chapter 5: Future Directions

Within this dissertation, I have investigated the development of biomaterial-based devices for liver cell therapy. In chapter 2 I have developed a PEGDA/HAMA-based, vascularizable dual compartment device for primary hepatocyte transplantation. The findings from this study indicate that the device was capable of maintaining the function of two different donor cell sources for one month. Given this preliminary success, future studies should determine the maximum time the transplanted device would remain functional in mice. Upon obtaining this result, the device can be applied to rescuing the phenotype of different liver or liver related diseases, like hemophilia B or alpha-1-anti trypsin deficiency that can be treated by augmenting liver function. First testing can be done in mouse models then if successful, larger animal testing can be conducted. In addition to testing in animal models, the device can also be further optimized by incorporating stem cells. Successful incorporation of stem cells will mean access to a theoretically unlimited cell source for liver therapy, as opposed to the limited primary hepatocyte cell source. Thus, the dual compartment device can be used to investigate the optimal ECM environment for maintaining functioning stem cell derived hepatocytes *in vivo*. Such insights could have major implications in the future of cell transplantation therapies for treating liver diseases.

In Chapter 3, we recognized that the device developed in chapter 2 has some limitations, making it only suitable for autogeneic and HLA matched allogeneic cell transplantation. Thus, we created a new device, chitosan cell pouch, which protected the transplanted cells from interaction with the host cells. We further developed the device by modifying it to mitigate the immune response and fibrous capsule formation. Such a

device could theoretically be used in allogeneic and xenogeneic transplantations without requiring immune suppression. To test this theory we successfully transplanted HepG2 cells in immune competent mice. The cells remained functional for 1 month and formed no visible fibrous capsule. Building upon this outcome, we can first extend the experimental time point to see how long the pouch can remain functional. We can also test the pouch in multiple strains of immune competent mice and then bigger animals to ensure that it can indeed be successfully transplanted in multiple organisms without eliciting an immune response. The potential to deliver HepG2 cells safely for liver therapy could provide a therapy with an unlimited cell source that does not rely on costly and limited primary cells.

In Chapter 4, we tested the ability of the chitosan cell pouch to deliver primary mice and primary human cells in immune competent mice. Even though we already saw success in HepG2 cells, it was important to test primary cell delivery since they are more sensitive to their environment and have been know to lose function over time. Furthermore, even though primary cells are limited, they have been shown to perform more functions than HepG2 cells. Our results show sustained function up to one month. Furthermore, we used the cell pouch to optimize ECM conditions for improving liver function. Additionally, we showed that the cells produced alpha-1-antitrypsin, which suggests that with further testing and development, the chitosan pouch can serve as a treatment for this deficiency. Again, further testing should be done to see whether the pouch could produce enough alpha-1-antitrysin to treat the deficiency and rescue the phenotype long term. The pouch should also be tested with stem cell derived hepatocytes to overcome the challenge of limited and expensive primary cells. If stem cells are

successful, this can open the door towards using the pouch for personalized medicine and treatments. For example, a patient's cells can be collected, programmed into stem cells and corrected for any liver deficiencies. The stem cells would then be differentiated and matured, then transplanted back into the patient via the modified chitosan cell pouch. Beyond being used to combat other varieties of liver diseases, the pouch can also be extended to deliver other cell types such is islet cells for insulin production.